

SLAC-240  
UC-34d  
(T/E)

LONG-RANGE INTERACTIONS IN LATTICE FIELD THEORY\*

Jeffrey Mark Rabin

Stanford Linear Accelerator Center  
Stanford University  
Stanford, California 94305

June 1981

Prepared for the Department of Energy  
under contract number DE-AC03-76SF00515

Printed in the United States of America. Available from the National Technical Information Service, U.S. Department of Commerce, 5285 Port Royal Road, Springfield, VA 22161. Price: Printed Copy A07, Microfiche A01.

---

\* Ph.D. dissertation.

# LONG-RANGE INTERACTIONS IN LATTICE FIELD THEORY

Jeffrey Mark Rabin  
Stanford University  
June 1981

## ABSTRACT

Lattice quantum field theories containing fermions can be formulated in a chirally invariant way provided long-range interactions are introduced. I establish that in weak-coupling perturbation theory such a lattice theory is renormalizable when the corresponding continuum theory is, and that the continuum theory is indeed recovered in the perturbative continuum limit. In the strong-coupling limit of these theories one is led to study an effective Hamiltonian describing a Heisenberg antiferromagnet with long-range interactions. Using block-spin renormalization group methods I find a critical rate of falloff of the interactions, approximately as inverse distance squared, which separates a nearest-neighbor-antiferromagnetic phase from a phase displaying identifiable long-range effects. I point out a duality-type symmetry which is present in some block-spin calculations.

#### ACKNOWLEDGEMENTS

I thank my advisers, Sid Drell and Helen Quinn, for constant advice, guidance, and encouragement. I am grateful for the opportunity to work at SLAC, where graduate students are treated as colleagues rather than slaves, and I thank Marvin Weinstein, Stan Brodsky, Ben Svetitsky, and the other members of the Theory Group for sharing their staggering collective knowledge of physics with me.

I thank Roberto Peccei, Alan Schwettman, Lenny Susskind, Dirk Walecka, and Roger Freedman of the Stanford Physics Department for their fine examples of how to do and teach physics.

I thank my roommates, Brent Hailpern, Tom Vogel, and Jim Shinkle (sequential, not simultaneous), and my friends, including but not restricted to Devaney Schneider, Christine Cory, Paula Kutzler, Ron Fellman, and Nikki Baumrind for helping me fill the past five years with things other than and perhaps (gasp!) more important than physics.

Finally I thank my parents, who have supported me in my arcane and incomprehensible studies of chess, physics, and mathematics simply because those were my choices and they love me.

## TABLE OF CONTENTS

	Page
ABSTRACT . . . . .	iii
ACKNOWLEDGEMENTS . . . . .	iv
TABLE OF CONTENTS . . . . .	v
LIST OF FIGURES . . . . .	vii
 CHAPTER	
I. INTRODUCTION . . . . .	1
II. PERTURBATION THEORY FOR SLAC LATTICE FERMIONS . . . . .	4
1. Introduction . . . . .	4
2. Lattice Fermions . . . . .	9
3. Wilson's Lattice QED . . . . .	16
4. Faithful Lattice Transcription of QED . . . . .	23
5. SLAC Lattice Gauge Theory . . . . .	28
6. Proof of Renormalizability . . . . .	44
7. Structure of Counterterms . . . . .	48
8. Concluding Remarks . . . . .	60
III. REAL-SPACE RENORMALIZATION GROUP METHODS . . . . .	63
1. Introduction . . . . .	63
2. Nearest-Neighbor Heisenberg-Ising Antiferromagnet . . .	65
3. Two-Site Calculation for the Isotropic Heisenberg Model . . . . .	77
4. Improving the Three-Site Calculation . . . . .	92
5. Concluding Remarks . . . . .	94

	Page
CHAPTER	
IV. THE LONG-RANGE HEISENBERG ANTIFERROMAGNET . . . . .	96
1. Introduction . . . . .	96
2. Exact Results . . . . .	100
3. Simple Calculation Using Three-Site Blocks . . . . .	103
4. Improved Calculation Using Nine-Site Blocks . . . . .	115
5. Concluding Remarks . . . . .	119
APPENDIX A . . . . .	121
APPENDIX B . . . . .	123
APPENDIX C . . . . .	127
REFERENCES . . . . .	130

## LIST OF FIGURES

FIGURE	Page
1. Spectrum-doubling fermion dispersion relation . . . . .	14
2. The SLAC derivative . . . . .	15
3. Feynman rules for Wilson's lattice QED . . . . .	19
4. Feynman rules for SLAC lattice QED . . . . .	31
5. Summation of tadpole diagrams to cure infrared divergences . . . . .	36
6. The "smoothed" SLAC derivative . . . . .	39
7. Summation of tadpole corrections to the fermion propagator . . . . .	41
8. One-loop scalar self-energy . . . . .	50
9. One-loop vertex correction . . . . .	53
10. Two-loop scalar self-energy . . . . .	56
11. Heisenberg-Ising model ground state energy density . . . .	75
12. Heisenberg-Ising model mass gap and end-to-end order . . .	76
13. Dimerized Heisenberg chain . . . . .	85
14. Heisenberg model renormalization-group trajectories . . .	86
15. Ground state energy density for the Heisenberg model with long-range interactions . . . . .	111

## CHAPTER I

### INTRODUCTION

The outstanding development in high energy physics during the past decade has been the re-emergence of relativistic quantum field theory as the unified theoretical framework for understanding the fundamental interactions. On the one hand, our command of perturbative field theory has been dramatically strengthened by the understanding of non-Abelian gauge theories and spontaneous symmetry breakdown, resulting in the unprecedented construction of unified, renormalizable theories of strong, weak, and electromagnetic interactions. On the other, real progress is finally being made in understanding nonperturbative phenomena in field theory.

It is no exaggeration to say that most of the results in nonperturbative field theory have come from lattice techniques. The lattice provides a regularization scheme which works independent of perturbation theory; many "continuum" calculations implicitly assume the presence of such a regularization. The very powerful renormalization group concepts of Wilson<sup>1</sup> give meaning to the renormalized continuum limit of a lattice theory, again without reference to perturbation theory. And lattice theories admit treatment by many approximation methods not available in the continuum: strong-coupling expansions,<sup>2</sup> block-spin renormalization group calculations,<sup>3-8</sup> Monte Carlo simulations,<sup>9</sup> variational methods,<sup>10</sup> and so forth. Experience derived from problems in solid-state physics is also very useful.

It is often pointed out that no regularization scheme can preserve all the desirable properties of relativistic quantum field theory: if it could we would take the finite regularized theory itself as a fundamental description of nature and throw away the unregulated, ill-defined field theory we started with. Thus dimensional regularization encounters difficulty with operators involving  $\gamma_5$ . For a similar reason (the axial current anomaly) there are difficulties in formulating Dirac fermions in the lattice regularization (in addition to the obvious loss of Lorentz invariance). This is discussed in Chapter II where I show that a simple lattice formulation of the Dirac equation with chiral symmetry requires long-range couplings on the lattice which fall off no faster than  $1/\text{distance}$ . This thesis discusses various issues arising from the existence of such long-range interactions in lattice theories.

In most discussions of lattice theories, long-range interactions are summarily excluded from the universe of discourse. This leads to a welcome reduction in the size of the space of all possible couplings, which is the appropriate setting for discussing the renormalization group. It also allows cavalier treatment of problems such as integration by parts, boundary conditions, and infinite-volume limits. Such issues will be important for the systems with long-range interactions discussed herein.

Chapter II of this thesis deals directly with the renormalization problem in lattice field theories where the long-range interactions arise from a chirally symmetric treatment of lattice fermions. If the lattice is to be a useful regulator for continuum field theory in general, it should in particular be a satisfactory perturbative regulator.

This means that it must be possible to define an order-by-order perturbative renormalization program such that the renormalized S-matrix elements have finite limits when the lattice spacing goes to zero, and these finite values agree with those obtained using any other regulator. It has been shown that this is possible for lattice theories with nearest-neighbor interactions,<sup>11</sup> but the proof does not go through in the presence of long-range interactions, due in part to the infinite-volume limit problem alluded to above. This circumstance has led some authors to conclude that the chirally symmetric lattice fermion theories are nonrenormalizable.<sup>12</sup> This is not so, and Chapter II generalizes the existing renormalizability proofs to handle these theories.

Chapters III and IV are devoted to nonperturbative studies of one-dimensional lattice spin systems using block-spin renormalization group techniques developed at SLAC. These spin systems, generalized Heisenberg antiferromagnets with interactions falling off as  $(\text{distance})^{-p}$ , arise naturally as effective Hamiltonians for the strong-coupling limit of the chirally symmetric fermion theories of Chapter II. The principal result is the identification of a critical rate of falloff of the interaction,  $p \approx 1.85$ , separating two phases of the theory. A faster falloff gives the same qualitative behavior as a nearest-neighbor interaction, long-range effects becoming important only with a slower falloff. In the course of carrying out the block-spin calculations a new type of duality transformation is encountered: it is a symmetry of the system after one blocking operation which is induced by the translation symmetry of the original spin system.

## CHAPTER II

### PERTURBATION THEORY FOR SLAC LATTICE FERMIONS

#### 1. Introduction

Rigorous formulation of a continuum quantum field theory normally involves defining the theory as a singular limit of a cutoff or regularized theory. In perturbation theory many satisfactory regularization schemes exist, including Pauli-Villars, dimensional regularization, and others. However, for nonperturbative studies of gauge theories, interest has focused on the lattice regularization, which has the virtue of preserving exact local gauge invariance. Block-spin renormalization group, Monte Carlo, strong-coupling, and rigorous mathematical methods<sup>2-10,13</sup> have provided a great deal of information concerning the phase structure and continuum limit of pure gauge theories on a lattice.

The extension of lattice techniques to realistic theories such as QCD has been hindered by uncertainty regarding the proper treatment of lattice fermions. Straightforward transcription of the Dirac equation to the lattice by replacing derivatives by nearest-neighbor differences leads to the so-called spectrum-doubling problem: the continuum limit of the latticized Dirac equation describes  $2^d$  fermions rather than just one, where  $d$  is the number of dimensions of space-time which are latticized. Of the many proposed solutions for this problem, two will be discussed here. Wilson<sup>14</sup> adds a term with no  $\gamma$ -matrix structure to the lattice Dirac equation. This term functions as a momentum dependent "mass", giving the extra fermions masses on the order of the cutoff and removing them from the spectrum in the continuum limit. As an additional

mass term, it also destroys the global chiral symmetry of the Dirac theory at  $m=0$ . The SLAC group<sup>4,15</sup> obtains the correct fermion spectrum and preserves chiral symmetry by transcribing the continuum derivative as a nonlocal lattice difference operator. The definition is such that in momentum space the lattice derivative acts as multiplication by  $ip_\mu$ .

Clearly, if the spectrum-doubling problem is connected with chiral symmetry, then it must be fully understood before lattice methods can give reliable information about the symmetry structure of QCD. Indeed, an important issue connected with chiral symmetry in any gauge theory is the axial anomaly. Any lattice gauge theory with continuous chiral symmetry must answer the following question. In consequence of the continuous symmetry, there will be a conserved axial current on the lattice. The naive manipulations leading to a non-anomalous Ward identity for this current are valid in the presence of the lattice regularization. Does the continuum limit of this current exist? If so, doesn't that yield a continuum axial current with no anomaly, and isn't that impossible?

The straightforward transcription of the Dirac equation answers this question by doubling the spectrum: the anomaly is cancelled between the different fermion species.<sup>16</sup> The Wilson formulation answers by explicitly breaking the lattice chiral symmetry. An extra term appears in the Ward identity and becomes the anomaly in the continuum limit.<sup>16,17</sup> In this chapter I will show that the SLAC theory encounters infrared divergences in perturbation theory which need careful treatment. Order by order the continuum limit of the conserved axial current does not exist due to these infrared divergences.

It is becoming generally recognized that an undoubled spectrum, continuous chiral symmetry, and locality of interactions are incompatible

though desirable properties of a lattice fermion scheme. Indeed, in the literature one can find the claim<sup>16,18</sup> that a lattice fermion theory with undoubled spectrum and continuous chiral symmetry is itself impossible, although the arguments in support of these claims involve additional assumptions. One purpose of the present work is to clarify the relations between these three properties of lattice fermion schemes.

Before using a particular regularization scheme for nonperturbative investigations, one would like to have confidence that it yields acceptable results in the familiar context of perturbation theory. Sharatchandra<sup>11</sup> has shown that Wilson's formulation of QED on a four-dimensional Euclidean lattice passes this test. He showed that in perturbation theory a multiplicative renormalization of fields and parameters suffices to remove all divergences in the  $a \rightarrow 0$  limit of the S-matrix, which then agrees with the S-matrix of continuum QED. My objective in this chapter is to give the corresponding analysis for the SLAC version of QED. In this case multiplicative renormalization does not suffice: additional counterterms are required. This is to be expected, since once long-range interactions are admitted the SLAC Lagrangian is by no means the most general one consistent with its symmetries. The analysis, like Sharatchandra's, should extend to QCD as well.

Perturbation theory with SLAC lattice fermions has been studied by Karsten and Smit in the four-dimensional Euclidean lattice formulation.<sup>12,16,19</sup> They computed both the one-loop vacuum polarization and the VVA triangle diagrams. They concluded that the axial current did not develop an anomaly in the continuum limit. Its matrix elements, along with the vacuum polarization, were nonlocal, not Lorentz covariant, and

infrared singular in the continuum limit. Furthermore, the theory appeared nonrenormalizable in that infinitely many Green's functions were superficially divergent. Nakawaki<sup>20</sup> reached similar conclusions from a study of the SLAC theory in Hamiltonian form. In the present work I show that the perturbation expansion of Karsten and Smit breaks down owing to the infrared singularities. I describe a resummation of the perturbation series which removes these divergences, and carry out a renormalization program to all orders of the modified expansion. The renormalized Green's functions at each order in this expansion go over, for  $a \rightarrow 0$ , to those of continuum QED to the same order.

The discussion is organized as follows. Section 2 reviews the fermion doubling problem and explores the reasons it occurs. The SLAC group's solution to the problem is discussed, and the "topological" connection between spectrum doubling, chiral symmetry, and the range of interactions is explained. In Sect. 3 I summarize Sharatchandra's arguments for the renormalizability of Wilson's lattice QED, which form the basis for the arguments I subsequently apply to the SLAC theory. In Sect. 4 I show how continuum QED in a fixed gauge can be faithfully transcribed onto a lattice. The SLAC derivative and long-range interactions appear automatically. Although this is not the SLAC lattice gauge theory which has been discussed in the literature, it provides a simple counterexample to the claim that no lattice version of QED with undoubled spectrum and continuous chiral symmetry is possible. Section 5 begins the discussion of the SLAC lattice gauge theory studied by Karsten and Smit. I derive the Feynman rules, check the classical continuum limit of the Lagrangian, and exhibit the conserved currents and Ward identities. The

theory appears nonrenormalizable by power counting. However, the perturbation expansion is shown to be invalid due to infrared divergences which arise as a direct consequence of having an undoubled fermion spectrum. The summation of tadpole diagrams is shown to remove both the infrared divergences and the problems with power counting. Section 6 begins the discussion of renormalization. The obstacle to direct application of Sharatchandra's methods is the inability to expand integrands in powers of external momenta. I divide the integrals into subregions, in each of which the Taylor expansion in external momenta is possible. I then give the prescription for order-by-order construction of counterterms, and show that in the presence of the counterterms the  $a \rightarrow 0$  limit gives ordinary continuum QED. Section 7 supplements this rather abstract discussion by applying the renormalization prescription to one- and two-loop examples. Although detailed calculations are not carried out, the form of the necessary counterterms is clarified. I consider to what extent the counterterms can be generated by rescaling fields and parameters. Finally, I show that in the renormalized perturbation expansion the conserved axial current still has divergent matrix elements. These can be made finite by redefining the current, at the cost of introducing the usual anomaly. Section 8 summarizes the conclusions and points out remaining problems. In particular I consider whether the properties of the SLAC lattice gauge theory established in perturbation theory will persist in the exact nonperturbative solution.

Notation: The Einstein summation convention is not used in this chapter. Summations will be indicated explicitly.

## 2. Lattice Fermions

This section reviews the spectrum-doubling problem of lattice fermions and motivates its solution via the "SLAC derivative".

Consider the Klein-Gordon equation for a scalar field,

$$\left( \frac{\partial^2}{\partial t^2} - \nabla^2 + m^2 \right) \phi(\vec{x}, t) = 0 \quad . \quad (2.1)$$

The problem of transcribing this equation onto a three-dimensional lattice with continuous time is solved by making  $\phi$  a function on lattice sites indexed by  $\vec{x}$  and replacing  $\nabla^2$  by an appropriate difference operator. Plausible choices are  $\nabla_+^2$ ,  $\nabla_-^2$ ,  $\nabla_\pm^2$ , and  $\vec{\nabla}_- \cdot \vec{\nabla}_+$ , where

$$\nabla_+^i f(\vec{x}) = \frac{1}{a} \left[ f(\vec{x} + \vec{a}^i) - f(\vec{x}) \right] \quad , \quad (2.2a)$$

$$\nabla_-^i f(\vec{x}) = \frac{1}{a} \left[ f(\vec{x}) - f(\vec{x} - \vec{a}^i) \right] \quad , \quad (2.2b)$$

$$\nabla_\pm^i f(\vec{x}) = \frac{1}{2a} \left[ f(\vec{x} + \vec{a}^i) - f(\vec{x} - \vec{a}^i) \right] \quad . \quad (2.2c)$$

(In this chapter the variable  $\vec{x}$  indexing lattice sites will always carry dimensions:  $x_i = n_i a$  where  $a$  is the lattice spacing and  $n_i$  is an integer.  $\vec{a}^i$  is a vector of length  $a$  in the  $i$  direction.) The spectrum of the lattice Klein-Gordon equation is found by seeking solutions of the form

$$\phi(\vec{x}, t) \sim e^{-iEt} e^{i\vec{k} \cdot \vec{x}} \quad ,$$

leading to the dispersion relations

$$\nabla_+^2 : E^2 = \frac{4}{a^2} \sum_i e^{ik_i a} \sin^2 \frac{1}{2} k_i a + m^2 , \quad (2.3a)$$

$$\nabla_-^2 : E^2 = \frac{4}{a^2} \sum_i e^{-ik_i a} \sin^2 \frac{1}{2} k_i a + m^2 , \quad (2.3b)$$

$$\nabla_{\pm}^2 : E^2 = \frac{1}{a^2} \sum_i \sin^2 k_i a + m^2 , \quad (2.3c)$$

$$\vec{\nabla}_- \cdot \vec{\nabla}_+ : E^2 = \frac{4}{a^2} \sum_i \sin^2 \frac{1}{2} k_i a + m^2 . \quad (2.3d)$$

(On an infinite lattice  $k_i$  is a continuous variable which can be chosen to run from  $-\pi/a$  to  $+\pi/a$ . The notation  $\Lambda = \pi/a$  will sometimes be used.)

All these expressions reduce to the usual continuum dispersion relation when  $a \rightarrow 0$  with  $\vec{k}$  fixed. However,  $\vec{\nabla}_+$  and  $\vec{\nabla}_-$  are not Hermitian: the energy in Eqs. (2.3a) and (2.3b) is not real. The remaining possibilities differ only in the period of the sine functions. Equation (2.3d) has the  $2\pi/a$  periodicity of the lattice while Eq. (2.3c) has period  $\pi/a$ . This signals spectrum doubling. For an acceptable spectrum only the spatially constant ( $\vec{k} = 0$ ) solution should minimize the energy. For Eq. (2.3c) this solution is degenerate with seven others having  $k_i = \pi/a$  for some values of  $i$  ( $\phi$  alternates sign in some lattice directions). About each of these solutions there is a band of long-wavelength excitations, resulting in eight low-lying particle states in the continuum limit compared to one for Eq. (2.3d).

It is not coincidental that Eq. (2.3d) alone is satisfactory. The gradient of a function  $f(\vec{x})$  on lattice sites is naturally defined as the

function on links which is the sum (with sign changes for the orientation of the link) of the values of  $f$  at the sites bounding a given link.

This is  $\nabla_+^i f$ . The divergence of a function  $f_i(x)$  on links is a function on sites given by the sum (with sign changes for orientation) of the values of  $f_i$  on links impinging on a given site. This is  $\sum_i \nabla_-^i f_i$ . Hence the Laplacian is naturally given by  $\vec{\nabla}_- \cdot \vec{\nabla}_+$ . The different derivatives represent the lattice boundary and coboundary operators,<sup>13</sup> which are not equal.

From a more abstract point of view, what is happening is the following. Associated with a scalar, vector, or antisymmetric tensor field there is a differential 0-form, 1-form, or 2-form. A rotationally covariant differential operator acting on the field can be expressed in terms of the exterior differential operators  $d$  and  $\delta$  acting on the form. A natural latticization is available by associating  $n$ -forms with  $n$ -cochains (functions on sites, links, or plaquettes for  $n = 0, 1, 2$ ) and  $d$  and  $\delta$  with the boundary and coboundary operators represented here by  $\nabla_+^i$  and  $\vec{\nabla}_-$ . The problems with fermions arise because they fall into spinor, rather than tensor representations of the rotation group and so have no associated  $n$ -forms.

Consider now the Dirac equation,

$$(i\gamma \cdot \partial - m)\psi = 0 , \quad (2.4)$$

which is seen to have the same dispersion relation as the Klein-Gordon equation by applying  $i\gamma \cdot \partial + m$  to both sides. Assume this equation is to be latticized by substituting a difference operator for the spatial derivatives,  $\psi$  being defined at lattice sites. This assumption is by no means necessary, but it does guarantee that the lattice Dirac equation

will have the usual chiral invariance when  $m = 0$ . The fermion dispersion relation will be that of the Klein-Gordon equation whose Laplacian is the square of the Dirac difference operator. The acceptable dispersion relation (2.3d) cannot be obtained!

The Dirac equation requires a Hermitian difference operator whose square is an acceptable Laplacian. The SLAC group<sup>4,15</sup> achieves this in terms of the Fourier transform of a lattice function  $f(\vec{x})$ ,

$$\tilde{f}(\vec{p}) = a^3 \sum_{\vec{x}} e^{-i\vec{p}\cdot\vec{x}} f(\vec{x}), \quad f(\vec{x}) = \frac{1}{(2\pi)^3} \int_{-\Lambda}^{\Lambda} d^3 p e^{i\vec{p}\cdot\vec{x}} \tilde{f}(\vec{p}), \quad (2.5)$$

by defining  $\nabla_j f(\vec{x})$  as the inverse transform of  $i p_j \tilde{f}(\vec{p})$ . This leads to the exact relativistic spectrum  $E^2 = p^2 + m^2$  on the lattice. In coordinate space the definition is

$$\nabla_j f(\vec{x}) = \sum_{n=1}^{\infty} \frac{(-1)^{n+1}}{na} \left[ f(\vec{x} + n\vec{a}_j) - f(\vec{x} - n\vec{a}_j) \right]. \quad (2.6)$$

The nonlocality of this operator is essential for avoiding the spectrum doubling. Indeed, a general derivative operator may be written

$$\nabla_j f(\vec{x}) = \sum_{\vec{y}} D_j(\vec{x} - \vec{y}) f(\vec{y}), \quad (2.7a)$$

with Fourier transform

$$\nabla_j \tilde{f}(\vec{p}) = i D_j(\vec{p}) \tilde{f}(\vec{p}), \quad (2.7b)$$

where the factor  $i$  has been extracted for convenience. The fermion dispersion relation will be

$$E^2 = \sum_j \tilde{D}_j^2(\vec{p}) + m^2 , \quad (2.8)$$

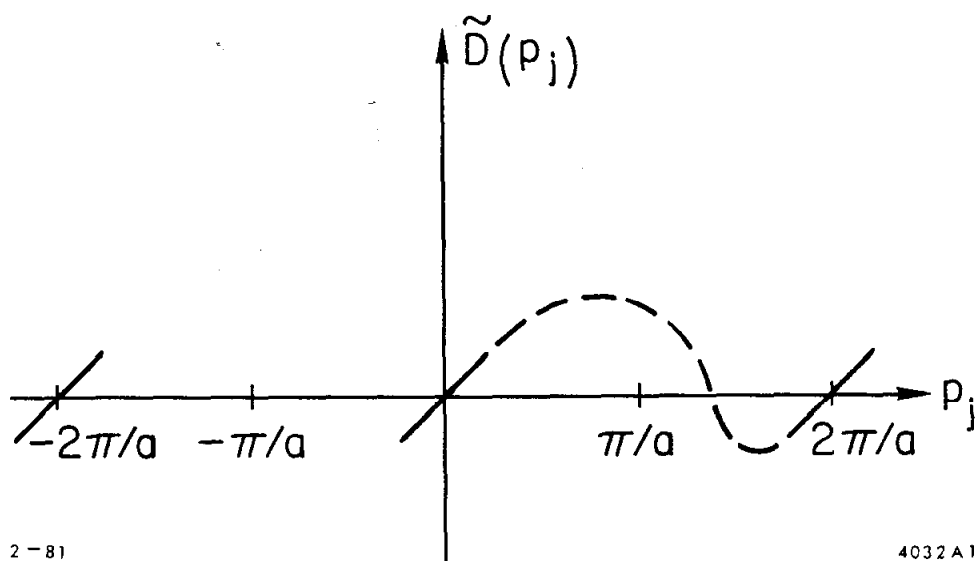
and spectrum doubling occurs if  $\sum_j \tilde{D}_j^2(\vec{p}) = 0$  has solutions other than  $\vec{p} = 2n\pi/a$ . Usually  $\tilde{D}_j(\vec{p}) = \tilde{D}(p_j)$  is a function of  $p_j$  alone, but in any case one can fix  $p_i = 0$ ,  $i \neq j$ , and study the function  $\tilde{D}(p_j) = \tilde{D}_j(p)$  alone. Hermiticity requires  $\tilde{D}$  to be real, a satisfactory continuum limit requires  $\tilde{D}(p_j) \rightarrow p_j$  as  $a \rightarrow 0$  with  $p_j$  fixed, and on general grounds  $\tilde{D}$  has period  $2\pi/a$ . It is evident from Fig. 1 that if  $\tilde{D}$  is continuous, it has at least one zero for  $0 < p_j < 2\pi/a$ , with a band of low-lying states around this zero to become an extra fermion in the continuum limit. The SLAC derivative (Fig. 2) escapes this conclusion due to its discontinuity at  $p_j = \pi/a$ . One recalls that the Fourier coefficients of a discontinuous function fall off as  $1/n$  or slower, so  $D_j(\vec{x} - \vec{y})$  is necessarily nonlocal. This argument, which also appears in Ref. 16, is a simple and intuitive case of the more general topological theorem of Ref. 18.

It is amusing to note that, because a Fourier series converges to the mean at a point of discontinuity, the SLAC function  $\tilde{D}(p_j) = p_j$  for  $p_j \in (-\pi/a, \pi/a)$ , extended periodically, does have a zero at  $p_j = \pi/a$ . However, there is no band of low-lying states surrounding this point.

It is quite possible for  $\tilde{D}(p_j)$  to have more than two zeroes. The choice

$$\nabla_j f(\vec{x}) = \frac{1}{4a} \left[ f(\vec{x} + 2\vec{a}_j) - f(\vec{x} - 2\vec{a}_j) \right] ,$$

for example, leads to "spectrum quadrupling".



2-81

4032 A1

Fig. 1. General behavior of a continuous function  $\tilde{D}(p_j)$  appearing in the fermion dispersion relation, illustrating the necessity of spectrum doubling.

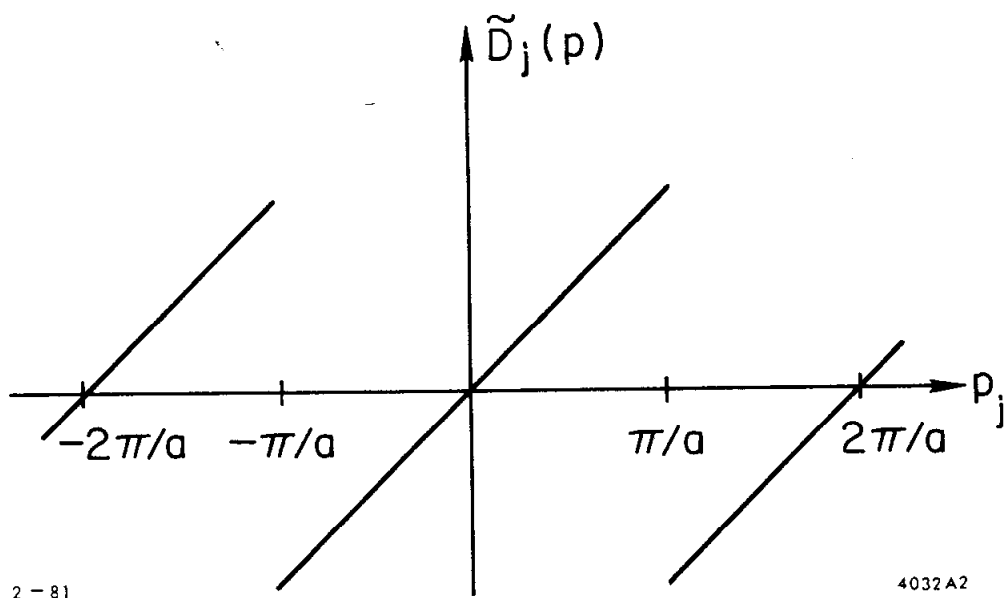


Fig. 2. The SLAC derivative  $\tilde{D}_j(p)$ , which avoids spectrum doubling by virtue of discontinuities at  $\pm\pi/a$ .

It should be evident from this discussion that there are interesting geometric and topological issues connected with latticizing fermions. Further research along these lines is in progress.

### 3. Wilson's Lattice QED

This section reviews Wilson's<sup>14</sup> lattice formulation of QED and Sharatchandra's<sup>11</sup> conclusions concerning its perturbative renormalizability. The method of Sharatchandra's proof is summarized in some detail since it provides a canonical set of arguments for establishing the perturbative equivalence of lattice and continuum theories. The analysis of the SLAC lattice QED formulation to follow will be based heavily on these arguments.

In this chapter, detailed discussions of lattice perturbation theory will be carried out in the four-dimensional Euclidean, rather than the Hamiltonian, formalism. This makes available the technical conveniences of the straightforward path-integral quantization and manifest symmetry between time and space coordinates characteristic of this formalism.

Wilson's lattice QED action is:

$$\begin{aligned}
 I = & a^4 \sum_{x,\mu,\nu} \frac{1}{4} F_{\mu\nu}^2(x) + a^4 \sum_{x,\mu} \frac{1}{2\lambda} \left[ \nabla_\mu^- A_\mu(x) \right]^2 \\
 & - a^4 \sum_{x,\mu} \bar{\psi}(x) \frac{1}{i} \gamma_\mu \frac{1}{2a} \left[ \psi(x + a_\mu) e^{ieaA_\mu(x)} - \psi(x - a_\mu) e^{-ieaA_\mu(x-a_\mu)} \right] \\
 & - a^4 \sum_{x,\mu} \bar{\psi}(x) \frac{1}{2a} \left[ \psi(x + a_\mu) e^{ieaA_\mu(x)} + \psi(x - a_\mu) e^{-ieaA_\mu(x-a_\mu)} - 2\psi(x) \right] \\
 & - a^4 \sum_x m\bar{\psi}(x)\psi(x) ,
 \end{aligned} \tag{2.9}$$

where  $F_{\mu\nu}(x) = \nabla_\mu^+ A_\nu(x) - \nabla_\nu^+ A_\mu(x)$ . (The  $\gamma$ -matrix convention is  $\{\gamma_\mu, \gamma_\nu\} = -2\delta_{\mu\nu}$ .)

For  $e = 0$ , the free fermion action is constructed using the derivative  $\nabla_\mu^\pm$  and would therefore yield a doubled spectrum if not for the additional terms in the third line of Eq. (2.9). In momentum space these terms read

$$- \left( \frac{2}{a} \sin^2 \frac{1}{2} p_\mu a \right) \tilde{\psi}(p) \tilde{\psi}(p) ,$$

and they vanish for  $p \rightarrow 0$  or for  $a \rightarrow 0$  with  $p$  fixed. However, they give "masses" of order  $\Lambda$  to the extra fermions with  $p_\mu = \pi/a$ , removing them from the spectrum in the continuum limit. They also explicitly break chiral symmetry, as is appropriate for a "mass" term.

The coupling to the gauge field is introduced in a manner consistent with invariance under the local gauge transformations

$$\psi(x) \rightarrow e^{-ie\chi(x)} \psi(x) ,$$

$$A_\mu(x) \rightarrow A_\mu(x) + \nabla_\mu^+ \chi(x) . \quad (2.10)$$

The second term in Eq. (2.9) serves to fix a "covariant" gauge. The form of the photon kinetic energy (not periodic in  $A_\mu$ ) identifies this as the noncompact formulation of QED; the compact formulation would replace  $F_{\mu\nu}^2(x)$  by

$$-\frac{2}{e^2 a^4} \left( e^{iea^2 F_{\mu\nu}(x)} - 1 \right) .$$

Finally, note that the lattice derivatives in Eqs. (2.9) and (2.10) are used "naturally" in the sense of Sect. 2:  $\nabla_\mu^+$  is used to create the plaquette variable  $F_{\mu\nu}$  from the link variable  $A_\mu$  while  $\nabla_\mu^-$  forms the scalar divergence of the vector  $A_\mu$ .

Expanding the exponentials in Eq. (2.9) and introducing the Fourier-transformed fields permits one to read off the Feynman rules from the coefficients of the terms in the action. For the photon field it is convenient to define the Fourier transform by

$$A_\mu(x) = \int_{-\Lambda}^{\Lambda} \frac{d^4 p}{(2\pi)^4} e^{ip \cdot (x + \frac{1}{2}a_\mu)} \tilde{A}_\mu(p) , \quad (2.11)$$

so as to get real expressions for propagators and vertex functions. For example, the Fourier transform of  $-i\nabla_\mu^- A_\mu(x)$  will be  $(2/a) \sin(\frac{1}{2}p_\mu a) \tilde{A}_\mu(p)$  rather than  $(1/ia)(1-e^{-ip_\mu a}) \tilde{A}_\mu(p)$ . Some of the resulting Feynman rules are given in Fig. 3.

$$\mu \xrightarrow{\text{wavy}} p \xrightarrow{\text{wavy}} \nu \quad \Delta_{\mu\nu}(p) = \frac{1}{S^2(p)} \left[ \delta_{\mu\nu} - (1-\lambda) \frac{S_\mu(p) S_\nu(p)}{S^2(p)} \right]$$

$$\xrightarrow{\text{---}} p \quad S_F(p) = \left[ \frac{1}{a} \sum_\mu \left( \gamma_\mu \sin p_\mu a + 2 \sin^2 \frac{1}{2} p_\mu a \right) + m \right]^{-1}$$

$$-e \left[ \gamma_\mu \cos \frac{1}{2} (p+q)_\mu a + a \sin \frac{1}{2} (p+q)_\mu a \right]$$

$$a e^2 \delta_{\mu\nu} \left[ \gamma_\mu \sin \frac{1}{2} (p+q)_\mu a - a \cos \frac{1}{2} (p+q)_\mu a \right]$$

Fig. 3. Some of the Feynman rules for Wilson's lattice QED. There are n-photon vertices for all  $n > 0$ .  $S_\mu(p) \equiv (2/a) \sin \frac{1}{2} p_\mu a$ .

Strictly speaking, the Feynman rules require an integration over the momentum of each internal line. In the continuum theory, many of these integrations are trivial because of the momentum-conserving delta functions. On the lattice, however, one has at each vertex a factor

$$a^4 \sum_{\mathbf{x}} \exp i(\sum \mathbf{k}) \cdot \mathbf{x} = (2\pi)^4 \delta_{\text{per}}^4(\sum \mathbf{k}) ,$$

where

$$\delta_{\text{per}}(\mathbf{q}) \equiv \sum_{n=-\infty}^{\infty} \delta(\mathbf{q} + 2n\Lambda) . \quad (2.12)$$

It is shown in Appendix A that because the Feynman integrands are themselves periodic functions of momenta, the trivial integrations can still be done. Thus even on the lattice one can label Feynman graph lines with exactly conserved momenta and perform nontrivial integrations only over a set of loop momenta.

Sharatchandra showed that this set of Feynman rules defines a multiplicatively renormalizable lattice QED: fields and parameters can be rescaled so that when  $a \rightarrow 0$  the Green's functions are finite and identical to those of ordinary QED. (In fact, Sharatchandra considered compact QED, which is technically more complicated.) This is demonstrated in four steps.

1. The Feynman rules reduce to the continuum Feynman rules when  $a \rightarrow 0$  with momenta fixed. Since the Feynman rules reflect the momentum-space coefficients in the action, this merely means that the action has the correct classical continuum limit. However, it does imply

that if a normal diagram (one containing no multiphoton vertices) converges as  $a \rightarrow 0$ , it agrees with the continuum result for the diagram.

2. The list of primitively divergent diagrams and their superficial degrees of divergence (for  $a \rightarrow 0$ ) coincides with the list for continuum QED. For normal diagrams this can be shown by bounding lattice quantities by continuum quantities. For example, for the photon propagator,

$$\frac{2}{\pi} p_\mu \leq \frac{2}{a} \sin \frac{1}{2} p_\mu a \leq p_\mu , \quad 0 \leq p_\mu \leq \frac{\pi}{a} ,$$

implies

$$\frac{1}{p^2} \leq \frac{1}{\sum_{\mu} \frac{4}{a^2} \sin^2 \frac{1}{2} p_\mu a} \leq \frac{\pi^2}{4} \frac{1}{p^2} , \quad |p_\mu| \leq \frac{\pi}{a} .$$

Now imagine shrinking some internal fermion propagator to a point in a normal diagram. The loss of this propagator increases  $D$  by one unit, but a two-photon vertex is created which carries an explicit factor  $a$  according to Fig. 3. Hence  $D$  is unchanged. This argument generalizes to show that the presence of multiphoton vertices does not interfere with power counting.

3. All Feynman integrands possess Taylor expansions in powers of their external momenta. Ignoring infrared problems, e.g., by assuming a photon mass, this means that the BPH procedure of subtracting the first  $D+1$  terms in the Taylor expansions of divergent subgraphs, with combinatorics handled by a forest formula, can be

implemented. It follows from point (1) that normal diagrams take on their continuum values when  $a \rightarrow 0$  after the subtractions are done. If a divergent subgraph contains a multiphoton vertex then it has the form  $a^N$  times an integral of  $\mathcal{O}(1/a^{N+D})$ ,  $N \geq 1$ . After  $D+1$  subtractions this becomes  $a^N \mathcal{O}(1/a^{N-1})$ , so all such diagrams vanish when  $a \rightarrow 0$ .

4. It remains to enumerate the counterterms which are required to implement the BPH subtractions. As in the continuum theory, the Ward identities are useful here. They are derived, as usual, by making a change of variables corresponding to an infinitesimal gauge transformation in the path integral for the vacuum functional in the presence of sources. The action proper is invariant under such a transformation but the gauge-fixing and source terms are not. The Ward identities state that the contribution of these terms does not affect the vacuum functional. It should be evident from Eqs. (2.9) and (2.10) that the Ward identities differ from their continuum versions only in the replacement of  $\partial_\mu$  by  $\nabla_\mu^-$ . They read, in momentum space,

$$\sum_\mu S_\mu(k) \Gamma_\mu(p+k, p) = S_F^{-1}(p+k) - S_F^{-1}(p) , \quad (2.13)$$

$$\sum_\mu S_\mu(k) \Pi_{\mu\nu}(k) = 0 , \quad (2.14)$$

$$\sum_\mu S_\mu(k_1) I_{\mu\nu\lambda\pi}(k_1, k_2, k_3, k_4) = 0 , \quad (2.15)$$

where  $S_\mu(k) \equiv \frac{2}{a} \sin \frac{1}{2} k_\mu a$  and  $I_{\mu\nu\lambda\pi}$  is the photon-photon scattering

amplitude. By substituting the Taylor expansions of the amplitudes into the Ward identities and using the lattice cubic symmetries one can show that  $I_{\mu\nu\lambda\pi}$  is not divergent, the divergent terms are at worst logarithmic, and the momentum dependence and tensor structure of these terms is exactly as in continuum QED. Because the action differs by terms of order  $a$  from the continuum QED action, it follows that multiplicative renormalization of fields and parameters generates precisely the needed counterterms, plus additional terms of order  $a \ln a$  which have no effect when  $a \rightarrow 0$ .

These arguments have been reviewed in detail so that the reader will understand exactly what ingredients go into a proof of perturbative equivalence of lattice and continuum field theories. In Sect. 5 I will discuss the problems that arise in applying the same arguments to the SLAC version of lattice QED.

#### 4. Faithful Lattice Transcription of QED

In Sect. 2 it was pointed out that with the SLAC derivative one can construct a lattice free fermion theory with continuous chiral symmetry and a sensible spectrum. I now give an "existence proof", showing that in fact a lattice QED can be formulated which continues to enjoy these properties and makes sense in weak-coupling perturbation theory. This serves as a simple counterexample to statements in the literature that no such formulation is possible.<sup>16,18</sup>

The idea here is to make contact between continuum and lattice field theories via a momentum-space formulation which both share. This tech-

nique has been used by the SLAC group<sup>4</sup> and by others<sup>21</sup> and in fact motivates the introduction of the SLAC gradient.

The Euclidean action for ordinary continuum QED reads:

$$I = \int d^4x \left\{ \sum_{\mu\nu} \frac{1}{4} F_{\mu\nu}^2 - \sum_{\mu} \bar{\psi}(x) \frac{1}{i} \gamma_{\mu} [\partial_{\mu} + ieA_{\mu}(x)] \psi(x) - m\bar{\psi}(x)\psi(x) \right\} . \quad (2.16)$$

The first step is to fix the Coulomb gauge and eliminate the dependent variable  $A_0$  by means of its equation of motion:

$$I = \int d^4x \left[ \frac{1}{2} (\partial_0 \vec{A})^2 + \frac{1}{2} (\vec{\nabla} \times \vec{A})^2 - \sum_{\mu} \bar{\psi}(x) \frac{1}{i} \gamma_{\mu} \partial_{\mu} \psi(x) - m\bar{\psi}(x)\psi(x) - \sum_j e\bar{\psi}(x) \gamma_j A_j(x) \psi(x) + e^2 \int d^4x' \frac{\delta(t-t')}{8\pi |\vec{x} - \vec{x}'|} \psi^\dagger(x)\psi(x) \psi^\dagger(x')\psi(x') \right] . \quad (2.17)$$

It is to be emphasized that  $I$  is manifestly gauge-invariant because it is written in terms of gauge-invariant fields:  $\vec{A}$  is now the transverse photon field and  $\psi$  is the Coulomb gauge (physical) electron field. All gauge degrees of freedom have been removed. These degrees of freedom are not true quantum variables and should not be included in the transcription to the lattice. The action (2.17) is now written in momentum space:

$$\begin{aligned}
 I = & \int \frac{d^4 k}{(2\pi)^4} \left[ \frac{1}{2} k^2 \vec{\tilde{A}}(k) \cdot \vec{\tilde{A}}(-k) - \tilde{\bar{\psi}}(k) \gamma^\mu k \tilde{\psi}(k) - m \tilde{\bar{\psi}}(k) \tilde{\psi}(k) \right. \\
 & - e \int \frac{d^4 p d^4 q}{(2\pi)^8} \tilde{\bar{\psi}}(k) \gamma^\mu \vec{\tilde{A}}(p) \tilde{\psi}(q) \delta^4(p + q - k) \\
 & \left. + \frac{1}{2} e^2 \int \frac{d^4 p d^4 q d^4 l}{(2\pi)^8} \frac{1}{|\vec{l} - \vec{k}|^2} \tilde{\psi}^\dagger(k) \tilde{\bar{\psi}}(l) \tilde{\psi}^\dagger(p) \tilde{\psi}(q) \delta^4(k + p - l - q) \right] . \tag{2.18}
 \end{aligned}$$

Next, impose a cutoff  $\Lambda$  on the magnitude of each component of momentum in Eq. (2.18). (This is why it was necessary to write  $I$  in terms of explicitly gauge-invariant variables. Had that not been done, gauge invariance would have been lost at this point.) The resulting action could equally well be interpreted as the momentum-space action of a lattice field theory, namely:

$$\begin{aligned}
 I_{\text{lattice}} = & a^8 \sum_{x,y} \frac{1}{2} d(x-y) \vec{A}(x) \cdot \vec{A}(y) - a^8 \sum_{x,y,\mu} \bar{\psi}(x) \frac{1}{i} \gamma_\mu D_\mu(x-y) \psi(y) \\
 & - a^4 \sum_x m \bar{\psi}(x) \psi(x) - a^{12} \sum_{x,y,z,j} e f(x,y,z) \bar{\psi}(x) \gamma_j A_j(y) \psi(z) \\
 & + a^{16} \sum_{x,x',y,y'} \frac{1}{2} e^2 g(x,x',y,y') \psi^\dagger(x) \psi(x') \psi^\dagger(y) \psi(y') , \tag{2.19}
 \end{aligned}$$

where

$$d(x-y) = \int_{-\Lambda}^{\Lambda} \frac{d^4 k}{(2\pi)^4} k^2 e^{ik \cdot (x-y)} ,$$

$$D_\mu(x-y) = \int_{-\Lambda}^{\Lambda} \frac{d^4 k}{(2\pi)^4} i k_\mu e^{ik \cdot (x-y)} ,$$

$$f(x, y, z) = \int_{-\Lambda}^{\Lambda} \frac{d^4 k d^4 p d^4 q}{(2\pi)^8} e^{i(k \cdot x - p \cdot y - q \cdot z)} \delta^4(p + q - k),$$

$$g(x, x', y, y') = \int_{-\Lambda}^{\Lambda} \frac{d^4 k d^4 p d^4 q d^4 \ell}{(2\pi)^{12}} \frac{1}{|\vec{\ell} - \vec{k}|^2} e^{i(k \cdot x + p \cdot y - \ell \cdot x' - q \cdot y')} \delta^4(p + k - \ell - q).$$

The nonlocal coefficient functions here are all translation-invariant and, except for  $g(x, x', y, y')$  which contains the noncovariance associated with the Coulomb interaction, invariant under the lattice cubic symmetries.

$D_\mu(x - y)$  is just the SLAC derivative operator. Note also that in this formulation there is no possibility of assigning the photon field  $A_j(x)$  to the links of the lattice: all fields are treated on an equal footing and may as well be situated on the sites.

The lattice theory (2.19) may be quantized by the path-integral technique provided one integrates only over transverse gauge fields with  $\vec{k} \cdot \vec{A}(k) = 0$ . It is evident that in all respects - including perturbation theory - the theory is equivalent to Coulomb gauge continuum QED regularized by a momentum cutoff. To each continuum operator there corresponds a lattice operator, obtained by a double Fourier transform, with the same regularized matrix elements. The fermion spectrum is sensible and there is chiral symmetry for  $m = 0$ . Also, there are no umklapp processes: momentum conservation in Feynman diagrams is exact rather than periodic, and propagators and vertex functions are identical to those of continuum QED. The theory can be given a finite  $a \rightarrow 0$  limit by including in the momentum-space action the counterterms needed to renormalize continuum QED. Because of the momentum-cutoff regularization, photon mass counter-terms will be needed. For  $\phi^4$  theory in 1+1 dimensions all necessary

counterterms are known exactly and this program has been carried out explicitly by Bronzan.<sup>21</sup>

Although this procedure provides a lattice theory which faithfully represents continuum QED, it is not a lattice gauge theory. A lattice gauge theory possesses a local gauge group on the lattice under which the action is invariant but the fields transform nontrivially. The above theory does not qualify because the gauge freedom in the fields was removed before transcription to the lattice. In the next section I discuss the lattice gauge theory constructed using the SLAC derivative.

The lattice theory constructed above possesses neither a local gauge symmetry nor periodic momentum conservation. It is easy to understand qualitatively why these properties are connected. At a technical level, perturbative proofs of Ward identities require shifts of integration variables which are made possible by periodicity. More generally, consider a term in the lattice action

$$F(x_1, x_2, \dots, x_n) \phi(x_1) \phi(x_2) \dots \phi(x_n),$$

where  $\phi$  is a generic field. Assuming that  $F$  is translation invariant its Fourier transform  $F(p_1, p_2, \dots, p_n)$  can have support only when  $\sum p_i = 0$  mod  $2\pi/a$ . To obtain exact momentum conservation  $F$  must be so chosen that its support lies in the subregion  $\sum p_i = 0$ : not all momenta can be allowed to become large simultaneously. This is the case for the coefficient functions in Eq. (2.19). However, a gauge symmetry which is local in coordinate space will affect the high-momentum components of fields. A gauge-invariant coupling term will couple high-momentum components of

fields, so that in general the support of  $F$  cannot be restricted to

$$\sum p_i = 0.$$

## 5. SLAC Lattice Gauge Theory

### A. Introduction

This section begins the discussion of the lattice gauge theory with action

$$I = a^4 \sum_{x,\mu,\nu} \frac{1}{4} F_{\mu\nu}^2(x) + a^4 \sum_{x,\mu} \frac{1}{2\lambda} \left[ \nabla_\mu^- A_\mu(x) \right]^2 \\ - a^8 \sum_{x,y,\mu} \bar{\psi}(x) \gamma_\mu \frac{1}{i} D_\mu(x-y) \psi(y) \exp iea \sum_{z=x}^y A_\mu(z) \\ - a^4 \sum_x m \bar{\psi}(x) \psi(x) , \quad (2.20)$$

where  $F_{\mu\nu}(x) = \nabla_\mu^+ A_\nu(x) - \nabla_\nu^+ A_\mu(x)$ ,

$$\text{and } D_\mu(x) = \int_{-\Lambda}^{\Lambda} \frac{d^4 k}{(2\pi)^4} i k_\mu e^{ik \cdot x} \\ = (-1)^{x_\mu/a} / a^4 x_\mu \text{ if } x_\mu \neq 0 \text{ but } x_\nu = 0 \text{ for all } \nu \neq \mu \\ = 0 \text{ otherwise,} \quad (2.21)$$

and the notation  $\sum_{z=x}^y A_\mu(z)$  means the following. Owing to the presence in Eq. (2.20) of the SLAC derivative function  $D_\mu(x-y)$ , the summation need only be defined in case  $x_\mu \neq y_\mu$  but  $x_\nu = y_\nu$  for all  $\nu \neq \mu$  ( $x$  and  $y$  are separated in the  $\mu$  direction only). In that case it means the sum

of the values of  $A_\mu$  on the oriented links between  $x$  and  $y$ :

$$\sum_{z=x}^y A_\mu(z) \text{ means}$$

$$\theta(y_\mu - x_\mu) \sum_{n=0}^{(y_\mu - x_\mu - a)/a} A_\mu(x + na_\mu) - \theta(x_\mu - y_\mu) \sum_{n=0}^{(x_\mu - y_\mu - a)/a} A_\mu(y + na_\mu)$$

For  $e = 0$  the fermion action is that of the SLAC formulation, with undoubled spectrum and continuous chiral symmetry for  $m = 0$ . The action is invariant under the gauge transformations of Eq. (2.10). Since the photon action is exactly as in the Wilson formulation it should be clear that the Ward identities are still given by Eqs. (2.13) - (2.15). In particular, the nearest-neighbor derivative, not the SLAC derivative, appears in Ward identities. (Nakawaki<sup>20</sup> has considered a lattice theory in which all derivatives are taken to be  $ik_\mu$  in momentum space. This simply replaces  $S_\mu(k)$  by  $k_\mu$  everywhere without affecting the arguments to follow.) However, the consequences of the Ward identities are vastly different for the theories (2.9) and (2.20) due to the different fermion spectra. This will emerge shortly.

The theory (2.20) possesses a conserved electromagnetic current which can be identified by considering the coupling to an external field:

$$\sum_\mu \bar{\psi}_\mu j_\mu(z) = 0 ,$$

$$j_\mu(z) = \frac{\delta I}{a^4 \delta A_\mu^{\text{ext}}(z)} \Bigg|_{A_\mu^{\text{ext}} = 0} \quad (2.22)$$

$$= -ea^5 \sum_{\substack{x, y \\ x_\mu \leq z_\mu < y_\mu \\ z_\nu = x_\nu, \nu \neq \mu}} \bar{\psi}(x) \gamma_\mu D_\mu(x-y) \psi(y) \exp iea \sum_{w=x}^y A_\mu(w) + \text{h.c.} .$$

There is also an axial current, conserved for  $m = 0$ :

$$\sum_{\mu} \nabla_{\mu}^{-} j_{\mu}^5(z) = 2im\bar{\psi}(z)\gamma_5\psi(z) , \quad (2.23)$$

$$j_{\mu}^5(z) = a^5 \sum_{\substack{x,y \\ x_{\mu} \leq z_{\mu} < y_{\mu} \\ z_v = x_v, v \neq \mu}} \bar{\psi}(x)\gamma_{\mu}\gamma_5 D_{\mu}(x-y)\psi(y) \exp ie a \sum_{w=x}^y A_{\mu}(w) + h.c.$$

Both these currents are gauge invariant.

By expanding the exponential in the action and introducing Fourier transforms, one derives what I shall call the naive Feynman rules.

These are given in Fig. 4. Momentum conservation in this theory is once again modulo  $2\pi/a$ . The first point to observe is that the continuum Feynman rules are indeed recovered when  $a \rightarrow 0$  with all momenta fixed. This verifies that the action has the correct classical continuum limit, a fact which is not immediately apparent from Eq. (2.20). The most striking feature of the naive Feynman rules, however, is the presence of infrared singularities in the vertex functions. The one-photon vertex, for example,

$$e\gamma_{\mu} \frac{\tilde{D}_{\mu}(p) - \tilde{D}_{\mu}(p+k)}{S_{\mu}(k)} ,$$

behaves as  $-2\pi e\gamma_{\mu}/ak_{\mu}$  as  $k_{\mu} \rightarrow 0^+$  with  $p_{\mu} \rightarrow \pi/a$  from below and  $p_{\mu} + k_{\mu} \rightarrow \pi/a$  from above. This is a consequence of the discontinuity in  $\tilde{D}_{\mu}(p)$  at  $p_{\mu} = \pi/a$ , and thus, indirectly, of the Ward identity (2.13) relating the vertex to the fermion propagator. These singularities have important consequences for the renormalization program a la Sharatchandra. Due to the singularities and discontinuities in the vertices, naive

$$\mu \text{---} p \text{---} \nu \quad \Delta_{\mu\nu}(p) = \frac{1}{S^2(p)} \left[ \delta_{\mu\nu} - (1-\lambda) \frac{S_\mu(p) S_\nu(p)}{S^2(p)} \right]$$

$$\text{---} \rightarrow p \quad S_F(p) = \left[ \sum_\mu \gamma_\mu \tilde{D}_\mu(p) + m \right]^{-1}$$

$$\text{---} \rightarrow q \quad \text{---} \rightarrow p \quad e \gamma_\mu \frac{\tilde{D}_\mu(p) - \tilde{D}_\mu(p+k)}{S_\mu(k)}$$

$$\text{---} \rightarrow q \quad \text{---} \rightarrow p \quad \frac{-e^2 \delta_{\mu\nu}}{S_\mu(k) S_\nu(l)} \gamma_\mu \left[ \tilde{D}_\mu(p) - \tilde{D}_\mu(p+k) - \tilde{D}_\mu(p+l) + \tilde{D}_\mu(p+k+l) \right]$$

$$\text{---} \rightarrow q \quad \text{---} \rightarrow p \quad \frac{e^n \delta_{\mu_1 \mu_2} \delta_{\mu_1 \mu_3} \dots \delta_{\mu_1 \mu_n}}{S_{\mu_1}(k_1) S_{\mu_2}(k_2) \dots S_{\mu_n}(k_n)} \gamma_{\mu_1} \Gamma_{\mu_1}^n(p; k_1, k_2, \dots k_n),$$

$$2-81 \\ 4032A4 \quad \Gamma_\mu^{n+1}(p; k_1, \dots k_{n+1}) = -\Gamma_\mu^n(p; k_1, \dots k_n) + \Gamma_\mu^n(p+k_{n+1}; k_1, \dots k_n)$$

Fig. 4. Naive Feynman rules for SLAC lattice QED.  
 $S_\mu(p) \equiv (2/a) \sin \frac{1}{2} p_\mu a.$

Feynman integrands do not possess Taylor expansions in powers of external momenta. Furthermore, the singularities alter the results of naive power counting. A diagram with  $F$  external fermion lines and  $B$  external boson lines would normally have superficial degree of divergence  $D = 4 - (3/2)F-B$ . Here, however, for each external photon line there is a factor  $1/S_\mu(k)$  which sits outside the integration and does not help to converge it. The integral is left with  $D = 4 - \frac{3}{2}F$ . The infinite class of diagrams with  $F = 0$  or  $2$  is superficially divergent! Due to the infrared singularities, then, the crucial steps 2 and 3 in the renormalization program of Sect. 3 do not go through for SLAC fermions, and the theory indeed appears non-renormalizable.

Karsten and Smit base their objections to the SLAC lattice gauge theory on the above points, which they have explicitly verified in the example of the one-loop vacuum polarization.<sup>12</sup> They found that  $\Pi_{\mu\nu}(k)$  had  $D = 2$  even after the cancellations due to gauge invariance. In the continuum limit there are infrared singular terms with unacceptable (nonlocal) tensor structure in both the divergent and finite terms, a typical structure being

$$\Pi_{\mu\nu}(k) \sim \frac{\delta_{\mu\nu}}{|k_\mu|} \sum_\lambda |k_\lambda| - \text{sign } k_\mu \text{ sign } k_\nu \quad (2.24)$$

+ other singular terms.

(Note that the Ward identity  $\sum_\mu k_\mu \Pi_{\mu\nu} = 0$  is satisfied!) Furthermore, since the necessary Taylor expansions do not exist, there is no natural way to make the separation into divergent terms and finite

remainders which defines the counterterms required. Since the Green's functions are not differentiable, the conventional normalization conditions do not make sense.

It is important to understand clearly the origin of the infrared singularities in the vertex functions. They come from the term in the action

$$-a^8 \sum_{x,y,\mu} \bar{\psi}(x) \gamma_\mu \frac{1}{i} D_\mu(x-y) \psi(y) \exp iea \sum_{z=x}^y A_\mu(z) . \quad (2.25)$$

The exponential factor, in momentum space, involves a geometric sum:

$$\begin{aligned} & \exp iea \sum_{z=x}^y \int_{-\Lambda}^{\Lambda} \frac{d^4 k}{(2\pi)^4} e^{ik \cdot z} e^{ik_\mu a/2} \tilde{A}_\mu(k) \\ &= \exp iea \int_{-\Lambda}^{\Lambda} \frac{d^4 k}{(2\pi)^4} \frac{e^{ik \cdot x} - e^{ik \cdot y}}{1 - e^{ik_\mu a}} e^{ik_\mu a/2} \tilde{A}_\mu(k) \\ &= \exp -e \int_{-\Lambda}^{\Lambda} \frac{d^4 k}{(2\pi)^4} \frac{e^{ik \cdot x} - e^{ik \cdot y}}{S_\mu(k)} \tilde{A}_\mu(k) . \end{aligned} \quad (2.26)$$

The singular factors  $1/S_\mu(k)$  enter the vertices via the expansion of this exponential in powers of  $e$ . However, consider the behavior of the integrand in the infrared region  $k_\mu \rightarrow 0$ ; it is proportional to  $i|x_\mu - y_\mu|$ . Since  $x$  and  $y$  are summed over all lattice sites in (2.25), the distance between them is unbounded. This means that the expansion of the exponential to any finite order  $n$  in  $e$  cannot be a uniformly valid approximation over the entire range of values of  $|x_\mu - y_\mu|$ . If the expansion is attempted anyway, its  $n$ th term will behave as  $|x_\mu - y_\mu|^{n-1}$ . Since

the function  $D_\mu(x-y)$  in (2.25) falls off only as  $|x_\mu - y_\mu|^{-1}$ , the individual terms in the perturbation expansion will be divergent in the infrared. The conclusion is that the infrared singularities in the naive Feynman rules are symptomatic of an invalid perturbation expansion which does not accurately represent the infrared behavior of the theory. I emphasize that the fault lies with the perturbative expansion rather than with any inconsistency in the theory. If the expansion in powers of  $e$  is avoided then the exponential enters the sum (2.25) as a rapidly oscillating phase when  $|x_\mu - y_\mu|$  is large. Such a phase factor actually improves convergence of the sum. Finally, note that perturbation theory can fail even when the fermion spectrum is doubled. If  $D_\mu(x-y)$  has a power-law falloff faster than  $|x_\mu - y_\mu|^{-1}$  then as pointed out in Sect. 2 the spectrum is doubled, but singularities will still appear at sufficiently high order in perturbation theory. The equivalent momentum-space statement is that even if  $\tilde{D}_\mu(p)$  is continuous, a discontinuity in its  $n$ th derivative induces a singularity in the  $(n+1)$ -photon vertex function. This follows from the recursion relation for the vertices in Fig. 4. A nonsingular perturbation expansion is obtained only if  $D_\mu(x-y)$  falls faster than any power of  $|x_\mu - y_\mu|$ . Such a  $D_\mu(x-y)$  strongly suppresses the contributions from the region of large  $|x_\mu - y_\mu|$  where the expansion of the exponential is invalid.

The failure of naive perturbation theory discussed above becomes evident from the structure of  $\Pi_{\mu\nu}$  in Eq. (2.24). Consider a diagram in which the one-loop  $\Pi_{\mu\nu}(k)$  appears as a subgraph. The integration over  $k$  encounters a  $1/k$  singularity. Such a singularity is not integrable, in contrast to the usual infrared singularities which often are, e.g.,

$\int d^4 k/k^2$ . Since the singularity arises from a vertex function rather than a propagator, it also is not regularized by a photon mass, and simply leads to a divergent amplitude indicating the breakdown of perturbation theory.

### B. Removal of the Infrared Problem

Now that the origin of the infrared problems which plague naive perturbation theory is clear, how can they be circumvented? The most obvious approach is simply to impose a cutoff on  $|x_\mu - y_\mu|$  in the nonlocal interaction Lagrangian:

$$\begin{aligned} & \sum_{x,y,\mu} \bar{\psi}(x) \gamma_\mu \frac{1}{i} D_\mu(x-y) \psi(y) \exp ie a \sum_{z=x}^y A_\mu(z) \\ \rightarrow & \sum_{x,y,\mu} \bar{\psi}(x) \gamma_\mu \frac{1}{i} D_\mu(x-y) \psi(y) \\ + & \sum_{\substack{x,y,\mu \\ |x_\mu - y_\mu| < Na}} \bar{\psi}(x) \gamma_\mu \frac{1}{i} D_\mu(x-y) \psi(y) \left[ \exp ie a \sum_{z=x}^y A_\mu(z) - 1 \right] . \end{aligned}$$

The cutoff permits a nonsingular expansion in powers of  $e$  but destroys manifest gauge invariance. Therefore the cutoff must be imposed in the fixed gauge in which quantization is performed. This should be a physical gauge, since otherwise the loss of the Ward identities will jeopardize unitarity.

I now show that in fact an ad hoc cutoff is unnecessary since the theory generates its own cutoff. Consider for example the bare one-photon vertex function, and add to it all diagrams in which additional photons are emitted and absorbed at the same vertex (Fig. 5). The sum gives the vertex function computed to lowest order in the interaction Lagrangian

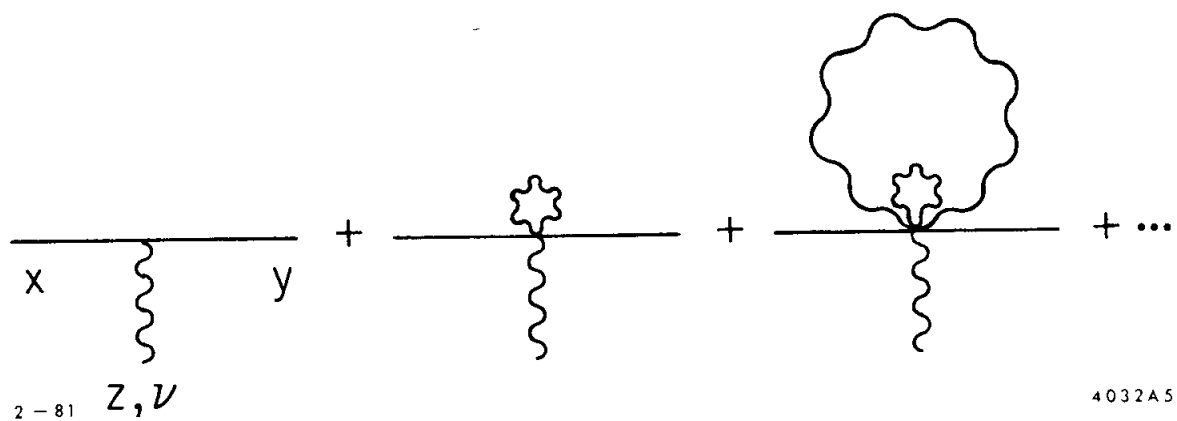


Fig. 5. A class of diagrams whose summation removes the infrared singularity from the vertex function and permits a non-singular perturbation expansion.

rather than lowest order in  $e$ . The diagrams are most easily summed in coordinate space, where they yield

$$\begin{aligned}
 & \sum_{x', y', \mu} \sum_{z' = x'}^{y'} iea S_F(x - x') \gamma_\mu D_\mu(x' - y') S_F(y' - y) \Delta_{\mu\nu}(z - z') \\
 & \times \left[ 1 - \frac{1}{2} e^2 a^2 \sum_{w_1 = x'}^{y'} \sum_{w_2 = x'}^{y'} \Delta_{\mu\mu}(w_1 - w_2) + \dots \right. \\
 & + \frac{(-1)^n}{(2n)!} (2n-1)(2n-3)\dots 1 (ea)^{2n} \sum_{w_1, \dots, w_{2n} = x'}^{y'} \Delta_{\mu\mu}(w_1 - w_2) \dots \\
 & \left. \Delta_{\mu\mu}(w_{2n-1} - w_{2n}) + \dots \right] , \tag{2.27}
 \end{aligned}$$

where the combinatorial factor  $(2n-1)(2n-3)\dots 1$  is the number of ways of pairing the points  $w_1, \dots, w_{2n}$  in the photon propagators. The sum in brackets exponentiates, giving

$$\begin{aligned}
 & \exp \left[ -\frac{1}{2} e^2 a^2 \sum_{w_1, w_2 = x'}^{y'} \Delta_{\mu\mu}(w_1 - w_2) \right] \\
 & = \exp \left[ -\frac{1}{2} e^2 a^2 \sum_{w_1, w_2 = x'}^{y'} \int_{-\Lambda}^{\Lambda} \frac{d^4 k}{(2\pi)^4} e^{ik \cdot (w_1 - w_2)} \Delta_{\mu\mu}(k) \right] \\
 & = \exp \left[ -\frac{1}{2} e^2 \int_{-\Lambda}^{\Lambda} \frac{d^4 k}{(2\pi)^4} \left| \frac{e^{ik \cdot x'} - e^{ik \cdot y'}}{S_\mu(k)} \right|^2 \Delta_{\mu\mu}(k) \right] . \tag{2.28}
 \end{aligned}$$

A similar calculation applies to the multiphoton vertex functions. The inclusion of these photon tadpole contributions to the vertex functions thus generates effective Feynman vertices which differ from the naive

ones of Fig. 4 only in the replacement

$$\begin{aligned} D_\mu(x-y) \rightarrow \tilde{D}_\mu(x-y) &\equiv D_\mu(x-y) \exp -\frac{1}{2} e^2 \int_{-\Lambda}^{\Lambda} \frac{d^4 k}{(2\pi)^4} \left| \frac{e^{ik \cdot x} - e^{ik \cdot y}}{S_\mu(k)} \right|^2 \Delta_{\mu\mu}(k) \\ &= D_\mu(x-y) \exp -\frac{1}{2} e^2 \int_{-\Lambda}^{\Lambda} \frac{d^4 k}{(2\pi)^4} a^2 \frac{\sin^2 \frac{1}{2} k_\mu (x-y)}{\sin^2 \frac{1}{2} k_\mu a} \Delta_{\mu\mu}(k). \quad (2.29) \end{aligned}$$

At issue is the large-distance behavior of  $\tilde{D}_\mu(x)$ . Since<sup>22</sup>

$$\frac{\sin^2 \frac{1}{2} nx}{n \sin^2 \frac{1}{2} x} \xrightarrow{n \rightarrow \infty} 2\pi \delta_{\text{per}}(x),$$

one has

$$\tilde{D}_\mu(x) \xrightarrow{x_\mu \rightarrow \infty} D_\mu(x) \exp -\pi e^2 \int_{-\Lambda}^{\Lambda} \frac{d^4 k}{(2\pi)^4} \Delta_{\mu\mu}(k) \delta(k_\mu) x_\mu, \quad (2.30)$$

and  $\tilde{D}_\mu(x)$  falls off exponentially fast. It follows that the Fourier transform  $\tilde{D}_\mu(p)$  and all its derivatives are continuous, and that there are no infrared singularities in any of the modified vertices. Although  $\tilde{D}_\mu(p)$  as a function of  $p_\mu$  has unit slope at  $p_\mu = 0$ , there is no reason for  $\tilde{D}_\mu(p)$  to share this property. This means that ultimately a finite renormalization will be required to express the theory in terms of a charge defined by the static limit of the electron-photon vertex rather than the parameter  $e$ . This is discussed more fully below. Figure 6 shows the expected behavior of  $\tilde{D}_\mu(p)$ .

In general, the summation of a selected class of diagrams is not a gauge-invariant procedure. This is reflected in the explicit appearance of the photon propagator in Eq. (2.29).  $\tilde{D}_\mu(x-y)$  is thus a gauge-dependent

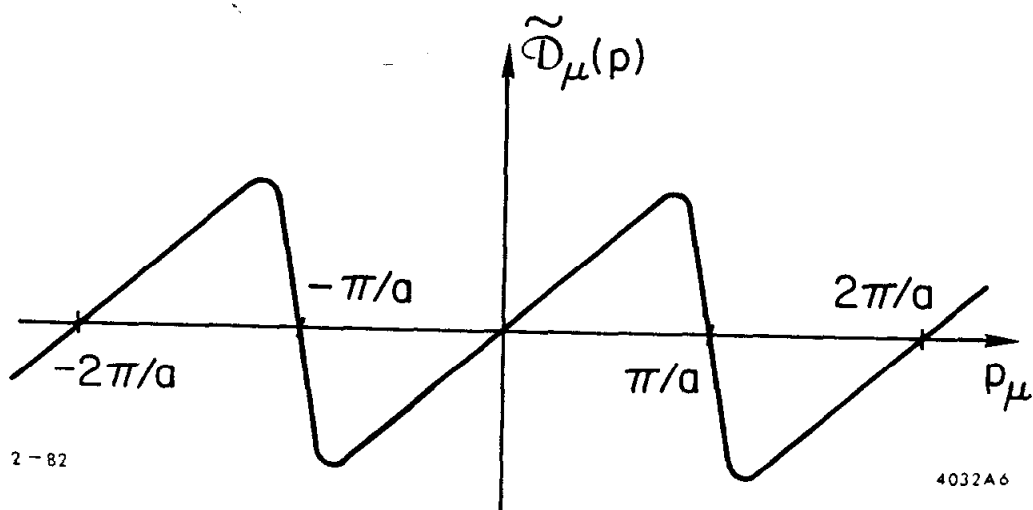


Fig. 6. Qualitative behavior of the function  $\tilde{D}_\mu(p)$  appearing in the effective Feynman rules.

function. It will be shown, however, that the S-matrix has a gauge-invariant continuum limit order by order in the modified perturbation expansion.

Summing the diagrams of Fig. 7 effects the replacement  $D_\mu(x-y) \rightarrow \mathcal{D}_\mu(x-y)$  in the fermion propagator, resulting in a doubled spectrum according to the analysis in Sect. 2. Since we wish to develop a perturbation expansion about the free field theory with undoubled fermion spectrum, this replacement must be undone by the addition of a counterterm

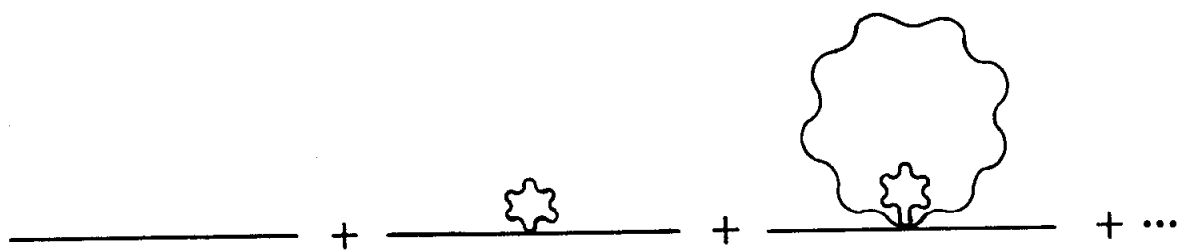
$$\sum_{x,y,\mu} \bar{\psi}(x) \gamma_\mu \frac{1}{i} [D_\mu(x-y) - \mathcal{D}_\mu(x-y)] \psi(y) , \quad (2.31)$$

again in the fixed, physical, quantization gauge. Of course this amounts to an assumption that the interacting theory (2.20) has the same qualitative spectrum as the noninteracting  $e=0$  theory. The validity of this assumption is discussed further in Sect. 8.

The resummation of perturbation theory discussed above is most clearly understood in the Hamiltonian formulation of the theory in the physical Coulomb gauge.<sup>23</sup> The Hamiltonian (now on a three-dimensional lattice) is

$$\begin{aligned} H = & a^3 \sum_{\vec{x}} \left[ \frac{1}{2} E_T^2(\vec{x}) + \frac{1}{2} B^2(\vec{x}) + m \bar{\psi}(\vec{x}) \psi(\vec{x}) \right] \\ & + a^6 \sum_{\vec{x}, \vec{y}} \frac{1}{2} e^2 \phi(\vec{x}-\vec{y}) \psi^\dagger(\vec{x}) \psi(\vec{x}) \psi^\dagger(\vec{y}) \psi(\vec{y}) \\ & + a^6 \sum_{\vec{x}, \vec{y}, j} \bar{\psi}(\vec{x}) \gamma_j \frac{1}{i} D_j(\vec{x}-\vec{y}) \psi(\vec{y}) \exp iea \sum_{\substack{\vec{z} \\ z=\vec{x}}} \vec{A}_j^T(\vec{z}) , \\ \vec{\nabla}_{-} \cdot \vec{\nabla}_{+} \phi(\vec{x}) = & -\delta_{\vec{x}, 0} , \quad \tilde{\phi}(\vec{k}) = 1/S^2(\vec{k}) , \quad \vec{\nabla}_{-} \cdot \vec{A}^T = 0 . \quad (2.32) \end{aligned}$$

The summation of photon tadpole diagrams simply corresponds to normal-



2 - 81

4032A7

Fig. 7. A class of diagrams whose summation would double the fermion spectrum.

ordering the exponential in Eq. (2.32). Including the counterterm analogous to (2.31) the Hamiltonian becomes:

$$\begin{aligned}
 H = & a^3 \sum_{\vec{x}} \left[ \frac{1}{2} E_T^2(\vec{x}) + \frac{1}{2} B^2(\vec{x}) + m \bar{\psi}(\vec{x}) \psi(\vec{x}) \right] \\
 & + a^6 \sum_{\substack{\vec{x}, \vec{y} \\ \vec{x}, \vec{y}}} \frac{1}{2} e^2 \bar{\psi}(\vec{x}-\vec{y}) \psi^\dagger(\vec{x}) \psi(\vec{x}) \psi^\dagger(\vec{y}) \psi(\vec{y}) \\
 & + a^6 \sum_{\substack{\vec{x}, \vec{y}, j \\ \vec{x}, \vec{y}}} \left[ \bar{\psi}(\vec{x}) \gamma_j \frac{1}{i} D_j(\vec{x}-\vec{y}) \psi(\vec{y}) \right. \\
 & \quad \left. + \bar{\psi}(\vec{x}) \gamma_j \frac{1}{i} \mathcal{D}_j(\vec{x}-\vec{y}) \psi(\vec{y}) : \exp iea \sum_{\substack{\vec{z} \\ \vec{z}=\vec{x}}} \vec{A}_j^T(\vec{z}) - 1 : \right] , \\
 \mathcal{D}_j(\vec{x}-\vec{y}) = & D_j(\vec{x}-\vec{y}) \exp -\frac{1}{2} e^2 \int_{-\Lambda}^{\Lambda} \frac{d^3 k}{(2\pi)^3 2|S(\vec{k})|} \left| \frac{e^{ik \cdot \vec{x}} - e^{ik \cdot \vec{y}}}{S_j(\vec{k})} \right|^2 \\
 & \times \left[ 1 - \frac{S_j^2(\vec{k})}{S^2(\vec{k})} \right] . \tag{2.33}
 \end{aligned}$$

$H$  is gauge invariant because the fields appearing in it are, but Ward identities which state that  $S_\mu(k)$  terms in the photon propagator do not contribute to physical quantities do not hold. This may be understood as follows. In a more general gauge, related to the Coulomb gauge by a time-independent gauge transformation, a structure  $\bar{\psi}(\vec{x}) D_j(\vec{x}-\vec{y}) \psi(\vec{y})$  in Eq. (2.33) appears as  $\bar{\psi}(\vec{x}) D_j(\vec{x}-\vec{y}) \psi(\vec{y}) \exp iea \sum_{\substack{\vec{z} \\ \vec{z}=\vec{x}}} \vec{A}_j^L(\vec{z})$ . Thus  $\vec{A}_L$  is coupled to the conserved current

$$j_i(\vec{z}) = -ea^4 \sum_{\substack{\vec{x}, \vec{y} \\ x_i \leq z_i < y_i \\ x_j = z_j, j \neq i}} \left[ \bar{\psi}(\vec{x}) \gamma_i D_i(\vec{x}-\vec{y}) \psi(\vec{y}) + \bar{\psi}(\vec{x}) \gamma_i D_i(\vec{x}-\vec{y}) \psi(\vec{y}) : \exp ie a \sum_{\substack{\vec{y} \\ \vec{z}=\vec{x}}} A_i^T(\vec{z}) - 1 : \right] + h.c.$$

(in Coulomb gauge) as required by gauge invariance, while  $\vec{A}_T$  couples to the nonconserved

$$j'_i(\vec{z}) = -ea^4 \sum_{\substack{\vec{x}, \vec{y} \\ x_i \leq z_i < y_i \\ x_j = z_j, j \neq i}} \bar{\psi}(\vec{x}) \gamma_i D_i(\vec{x}-\vec{y}) \psi(\vec{y}) : \exp ie a \sum_{\substack{\vec{y} \\ \vec{z}=\vec{x}}} A_i^T(\vec{z}) : + h.c.$$

[ $j_0(\vec{z}) = -e\bar{\psi}(\vec{z})\psi(\vec{z})$  in either case.] In continuum QED  $\vec{A}_L$  and  $\vec{A}_T$  enter the action only through the local field  $\vec{A}$ , so both couple to the same current.

The effective vertices possess all the properties required for a proof of renormalizability as in Sect. 3. The functions involved are  $C^\infty$  and possess the required Taylor expansions. Furthermore, naive power counting now works properly. A diagram with  $F$  external fermions and  $B$  external photons is  $1/S_\alpha(k_1)S_\beta(k_2)\dots S_\mu(k_B)$  times an integral with superficial  $D = 4 - \frac{3}{2}F$ . But the absence of infrared singularities requires that the Taylor expansions of the vertex functions in the integrand begin with the term of order  $k_{1\alpha}k_{2\beta}\dots k_{B\mu}$ , reducing  $D$  to  $4 - \frac{3}{2}F - B$ . Similarly the numerator of an  $n$ -photon vertex must go as  $k_{1\mu}k_{2\mu}\dots k_{n\mu}$  when the  $k$ 's are small, and this must be accompanied by a factor  $a^{n-1}$  on

dimensional grounds. Hence multiphoton vertices are accompanied by factors of  $a$  as required in the arguments of Sect. 3. However, one obstacle remains to the application of Sharatchandra's arguments to the SLAC lattice gauge theory: the presence in the fermion propagator of the discontinuous function  $\tilde{D}_\mu(p)$ . This problem is addressed next.

## 6. Proof of Renormalizability

So far it has been established that in the modified perturbation expansion for the SLAC lattice gauge theory, the vertices are infinitely differentiable functions of momenta and naive power counting correctly gives the degree of divergence of Feynman integrals. In general, diagrams will actually have their full superficial degrees of divergence since the Ward identities which normally reduce  $D$  do not hold order by order in this expansion. However, Feynman integrands still do not possess Taylor expansions because the fermion propagators contain the discontinuous function  $\tilde{D}_\mu(p)$ . This difficulty may exist in any lattice field theory in which there is (a) periodic momentum conservation, and (b) fermions with undoubled spectrum. In this section I explain how to carry out a subtractive renormalization program for such theories. The next section considers the form of the counterterms required to implement the subtractions.

Consider an arbitrary Feynman diagram. The corresponding amplitude takes the form

$$A(k) = \left[ \prod_{\text{lines}} \int_{-\Lambda}^{\Lambda} \frac{d^4 \ell}{(2\pi)^4} \right] I(\ell, k) \left[ \prod_{\text{vertices}} (2\pi)^4 \delta_{\text{per}}^4 (\sum \text{momenta}) \right] \quad (2.34)$$

where  $k$  denotes the external momenta and  $I$  is written using the Feynman rules. At this point  $I(\ell, k)$  possesses an expansion in powers of  $k$  because for  $|\ell_\mu| < \Lambda$ ,  $\tilde{D}_\mu(\ell) = \ell_\mu$  which is perfectly continuous.  $A(k)$  does not have an expansion, though, because the periodic  $\delta$ -functions contain additional dependence on  $k$ .

Choose now a subset  $\{q\}$  of the momenta  $\{\ell\}$  to act as independent loop momenta. According to Appendix A the trivial integrations over  $\{\ell\} - \{q\}$  may be done provided  $I(\ell, k)$  is a periodic function; provided, in other words, the fermion propagators are written in terms of the discontinuous  $\tilde{D}_\mu(\ell)$  instead of simply  $\ell_\mu$ . The integrations then result in a discontinuous integrand  $I(q, k)$ . However, since  $\tilde{D}_\mu(\ell)$  is piecewise continuous, the domain of integration can be divided into subregions with  $I(q, k)$  continuous in each.

An efficient way to do this is to return to Eq. (2.34) and to substitute for the periodic  $\delta$ -functions

$$\delta_{\text{per}}^4(p) = \prod_\mu \sum_{n_\mu=-\infty}^{\infty} \delta(p_\mu + 2n_\mu \Lambda) . \quad (2.35)$$

Since only finitely many lines enter each vertex of the graph, and all lines are restricted by  $|\ell_\mu| < \Lambda$ , only finitely many terms in the sum can actually contribute. Doing trivial integrations then yields

$$A(k) = \sum_j \left[ \prod_{\{q\}} \int_{-\Lambda}^{\Lambda} \frac{d^4 q}{(2\pi)^4} \right] I_j(q, k) \left\{ \prod_{\text{lines}, \mu} \theta[\Lambda - |\ell_j^\mu(q, k)|] \right\} , \quad (2.36)$$

i.e., a sum of integrals indexed by  $j$ . The integrands  $I_j(q, k)$  are

generally all different, as are the functions  $\ell_j^\mu(q, k)$  which give the  $\mu$ th component of the momentum in line  $\ell$  in terms of  $q$  and  $k$ . In writing  $I_j(q, k)$ ,  $\tilde{D}_\mu(\ell)$  is to be replaced by  $\ell_\mu$  as is permitted by the  $\theta$ -functions. Each integrand  $I_j(q, k)$  thus has a Taylor expansion in the variables  $k$ . Let  $j = 0$  label the integral with no umklapps -  $n_\mu = 0$  in Eq. (2.35) for every periodic  $\delta$ -function in Eq. (2.34). The terms  $j \neq 0$  are diagrams in which momentum components in multiples of  $2\Lambda$  enter vertices "from nowhere" in all possible ways.

Consider one particular integral labelled by  $j$ . The integral will be made finite in the limit  $a \rightarrow 0$  by replacing  $I_j(q, k)$  by a renormalized integrand  $R_j(q, k)$  via the following prescription. As in ordinary BPH renormalization, lay down forests of nonoverlapping boxes on the diagram, each box surrounding a renormalization part - a 2-, 3-, or 4-point function. Make the usual subtractions of the first  $D+1$  terms of the Taylor expansions of the boxed subgraphs, with the following exception. If a box contains an umklapp process (if the external momenta of the boxed subgraph do not sum to zero, but to a multiple of  $2\Lambda$ , which can happen only for 3- and 4-point functions) then no subtractions need be made for that box. The reason for this exception is the following. According to the usual criterion a Feynman integral converges if all subintegrations have  $D < 0$ , a subintegration being an integral over a subset of the  $q$ 's with all other momenta held fixed as  $a \rightarrow 0$ . The integration over the internal momenta of a boxed umklapp process does not count as a subintegration because the external momenta cannot be held fixed when  $a \rightarrow 0$ . Renormalized Green's functions are not required to be finite when their external momenta approach infinity!

After the subtractions are made, the  $j$ th integral is guaranteed to be finite when  $a \rightarrow 0$ , even ignoring the  $\theta$ -function constraints in Eq. (2.36). The  $\theta$ -functions impose additional restrictions on the region of integration, so including them does not make a formerly finite integral diverge. As in Sect. 3, if the diagram under consideration includes a multiphoton vertex then the explicit factors of  $a$  in such a vertex cause the renormalized diagram to vanish as  $a \rightarrow 0$ . For a normal diagram, the integrand  $I_0(q, k)$  of the no-umklapp term in Eq. (2.36) becomes the continuum Feynman integrand for the same diagram when  $a \rightarrow 0$  (provided the continuum parameter  $e$  is identified as the coefficient of  $\gamma_\mu$  in the zero-momentum limit of the lattice one-photon vertex). The  $\theta$ -functions make a negligible contribution in the limit  $a \rightarrow 0$ , so the renormalized  $j = 0$  integral at  $a = 0$  equals the corresponding renormalized continuum integral. Finally, consider the  $j \neq 0$  contributions to a normal diagram. The integral of  $R_j(q, k)$  is finite. Now consider the effect of the  $\theta$ -functions. There is a vertex of the graph at which some components of the three entering momenta sum to  $2n\Lambda$ ,  $n \neq 0$ . Since no momentum exceeds  $\Lambda$  ( $\theta$ -functions!), at least two momenta are large on the scale  $\Lambda$  (and incidentally  $n = \pm 1$ ). These large momenta may be traced through the graph; eventually a large momentum must flow through a line carrying one of the integration momenta  $q$ . But if one has an integral from  $-\Lambda$  to  $+\Lambda$ , finite when  $\Lambda \rightarrow \infty$ , and adds a  $\theta$ -function requiring the integration variable to be of order  $\Lambda$ , the result vanishes for  $\Lambda \rightarrow \infty$ . Hence all  $j \neq 0$  terms vanish for  $a \rightarrow 0$ .

It has now been shown that in the modified perturbation expansion for the SLAC lattice gauge theory the subtracted Feynman integrals yield

the usual results of continuum QED order by order when  $a \rightarrow 0$ . It follows trivially that the  $a \rightarrow 0$  limit of the S-matrix is in fact gauge-invariant despite the gauge dependence of the lattice expansion due to the summation of photon tadpoles. It is clear that the subtractions described above can be implemented by counterterms in the action, but the structure of these counterterms is not as simple as in the case of Wilson's QED. This is discussed next.

## 7. Structure of Counterterms

### A. Examples

This section presents some examples of the renormalization program just discussed for lattice theories with undoubled fermion spectra, with the purpose of exhibiting the types of counterterms to be expected. Since the Ward identities are not maintained order by order in the modified perturbation expansion for lattice QED, there is no formal difference between the renormalization program for lattice theories with and without local gauge invariance. Therefore, to save indices, the examples here are taken from a theory of SLAC fermions interacting with scalar mesons via a  $g\bar{\psi}(x)\psi(x)\phi(x)$  coupling.

### 1. Scalar Self-Energy

The one-loop scalar self-energy (Fig. 8) is given by

$$\begin{aligned}
 \Pi &= g^2 \text{Tr} \int_{-\Lambda}^{\Lambda} d^4 q d^4 \ell S_F(q) S_F(\ell) \delta_{\text{per}}^4(p + \ell - q) \delta_{\text{per}}^4(q - \ell - p') \\
 &= g^2 \text{Tr} \sum_{n,m} \int_{-\Lambda}^{\Lambda} d^4 q d^4 \ell S_F(q) S_F(\ell) \delta^4(p + \ell - q + 2n\Lambda) \delta^4(q - \ell - p' + 2m\Lambda) \\
 &= g^2 \text{Tr} \sum_{n,m} \int_{-\Lambda}^{\Lambda} d^4 \ell S_F(p + \ell + 2n\Lambda) S_F(\ell) \prod_{\mu} \theta(\Lambda - |p_{\mu} + \ell_{\mu} + 2n_{\mu}\Lambda|) \\
 &\quad \times \delta^4[p - p' + 2(m + n)\Lambda] , \tag{2.37}
 \end{aligned}$$

where  $m$  and  $n$  are four-vectors with integer components. The fact that all momentum components are bounded in magnitude by  $\Lambda$  imposes the restrictions  $m = -n$  and  $n_{\mu} = 0, \pm 1$ . Extracting the overall momentum conserving  $\delta$ -function gives

$$\Pi(p) = g^2 \text{Tr} \sum_{n_{\mu}=0,\pm 1} \int_{-\Lambda}^{\Lambda} d^4 \ell S_F(p + \ell + 2n\Lambda) S_F(\ell) \prod_{\mu} \theta(\Lambda - |p_{\mu} + \ell_{\mu} + 2n_{\mu}\Lambda|) , \tag{2.38}$$

where  $S_F(q)$  now means  $(\gamma \cdot q + m)^{-1}$ ,  $\tilde{D}_{\mu}(q)$  no longer appearing.

Consider first the no-umklapp ( $n = 0$ ) contribution:

$$\begin{aligned}
 &g^2 \prod_{\mu} \left[ \int_{\max(-\Lambda, -\Lambda - p_{\mu})}^{\min(\Lambda, \Lambda - p_{\mu})} d\ell_{\mu} \right] \text{Tr } S_F(p + \ell) S_F(\ell) \\
 &= g^2 \prod_{\mu} \left[ \theta(p_{\mu}) \int_{-\Lambda}^{\Lambda - p_{\mu}} d\ell_{\mu} + \theta(-p_{\mu}) \int_{-\Lambda - p_{\mu}}^{\Lambda} d\ell_{\mu} \right] \text{Tr } S_F(p + \ell) S_F(\ell) . \tag{2.39}
 \end{aligned}$$

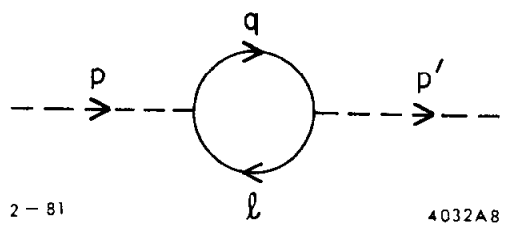


Fig. 8. The scalar self-energy in the lattice  $\bar{\psi}\psi\phi$  theory.

It is clear that apart from the  $\theta$ -functions the integrals have expansions in powers of  $p_\mu$  of which the terms up to  $\mathcal{O}(p^2)$  may be divergent, while subsequent terms must give the continuum results when  $a \rightarrow 0$  with  $p$  fixed. The discontinuous behavior of the integrand has been isolated in the  $\theta$ -functions which appear because one must know the sign of  $p_\mu$  to tell whether  $p_\mu + \ell_\mu > \Lambda$  or  $p_\mu + \ell_\mu < -\Lambda$  is possible for  $|\ell_\mu| < \Lambda$ . The required counterterms will have the form

$$\theta(\pm p_0) \theta(\pm p_1) \theta(\pm p_2) \theta(\pm p_3) \left( A + \sum_\mu B_\mu p_\mu + \sum_{\mu, \nu} C_{\mu\nu} p_\mu p_\nu \right) \tilde{\phi}(p) \tilde{\phi}(-p), \quad (2.40)$$

with  $A, B_\mu, C_{\mu\nu}$  divergent constants. Indeed, one can say more: since  $\Pi(p)$  has definite symmetry under  $p \rightarrow -p$ ,  $\theta(p_\mu)$  must appear in the even and odd combinations  $\theta(p_\mu) + \theta(-p_\mu) = 1$  and  $\theta(p_\mu) - \theta(-p_\mu) = \text{sign } p_\mu$ , giving counterterms

$$\left( A + \sum_\mu B_\mu |p_\mu| + \sum_{\mu\nu} C_{\mu\nu} p_\mu p_\nu + \sum_{\mu\nu} D_{\mu\nu} |p_\mu| |p_\nu| \right) \tilde{\phi}(p) \tilde{\phi}(-p) , \quad (2.41)$$

which may be further restricted by the lattice cubic symmetries. These counterterms will be nonlocal when expressed in position space, but this is to be expected since the bare action was nonlocal as well. It would be wrong to conclude from this nonlocality that infinitely many counterterms are required (counting separately the nearest-neighbor, next-nearest-neighbor, etc. terms) since in momentum space there are clearly finitely many divergent constants.

Next, examine a typical contribution to  $\Pi(p)$  containing an

umklapp ( $n_0 = 1$ ,  $\vec{n} = 0$ ):

$$g^2 \theta(-p_o) \int_{-\Lambda}^{-\Lambda-p_o} d\ell_o \left[ \prod_i \int_{\max(-\Lambda, -\Lambda-p_i)}^{\min(\Lambda, \Lambda-p_i)} d\ell_i \right] \text{Tr } S_F(p_o + \ell_o + 2\Lambda, \vec{p} + \vec{\ell}) S_F(\ell). \quad (2.42)$$

Evidently counterterms of the form (2.40) will suffice to make this finite for  $a \rightarrow 0$ . After the removal of the terms up to  $\mathcal{O}(p^2)$  in the expansion of the above integral, the remaining terms vanish because the umklapp restricts the  $\ell_0$  integration to a small region near  $-\Lambda$ , as expected from the arguments of Sec. VI. All umklapp contributions vanish similarly and when  $a \rightarrow 0$  the continuum result is recovered from the no-umklapp term.

## 2. Vertex Function

The one-loop vertex correction (Fig. 9) reads:

$$\begin{aligned} \Gamma &= g^3 \bar{v}(q) \int_{-\Lambda}^{\Lambda} d^4 k d^4 k' d^4 \ell S_F(k) S_F(k') \Delta(\ell) \delta_{per}^4(p+k'-k) \\ &\times \delta_{per}^4(k-\ell-q) \delta_{per}^4(\ell-k'-q') v(-q'), \end{aligned} \quad (2.43)$$

where  $\Delta(\ell) = 1/S^2(\ell)$ . This becomes

$$\begin{aligned} \Gamma &= g^3 \bar{v}(q) \sum_{n,n',n''} \int_{-\Lambda}^{\Lambda} d^4 k d^4 k' d^4 \ell S_F(k) S_F(k') \Delta(\ell) \\ &\times \delta^4(p+k'-k+2n\Lambda) \delta^4(k-\ell-q+2n'\Lambda) \delta^4(\ell-k'-q'+2n''\Lambda) v(-q') \\ &= g^3 \bar{v}(q) \sum_{n,n',n''} \int_{-\Lambda}^{\Lambda} d^4 \ell S_F(\ell+q-2n'\Lambda) S_F(\ell-q'+2n''\Lambda) \Delta(\ell) \\ &\times \prod_{\mu} \theta(\Lambda - |\ell_{\mu} + q_{\mu} - 2n'\Lambda|) \theta(\Lambda - |\ell_{\mu} - q'_{\mu} + 2n''\Lambda|) \delta^4[p-q-q'+2(n+n'+n'')\Lambda] v(-q'). \end{aligned} \quad (2.44)$$

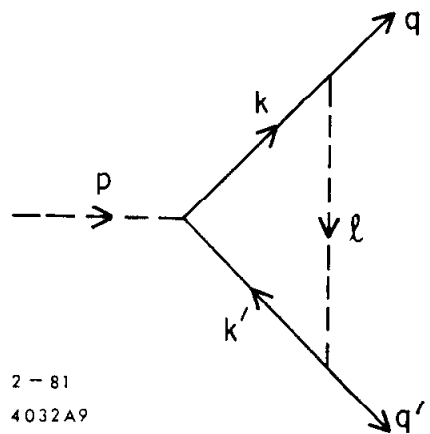


Fig. 9. Vertex correction in  $\bar{\psi}\psi\phi$  theory.

According to Sect. 6 subtractions are only required in the case of overall momentum conservation  $n + n' + n'' = 0$ . Consider the no-umklapp term  $n = n' = n'' = 0$ :

$$g^3 \bar{v}(q) \left[ \prod_{\mu} \int_{\max(-\Lambda, -\Lambda+q_{\mu}', -\Lambda-q_{\mu})}^{\min(\Lambda, \Lambda+q_{\mu}', \Lambda-q_{\mu})} d\ell_{\mu} \right] S_F(\ell+q) S_F(\ell-q') \Delta(\ell) \delta^4(p-q-q') v(-q'). \quad (2.45)$$

The conditions on the range of integration can be expressed using  $\theta$ -functions, but this is not necessary: since the integral is only logarithmically divergent, the limits of integration can be taken as  $-\Lambda$  to  $\Lambda$  with vanishing error as  $\Lambda \rightarrow \infty$ . The integrand requires only a subtraction of its value at  $q = q' = 0$ , which can evidently be effected by a counterterm of the same form as in the cutoff continuum theory.

For a typical umklapp term,  $n_0 = 0$ ,  $n'_0 = -1$ ,  $n''_0 = +1$ ,  $\vec{n} = \vec{n}' = \vec{n}'' = 0$ ,

$$g^3 \bar{v}(q) \theta(q'_0) \theta(-q'_0) \int_{-\Lambda}^{\min(-\Lambda-q'_0, -\Lambda+q'_0)} d\ell_0 \left[ \prod_i \int_{\max(-\Lambda, -\Lambda+q'_i, -\Lambda-q'_i)}^{\min(\Lambda, \Lambda+q'_i, \Lambda-q'_i)} d\ell_i \right] \times S_F(\ell_0 + q'_0 + 2\Lambda, \vec{\ell} + \vec{q}) S_F(\ell_0 - q'_0 + 2\Lambda, \vec{\ell} - \vec{q}) \Delta(\ell) \delta^4(p - q - q') v(-q'), \quad (2.46)$$

the situation is even better. Since the integrand has  $D = 0$ , the limited range of the  $\ell_0$  integral causes it to vanish as  $a \rightarrow 0$  and no counterterm is needed.

### 3. Two-Loop Scalar Self-Energy

This is included as an example of the vanishing of umklapp contributions beyond one-loop order. The only diagram which is not simply an

insertion of the one-loop fermion propagator gives (Fig. 10):

$$\Pi^{(4)} = g^4 (2\pi)^{-4} \text{Tr} \int_{-\Lambda}^{\Lambda} d^4 k d^4 k' d^4 \ell d^4 \ell' d^4 q S_F(k) S_F(k') \quad (2.47)$$

$$\times S_F(\ell') S_F(\ell) \Delta(q) \delta_{\text{per}}^4(p + k' - k) \delta_{\text{per}}^4(k - \ell - q) \delta_{\text{per}}^4(\ell - \ell' - p') \delta_{\text{per}}^4(\ell' + q - k') .$$

$$\Pi^{(4)}(p) = g^4 \text{Tr} \sum_{m, m', n} \int_{-\Lambda}^{\Lambda} d^4 k d^4 \ell S_F(k) S_F(k - p - 2m\Lambda) S_F(\ell - p + 2n\Lambda) S_F(\ell) \quad (2.48)$$

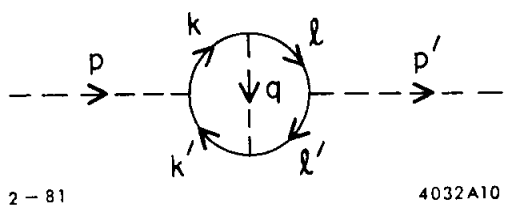
$$\times \Delta(k - \ell + 2m'\Lambda) \prod_{\mu} \theta(\Lambda - |k_{\mu} - p_{\mu} - 2m_{\mu}\Lambda|) \theta(\Lambda - |\ell_{\mu} - p_{\mu} + 2n_{\mu}\Lambda|) \theta(\Lambda - |k_{\mu} - \ell_{\mu} + 2m'_{\mu}\Lambda|) .$$

In addition to the overall  $D = 2$  integration there are various subintegrals having  $D = 0$ . The overlapping divergences in the no-umklapp term are handled exactly as in the continuum theory: the overall subtractions plus the inclusion of the vertex counterterms discussed above yield a finite result. Consider now the umklapp contribution

$$m = n = 0, m'_0 = -1, \vec{m}' = 0:$$

$$g^4 \left[ \prod_{\mu} \int_{\max(-\Lambda, -\Lambda + p_{\mu})}^{\min(\Lambda, \Lambda + p_{\mu})} dk_{\mu} d\ell_{\mu} \right] \text{Tr} S_F(k) S_F(k - p) S_F(\ell - p) S_F(\ell) \Delta(k_0 - \ell_0 - 2\Lambda, \vec{k} - \vec{\ell}) \times \theta(k_0 - \ell_0 - \Lambda) \prod_i \theta(\Lambda - |k_i - \ell_i|) \quad (2.49)$$

Here the explicitly indicated range of integration is not particularly small. However, there is the  $\theta$ -function restriction  $k_0 - \ell_0 > \Lambda$ . The subintegral over  $k$  at fixed  $\ell$  is therefore restricted to a small region near  $k_0 = \Lambda$ , which causes it to vanish as  $\Lambda \rightarrow \infty$  since it had  $D = 0$ .



2-81

4032A10

Fig. 10. A contribution to the two-loop scalar self-energy in  $\bar{\psi}\psi\phi$  theory.

Similarly for the  $\ell$ -subintegral at fixed  $k$ . Finally, a subintegral over  $k + \ell$  at fixed  $k - \ell$  vanishes as  $\Lambda \rightarrow \infty$  since a fixed  $k - \ell$  will fail to satisfy  $k_0 - \ell_0 > \Lambda$ . Then, after counterterms of the form (2.40) have removed the terms up to  $\mathcal{O}(p^2)$  in the integrand's Taylor expansion the result must vanish since  $k_0 - \ell_0 > \Lambda$  requires the integration variables to be large.

### B. Summary

From these examples it appears that in lattice theories with undoubled fermions one must expect momentum-space counterterms which are polynomials in the momenta, plus sign  $p_\mu$  functions times such polynomials. The dependence on sign  $p_\mu$  reflects the fact that although the lattice Green's functions do not have Taylor expansions about  $p_\mu = 0$ , they do possess "one-sided" Taylor expansions valid when  $p_\mu > 0$  or  $p_\mu < 0$ . The counterterms thus serve to impose appropriate normalization conditions on the left and right limits and derivatives of the Green's functions at  $p_\mu = 0$ . Only finitely many types of counterterms arise although they are nonlocal in position space. Some of the counterterms which are simple polynomials and only logarithmically divergent can be generated by rescaling fields and parameters, as in Wilson's QED, but others must be added by hand.

For SLAC lattice QED, Eq. (2.20), the prescription is as follows. First rescale fields and parameters in Eq. (2.20), writing it as a renormalized action plus counterterms. Next sum the photon tadpole diagrams to produce an infrared finite set of Feynman rules. Third, execute the renormalization program of this and the preceding sections. This both

determines the logarithmically divergent multiplicative renormalization constants and requires additional counterterms. In particular, photon mass and photon-photon scattering counterterms will be needed due to the absence of Ward identities. Finally, to make contact with continuum QED a finite charge renormalization is needed to express the theory in terms of a charge defined by the static limit of the effective one-photon vertex:  $e_{\text{physical}} = \tilde{\mathcal{D}}_\mu'(0)e$ . This prescription is straightforward in the covariant gauge of Eq. (2.20) in which  $\tilde{\mathcal{D}}_\mu'(0)$  is independent of  $\mu$ . However, the normal-ordering procedure for removing infrared problems violates unitarity unless carried out in a physical gauge, and physical gauges are never covariant. Then one must admit the possibility of non-covariant counterterms; in particular the bare coupling constant  $e_\mu$  associated with  $A_\mu$  can depend on  $\mu$ . (For example, in the Hamiltonian Coulomb gauge formulation the parameter  $e$  in the instantaneous Coulomb interaction must be allowed to renormalize independently of the coupling to the transverse photons.) After the rescalings

$$\psi \rightarrow Z_2^{\frac{1}{2}} \psi_R , \quad A_\mu \rightarrow Z_{3\mu}^{\frac{1}{2}} A_{R\mu} , \quad e_\mu \rightarrow e_{R\mu} Z_{1\mu} / Z_2 Z_{3\mu}^{\frac{1}{2}} , \quad (2.50)$$

and the summation of photon tadpole diagrams, it is the parameter  $e_{R\mu}$  which appears in the definition of  $\mathcal{D}_\mu(x-y)$ , Eq. (2.29). The final finite charge renormalization is then

$$e_{\text{physical}} = \tilde{\mathcal{D}}_\mu'(0) e_{R\mu} , \quad (2.51)$$

which implicitly determines  $e_{R\mu}$  in terms of the measured  $e_{\text{physical}}$ .

### C. The Axial Current

The fate of the axial current and the axial-vector Ward identity, Eq. (2.23), in the present treatment are easy to see. The axial current couples to vertices exactly like the photon, but with an extra factor  $\gamma_5$ . In naive perturbation theory its matrix elements, like most Green's functions, are infrared divergent. After the summation of photon tadpole diagrams, matrix elements of the normal-ordered current

$$j_\mu^5(z) = a^5 \sum_{x,y} \bar{\psi}(x) \gamma_\mu \gamma_5 \mathcal{D}_\mu(x-y) \psi(y) : \exp iea \sum_{w=x}^y A_\mu(w) : + h.c.$$

$x_\mu \leq z_\mu < y_\mu$   
 $z_v = x_\mu, v \neq \mu$

are guaranteed to be infrared-finite. However, in the resummed perturbation expansion the vector Ward identities are not available to reduce the degrees of divergence of graphs. This means that the VVA triangle diagrams involving this axial current (or any other) will be at least logarithmically divergent. As yet no renormalization prescription has been given for these diagrams. At this point one must decide which Ward identity is to be satisfied in the continuum limit and renormalize accordingly. To obtain a finite continuum limit obeying Lorentz and Bose symmetries and the vector Ward identity, certain counterterms must be added to the current and by the Adler-Bardeen theorem they cannot be chosen such that the axial Ward identity is also satisfied.

The important point to abstract from perturbation theory is that there is no reason to expect a nonlocal operator such as the conserved axial current (2.23) to have a finite continuum limit. In view of the anomaly there is every reason not to.

## 8. Concluding Remarks

### A. Summary

This chapter has considered various formulations of lattice QED with fermions, with particular emphasis on the SLAC lattice gauge theory (2.20). I have shown that if lattice QED is constructed from the free Dirac action by replacing derivatives by difference operators and then coupling to the photon in a locally gauge invariant way, an undoubled fermion spectrum implies that naive perturbation theory breaks down due to infrared divergences. Under the assumption that the full gauge theory continues to have an undoubled spectrum, a resummation of the perturbation series was carried out which removed the infrared problems. A renormalization program, applicable to any lattice fermion theory with undoubled spectrum, was carried out such that ordinary continuum QED was recovered order by order as  $a \rightarrow 0$ . In this scheme the lattice axial current which obeys a non-anomalous Ward identity had no finite continuum limit order by order. In view of the anomaly this must also be true to all orders.

### B. Beyond Perturbation Theory

The results of this chapter are rather formal in that they show what can be done with SLAC lattice QED in perturbation theory and what counterterms are needed to do it. Continuum QED at this time is defined by its renormalized perturbation series, but a lattice theory presumably has a meaning even beyond the region of validity of perturbation theory.

As remarked earlier, perturbation theory cannot predict a qualitative spectrum, but must instead be constructed around a zeroth order approximation which already has the correct qualitative spectrum. It is important to ask whether the perturbation theory constructed in this chapter accurately reflects the exact solution to the theory (2.20). In principle this should be determined by an exact renormalization-group treatment and analysis of the fixed points. The renormalization-group critical surface should determine an action containing the counterterms required in perturbation theory. What can be said in the absence of such information?

There seem to be two possible scenarios based on the Ward identity

$$\sum_{\mu} S_{\mu}(k) \Gamma_{\mu}(p+k, p) = S_F^{-1}(p+k) - S_F^{-1}(p), \quad (2.52)$$

which is an exact property of the theory. If the exact fermion propagator describes an undoubled spectrum then  $S_F^{-1}$  has a discontinuity at some point  $p_0$ . Letting  $p \rightarrow p_0$  and  $k \rightarrow 0$  in Eq. (2.52) shows that  $\Gamma_{\mu}$  must have a singularity there. This in itself is not a disaster since  $p_0$  is normally of order  $1/a$ . A disaster occurs only if this singularity propagates down into the low-momentum (continuum) limit of some Green's function. This happens in naive perturbation theory where loops of high-momentum particles contribute to the low-momentum behavior of, for example,  $\Pi_{\mu\nu}(p)$ . If it happens in general then the theory is sick. If it does not happen, so that singularities are confined to high momenta, then the continuum limit may be as described perturbatively above. The high-momentum singularities would be generated from the sum to all orders of the order by order nonsingular effective theory of Sect. 5.B. The conserved lattice

axial current has no continuum limit due probably to singular contributions to its matrix elements.

If no infrared singularities arise at any momentum, then  $S_F^{-1}$  must be continuous and the fermion spectrum doubles. This happens nonperturbatively since the spectrum is undoubled at  $e = 0$ . This scenario is suggested by the summation of the photon tadpole contributions to  $S_F$  (Fig 7). Summing perturbation theory to all orders would not introduce any singularities but would merely restore gauge invariance, which was lost order by order. The axial current could have a non-anomalous continuum limit, the anomaly being cancelled between the doubled fermion species. It is even possible that both these scenarios could occur, each characterizing a different phase of the lattice theory. The SLAC lattice gauge theory (2.20) could thus have an extremely rich and interesting structure beyond perturbation theory. In my opinion it is extremely important, though difficult, to learn which of these cases occurs. The possibility that the fermion spectrum multiplicity is determined dynamically does not seem to have been previously suggested, and would add a new dimension to our understanding of the realization of chiral symmetry in lattice theories.

## CHAPTER III

### REAL-SPACE RENORMALIZATION GROUP METHODS<sup>24</sup>

#### 1. Introduction

This chapter and the next are concerned with nonperturbative studies of lattice theories with long-range interactions. The method used is the real-space renormalization-group (RG) technique introduced by Drell et al. and subsequently applied to a variety of lattice field theories and spin systems.<sup>3-8</sup> It has been shown to yield accurate results for correlation functions and low-lying energy levels, and to locate phase transitions reliably. Furthermore, calculations using this technique can be systematically improved to provide accuracy limited only by the available computer time.

The goal is to use the RG method to study an antiferromagnetic Heisenberg spin chain with long-range interactions on a one-dimensional lattice at zero temperature:

$$H = \frac{1}{2} \sum_{\substack{i,j=1 \\ i \neq j}}^N (-1)^{i-j+1} \frac{1}{|i-j|^p} \vec{S}(i) \cdot \vec{S}(j) , \quad (3.1)$$

where  $\vec{S}(i)$  denotes a spin-1/2 operator acting at the  $i$ th lattice site. The relation of this model to one-dimensional fermion field theories formulated with the long-range SLAC derivative is discussed in Chapter IV. The model is also of independent interest owing to rigorous results obtained by Dyson<sup>25</sup> and Ruelle<sup>26</sup> for the analogous Ising model  $\vec{S} \rightarrow S_z$ . These results are also summarized in Chapter IV. In this chapter, I introduce the RG method and show that it successfully reveals the known

properties of the nearest-neighbor Heisenberg chain which is the  $p \rightarrow \infty$  limit of Eq. (3.1). Although both two- and three-site blocking techniques are successful for the nearest-neighbor chain, it will emerge that the three-site method is more reliable for studying the long-range model (3.1). That study is taken up in Chapter IV.

This chapter is organized as follows. In Sect. 2 the three-site blocking procedure is described and applied to the anisotropic nearest-neighbor spin chain (Heisenberg-Ising model). This is done to facilitate comparison with the calculation of Sect. 3: it will be useful to have studied the isotropic model of interest as a fixed point (in the RG sense) of a more general model. I find that the three-site calculation correctly reproduces the qualitative physics of the model and gives the ground state energy density to within 12%. Section 3 describes a two-site blocking calculation for the isotropic nearest-neighbor chain. After the first blocking the model has been embedded as an unstable fixed point in a more general model with integer-spin degrees of freedom. A naive application of the blocking procedure leads to entirely incorrect physics for the isotropic model due to the instability of the fixed point and the approximate nature of the calculation. The correct results emerge from a study of the RG trajectories. Although the problem is easily understood in this context, it makes the two-site calculation unsuitable for studying the long-range model (3.1) with its infinite-dimensional parameter space. The situation is further clarified by introducing a duality transformation for the integer-spin model. It is suggested that such duality transformations may be useful in other block-spin calculations as well. Section 4 describes ways to improve the three-site calculation of Sect. 2,

in particular by developing it into an approximate nine-site calculation. Section 5 contains concluding remarks.

## 2. Nearest-Neighbor Heisenberg-Ising Antiferromagnet

In this section the three-site blocking algorithm is described and applied to the nearest-neighbor model with Hamiltonian

$$H = \sum_{i=1}^{N-1} \left[ S_x(i) S_x(i+1) + S_y(i) S_y(i+1) + \gamma S_z(i) S_z(i+1) \right] ,$$
$$\gamma \geq 0 , \quad (3.2)$$

where the infinite volume limit  $N \rightarrow \infty$  will generally be assumed. The lattice sites may be grouped into blocks of three and labelled by ordered pairs  $(k, a)$  where  $k = 1, 2, \dots, N/3$  specifies the block and  $a = 1, 2, 3$  labels sites within that block. Thus the  $i^{\text{th}}$  lattice site may be relabelled  $(k, a)$  where  $i = 3k - 3 + a$ . Three-site blocks are convenient because the block states will have half-integer spin as do the original degrees of freedom. The Hamiltonian may now be decomposed into two pieces,  $H_{\text{in}}$  and  $H_{\text{out}}$ , where  $H_{\text{in}}$  couples sites within a single block and  $H_{\text{out}}$  couples sites in adjacent blocks:

$$H = H_{\text{in}} + H_{\text{out}} , \quad (3.3)$$

$$H_{\text{in}} = \sum_k \left[ S_x(k,1)S_x(k,2) + S_x(k,2)S_x(k,3) + S_y(k,1)S_y(k,2) \right. \\ \left. + S_y(k,2)S_y(k,3) + \gamma S_z(k,1)S_z(k,2) + \gamma S_z(k,2)S_z(k,3) \right] ,$$

$$H_{\text{out}} = \sum_k \left[ S_x(k,3)S_x(k+1,1) + S_y(k,3)S_y(k+1,1) + \gamma S_z(k,3)S_z(k+1,1) \right] .$$

To diagonalize  $H_{in}$ , it suffices to consider a single block:

$$H_{in} = \sum_k H_{block}(k) ,$$

$$\begin{aligned} H_{block} &= \vec{S}(1) \cdot \vec{S}(2) + \vec{S}(2) \cdot \vec{S}(3) + \epsilon \left[ S_z(1)S_z(2) + S_z(2)S_z(3) \right] \\ &= \frac{1}{2} \left\{ \left[ \vec{S}(1) + \vec{S}(2) + \vec{S}(3) \right]^2 - \left[ \vec{S}(1) + \vec{S}(3) \right]^2 - \frac{3}{4} \right\} \\ &\quad + \epsilon \left[ S_z(1)S_z(2) + S_z(2)S_z(3) \right] \end{aligned} \quad (3.4)$$

where  $\epsilon = \gamma - 1$ .

For  $\epsilon = 0$ ,  $H_{block}$  is rotationally invariant and its eigenstates are found by combining  $\vec{S}(1)$  and  $\vec{S}(3)$  to give a total spin 0 or 1, which is then coupled to  $\vec{S}(2)$ . These states form a spin-3/2 multiplet and two spin-1/2 doublets and are (notation is  $|S, S_z\rangle$ ):

$$\left. \begin{aligned} |\frac{3}{2}, \frac{3}{2}\rangle &= |\uparrow\uparrow\uparrow\rangle , \\ |\frac{3}{2}, \frac{1}{2}\rangle &= \frac{1}{\sqrt{3}} \left( |\uparrow\uparrow\uparrow\rangle + |\downarrow\uparrow\uparrow\rangle + |\uparrow\downarrow\uparrow\rangle \right) \\ |\frac{1}{2}, \frac{1}{2}\rangle_0 &= \frac{1}{\sqrt{2}} \left( |\uparrow\uparrow\downarrow\rangle - |\downarrow\uparrow\uparrow\rangle \right) , \\ |\frac{1}{2}, \frac{1}{2}\rangle_1 &= \frac{1}{\sqrt{6}} \left( 2|\uparrow\downarrow\uparrow\rangle - |\downarrow\uparrow\uparrow\rangle - |\uparrow\uparrow\downarrow\rangle \right) , \end{aligned} \right\} \text{energy} = +\frac{1}{2} , \quad (3.5)$$

plus the four corresponding states with all spins flipped and negative total  $S_z$ .

For  $\epsilon \neq 0$ ,  $H_{\text{block}}$  is invariant only under rotations about the z-axis (plus the discrete symmetry  $z \rightarrow -z$  which keeps the energy independent of the sign of  $S_z$ ) so that states of different total spin but equal  $S_z$  can mix. One finds that  $|\frac{3}{2}, \frac{3}{2}\rangle$  is still an eigenstate, with energy  $\frac{1}{2}\gamma$ ,  $|\frac{1}{2}, \frac{1}{2}\rangle_0$  is still an eigenstate with energy 0, but that  $|\frac{3}{2}, \frac{1}{2}\rangle_1$  and  $|\frac{1}{2}, \frac{1}{2}\rangle_1$  do mix. By diagonalizing a  $2 \times 2$  matrix, one finds that the lowest-energy eigenstate is

$$|\pm \frac{1}{2}\rangle \equiv (1 + 2x^2)^{-\frac{1}{2}} \left( |\frac{1}{2}, \frac{1}{2}\rangle_1 + \sqrt{2}x |\frac{3}{2}, \frac{1}{2}\rangle \right) ,$$
$$\text{energy} = -\frac{1}{4}(\gamma + \sqrt{\gamma^2 + 8}) ,$$
$$x \equiv 2(\gamma - 1)(8 + \gamma + 3\sqrt{\gamma^2 + 8})^{-\frac{1}{2}} . \quad (3.6)$$

Thus far the state of the lattice has been described in terms of the state—spin up or spin down—of the spin- $\frac{1}{2}$  particle at each site. Since the eight eigenstates of  $H_{\text{block}}$  form a complete set, an equally good description (corresponding to a different basis in the Hilbert space of states) is obtained by specifying the eigenstate of each block. However, it is physically reasonable to expect the low-lying states of the lattice to be predominantly formed from the low-lying eigenstates of  $H_{\text{block}}$ . I therefore make the approximation of restricting attention to the sector of states built from the block states  $|\pm \frac{1}{2}\rangle$  and  $|\mp \frac{1}{2}\rangle$  only,  $|\mp \frac{1}{2}\rangle$  being obtained from  $|\pm \frac{1}{2}\rangle$  under  $z \rightarrow -z$ . The next step is to write an effective Hamiltonian which has the same matrix elements as the original Hamiltonian within this sector of states.

More explicitly, the lowest-lying states of  $H_{\text{block}}$  are

$$\begin{aligned} |+\frac{1}{2}\rangle &= (1+2x^2)^{-\frac{1}{2}} \frac{1}{\sqrt{6}} \left[ |\uparrow\uparrow\uparrow\rangle (2x+2) + |\uparrow\uparrow\downarrow\rangle (2x-1) + |\uparrow\downarrow\uparrow\rangle (2x-1) \right], \\ |-\frac{1}{2}\rangle &= -(1+2x^2)^{-\frac{1}{2}} \frac{1}{\sqrt{6}} \left[ |\uparrow\uparrow\uparrow\rangle (2x+2) + |\uparrow\downarrow\uparrow\rangle (2x-1) + |\uparrow\uparrow\downarrow\rangle (2x-1) \right]. \end{aligned} \quad (3.7)$$

The overall sign difference between the states reflects Condon-Shortley phase conventions. The effective Hamiltonian is constructed from new spin operators  $\vec{S}'$  defined by  $\langle +\frac{1}{2}|S'_z|+\frac{1}{2}\rangle = \frac{1}{2}$ ,  $\langle -\frac{1}{2}|S'_z|-\frac{1}{2}\rangle = -\frac{1}{2}$ , etc.

With this definition it is easy to check that in each block

$$\begin{aligned} \langle S_x(1)\rangle &= \langle S_x(3)\rangle = \frac{2(1+x)(1-2x)}{3(1+2x^2)} \langle S'_x \rangle , \\ \langle S_y(1)\rangle &= \langle S_y(3)\rangle = \frac{2(1+x)(1-2x)}{3(1+2x^2)} \langle S'_y \rangle , \\ \langle S_z(1)\rangle &= \langle S_z(3)\rangle = \frac{2(1+x)^2}{3(1+2x^2)} \langle S'_z \rangle \end{aligned} \quad (3.8)$$

where the notation  $\langle \rangle$  indicates any one of the four matrix elements involving the states  $|\pm\frac{1}{2}\rangle$ , and the equality  $\langle \vec{S}(1)\rangle = \langle \vec{S}(3)\rangle$  follows from the even parity of these states. Using the relations (3.8) to eliminate the  $\vec{S}$  operators from  $H_{\text{out}}$ , and remembering that  $H_{\text{in}}$  has been diagonalized, the effective Hamiltonian can be written:

$$H^{(1)} = \sum_{k=1}^{N/3} a_1 + \sum_{k=1}^{(N/3)-1} b_1 \left[ S'_x(k)S'_x(k+1) + S'_y(k)S'_y(k+1) + \gamma_1 S'_z(k)S'_z(k+1) \right] , \quad (3.9)$$

$$a_1 = -\frac{1}{4}(\gamma + \sqrt{\gamma^2 + 8}) , \quad b_1 = \left[ \frac{2(1+x)(1-2x)}{3(1+2x^2)} \right]^2 , \quad \gamma_1 = \left( \frac{1+x}{1-2x} \right)^2 \gamma .$$

Because this Hamiltonian has the same form as the original one, apart from the energy shift  $a_1$  and the scale factor  $b_1$ , the blocks of the original lattice may be viewed as sites of a new lattice and an identical blocking procedure applied to  $H^{(1)}$ . In this way one generates a sequence of Hamiltonians  $H^{(m)}$  describing the physics of ever larger length scales (block sizes) and obeying the following renormalization group equations:

$$H^{(m)} = \sum_{k=1}^{N/3^m} a_m + \sum_{k=1}^{(N/3^m)-1} b_m \left[ S_x(k)S_x(k+1) + S_y(k)S_y(k+1) + \gamma_m S_z(k)S_z(k+1) \right],$$

$$a_{m+1} = 3a_m - \frac{1}{4}b_m \left( \gamma_m + \sqrt{\gamma_m^2 + 8} \right),$$

$$b_{m+1} = b_m \left[ \frac{2(1+x_m)(1-2x_m)}{3(1+2x_m^2)} \right]^2,$$

$$\gamma_{m+1} = \gamma_m \left( \frac{1+x_m}{1-2x_m} \right)^2,$$

$$a_0 = 0, \quad b_0 = 1, \quad \gamma_0 = \gamma,$$
(3.10)

where

$$x_m \equiv 2(\gamma_m - 1) \left( 8 + \gamma_m + 3\sqrt{\gamma_m^2 + 8} \right)^{-1}.$$

(The primes on the block spin operators in  $H^{(m)}$  have been dropped for simplicity.) Here  $a_m$  is a c-number contribution to the energy which after sufficiently many iterations of the blocking procedure becomes the dominant contribution. In fact, on the finite lattice of length  $N$ , after roughly  $m = \log_3 N$  iterations the whole lattice has been reduced to a single block and  $a_m$  is the only contribution to the energy. Since at

each iteration the number of lattice sites drops by a factor  $1/3$ , the energy per original lattice site is to be computed as  $a_m / 3^m \equiv \mathcal{E}_m$ .

Returning to an infinite lattice by letting  $N \rightarrow \infty$  one obtains an energy density given by  $\lim_{m \rightarrow \infty} \mathcal{E}_m$  where  $\mathcal{E}_m$  satisfies

$$\mathcal{E}_{m+1} = \mathcal{E}_m - \frac{1}{12 \times 3^m} b_m \left( \gamma_m + \sqrt{\gamma_m^2 + 8} \right) , \quad \mathcal{E}_0 = 0 . \quad (3.11)$$

Since the whole RG procedure may be viewed as a variational calculation in which the set of variational trial states is "thinned out" or "truncated" with each iteration, the energy density computed from (3.11) will always be an upper bound on the true energy density.

The RG equations have three fixed points in the region  $\gamma \geq 0 : \gamma = 0$  (isotropic XY model),  $\gamma = 1$  (isotropic Heisenberg model), and  $\gamma = \infty$  (Ising model). I now proceed to discuss them.

A)  $\gamma = 0$ . Near this point the RG equations become:

$$\gamma_{m+1} = \frac{1}{2} \gamma_m , \quad (3.12a)$$

$$b_{m+1} = \left[ \frac{1}{2} + \mathcal{O}(\gamma_m) \right] b_m , \quad (3.12b)$$

$$\mathcal{E}_{m+1} = \mathcal{E}_m - \frac{1}{12 \times 3^m} b_m \left( 2\sqrt{2} + \gamma_m \right) . \quad (3.12c)$$

Equation (3.12a) implies that if  $|\gamma|$  is small the system will be driven to the isotropic XY form: the  $\gamma = 0$  fixed point is stable. According to Eq. (3.12b),  $\lim_{m \rightarrow \infty} b_m = 0$  which implies that the isotropic XY model is a massless theory: after sufficiently many iterations it is possible to

construct variational trial states with arbitrarily small excitation energy. It is also possible to compute the energy density at the point  $\gamma = 0$ : (3.12b) and (3.12c) imply  $\mathcal{E}_{m+1} = \mathcal{E}_m - (\sqrt{2} / 6^{m+1})$ . This leads to a geometric series for  $\mathcal{E}_\infty$  whose sum is  $\mathcal{E}_\infty = -\sqrt{2} / 5 = -0.2828$ , to be compared with the exact result<sup>27</sup>  $\mathcal{E} = -1/\pi = -0.3183$ . The error is 11%.

B)  $\gamma = 1$ . Near this point  $\gamma = 1 + \epsilon$  with  $|\epsilon| \ll 1$ , and the RG equations become:

$$\epsilon_{m+1} = \frac{5}{3} \epsilon_m , \quad (3.13a)$$

$$b_{m+1} = \frac{4}{9} b_m \left( 1 - \frac{2}{9} \epsilon_m \right) , \quad (3.13b)$$

$$\mathcal{E}_{m+1} = \mathcal{E}_m - \frac{b_m}{3^{m+1}} \left( 1 + \epsilon_m \right) . \quad (3.13c)$$

Equation (3.13a) shows that this fixed point is unstable: however small  $\epsilon_0$  may be, after many iterations one will have  $\epsilon_m \sim 1$  and Eqs. (3.13) will cease to hold. According to (3.13b),  $b_m \rightarrow 0$  at  $\epsilon = 0$  so that the isotropic Heisenberg model is massless. Finally, using (3.13b,c) to compute the energy density at  $\epsilon = 0$  gives  $\mathcal{E}_{m+1} = \mathcal{E}_m - (1/3)(4/27)^m$ , a geometric series whose sum is  $\mathcal{E}_\infty = -9/23 = -0.3913$ . This differs by 12% from the exact result,<sup>28</sup>  $\mathcal{E} = -0.4431$ .

C)  $\gamma = \infty$ . In the limit  $\gamma \gg 1$  the RG equations become:

$$x_m = \frac{1}{2} \left( 1 - \frac{3}{\gamma_m} \right) , \quad (3.14a)$$

$$\gamma_{m+1} = \frac{1}{4} \gamma_m^3 \left( 1 - \frac{2}{\gamma_m} \right) , \quad (3.14b)$$

$$b_{m+1} = \frac{4}{\gamma_m^2} b_m \left(1 + \frac{6}{\gamma_m}\right) , \quad (3.14c)$$

$$\mathcal{E}_{m+1} = \mathcal{E}_m - \frac{1}{6 \times 3^m} b_m \gamma_m . \quad (3.14d)$$

Equation (3.14b) demonstrates the stability of the  $\gamma = \infty$  fixed point: once  $\gamma_m$  becomes large, it essentially cubes itself with each iteration. Equations (3.14b) and (3.14c) imply that for  $\gamma$  sufficiently large,

$$b_{m+1} \gamma_{m+1} = b_m \gamma_m = b_0 \gamma_0 = \gamma , \quad (3.15)$$

so that (3.14d) gives the energy density as  $\mathcal{E}_\infty = -\gamma \sum_{m=0}^{\infty} (1/(6 \times 3^m)) = -(\gamma/4)$ . This is the exact result for the Ising model  $\gamma \rightarrow \infty$ , which is easily understood since the block states  $|\pm\frac{1}{2}\rangle$  become in this limit:

$$|\pm\frac{1}{2}\rangle = |\uparrow\downarrow\uparrow\rangle - \frac{1}{\gamma} |\uparrow\uparrow\downarrow\rangle - \frac{1}{\gamma} |\downarrow\uparrow\uparrow\rangle ,$$

$$|\mp\frac{1}{2}\rangle = - |\uparrow\downarrow\uparrow\rangle + \frac{1}{\gamma} |\uparrow\downarrow\downarrow\rangle + \frac{1}{\gamma} |\downarrow\uparrow\downarrow\rangle , \quad (3.16)$$

so that the RG algorithm constructs the exact Ising ground state. The fact that  $b_m \rightarrow 0$  in this case is not sufficient to give a massless theory because  $\gamma_m \rightarrow \infty$ . The mass gap for any  $\gamma > 1$  is in fact given by  $b_\infty \gamma_\infty$ , which is the gap at the stable Ising fixed point. This quantity is shown to be nonzero in the discussion of end-to-end order given below.

The picture that emerges from this analysis is that for  $0 \leq \gamma < 1$  the system is driven to the massless isotropic XY form, while for  $\gamma > 1$  it is driven to the massive Ising form. The unstable fixed point  $\gamma = 1$

separates the two regimes. This is precisely the known behavior of this model.<sup>29</sup> One might ask how this approximate calculation is able to locate the correct phase transition exactly, at  $\gamma = 1$ . This is guaranteed by a symmetry: at  $\gamma = 1$  the system becomes rotationally invariant, and the RG transformation has been defined so as to preserve rotational invariance if it is initially present. This point will be important in Sect. 3.

It is also possible to calculate the end-to-end order in the ground state, defined as  $|\langle \vec{S}(1) \cdot \vec{S}(N) \rangle|$ . This is done, in direct analogy to the treatment of  $H$ , by replacing the operator  $\vec{S}(1) \cdot \vec{S}(N)$  with an effective operator having the same matrix elements in the sector of states retained at each iteration. Since the first and last spins on the lattice are also the first spin in the first block and the third spin in the last block, Eqs. (3.8) and (3.10) show that after  $m$  iterations the appropriate effective operator is:

$$[\vec{S}(1) \cdot \vec{S}(N)]_{\text{eff}}^{(m)} = b_m \left[ S_x(1) S_x\left(\frac{N}{3^m}\right) + S_y(1) S_y\left(\frac{N}{3^m}\right) \right] + \frac{1}{\gamma} b_m \gamma_m S_z(1) S_z\left(\frac{N}{3^m}\right). \quad (3.17)$$

Since  $b_m \rightarrow 0$  in all cases, the end-to-end order may be computed as:

$$|\langle \vec{S}(1) \cdot \vec{S}(N) \rangle| = |\langle S_z(1) S_z(\text{last}) \rangle| \frac{1}{\gamma} b_\infty \gamma_\infty, \quad (3.18)$$

where the expectation value on the right side is evaluated in the ground state of the fixed point Hamiltonian  $H^{(\infty)}$ . Clearly this predicts no end-to-end order for  $0 \leq \gamma \leq 1$ . The vanishing of the order for  $\gamma = 1$  may also be obtained as a consequence of the rotational symmetry of the theory and the cluster property  $\lim_{N \rightarrow \infty} [\langle \vec{S}(1) \cdot \vec{S}(N) \rangle - \langle \vec{S}(1) \rangle \cdot \langle \vec{S}(N) \rangle] = 0$ .

For  $\gamma > 1$  the system is driven to the Ising model for which

$|\langle S_z(1)S_z(\text{last})\rangle| = \frac{1}{4}$ . Using Eqs. (3.10) one has for  $\gamma > 1$

$$|\langle \vec{S}(1) \cdot \vec{S}(N) \rangle| = \frac{1}{4} \prod_{n=0}^{\infty} \frac{4}{9} \frac{(1+x_n)^4}{(1+2x_n^2)^2} . \quad (3.19)$$

This infinite product is in fact convergent and nonzero. For  $m$  sufficiently large that  $\gamma_m \gg 1$  one finds from (3.14a) that  $(4/9) \times ((1+x_m)^4 / (1+2x_m^2)^2) = 1 - O(\gamma_m^{-2})$ . The product (3.19) is finite and nonzero if and only if the sum  $\sum_{n>m} \log [1 - O(\gamma_n^{-2})] = - \sum_{n>m} O(\gamma_n^{-2})$  converges. Since  $\gamma_{n+1} \sim \gamma_n^3$  for  $n > m$ , the sum is highly convergent. It is important to note that the end-to-end order depends not only on which fixed point is ultimately reached, but also on the rapidity with which it is approached.

It is also easy to obtain the limiting behavior of the end-to-end order as  $\gamma \rightarrow 1^+$  using Eq. (3.19). Set  $\gamma = 1 + \epsilon$  with  $|\epsilon| \ll 1$ . According to Eq. (3.13a) one iteration of the RG equations changes  $\epsilon$  into  $(5/3)\epsilon$ . Since  $x_n = 0$  for  $\gamma = 1$ , it follows from Eq. (3.19) that

$$\text{Order}(\epsilon) = \frac{4}{9} \text{Order}\left(\frac{5}{3}\epsilon\right), \quad (3.20a)$$

a functional equation which is solved by

$$\text{Order}(\epsilon) \sim \epsilon^{1.6}, \quad 0 < \epsilon \ll 1, \quad \text{where } 1.6 = \frac{\log(4/9)}{\log(5/3)} . \quad (3.20b)$$

Figures 11 and 12 show the results of numerical iteration of the RG equations. Figure 11 compares the ground state energy density computed from (3.11) with the exact solution of Orbach,<sup>28</sup> while Fig. 12 displays

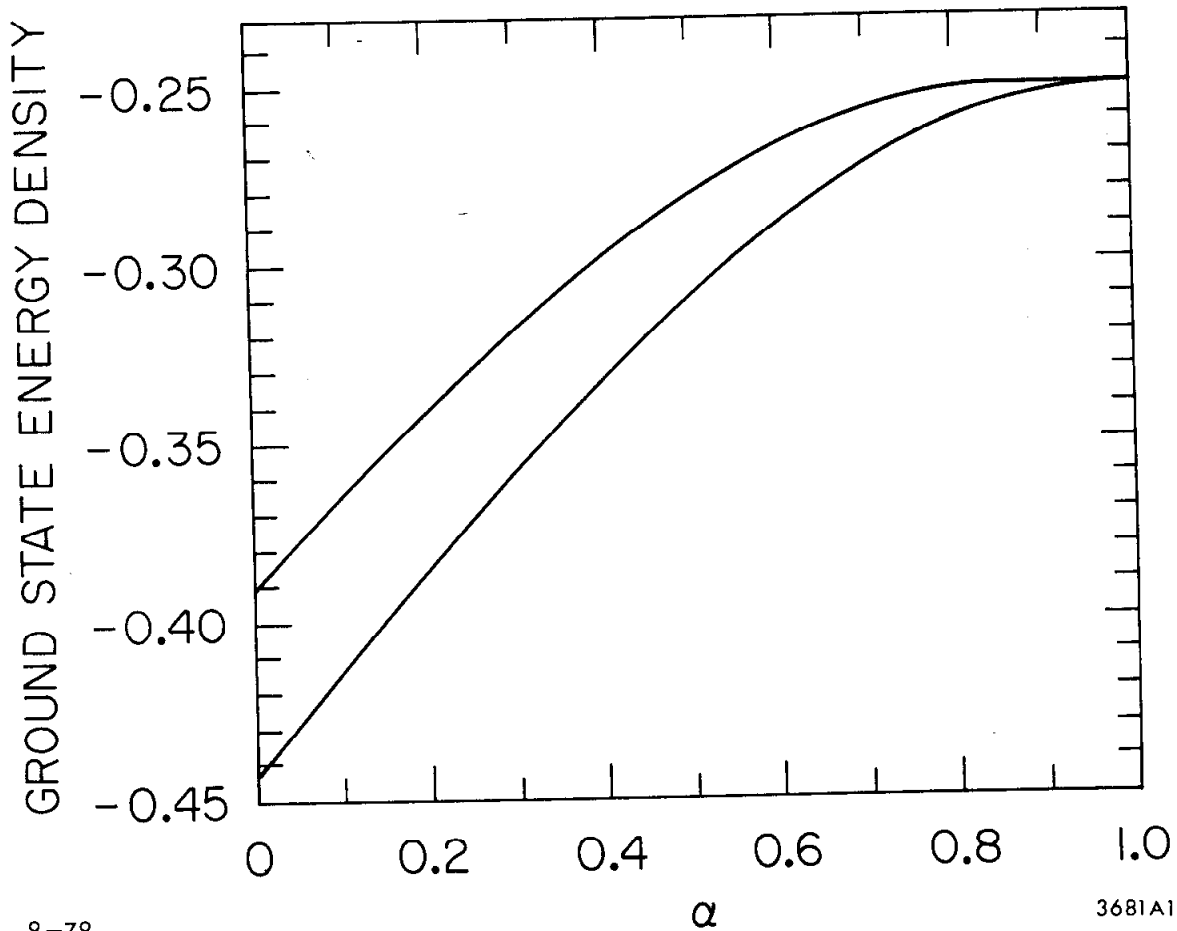
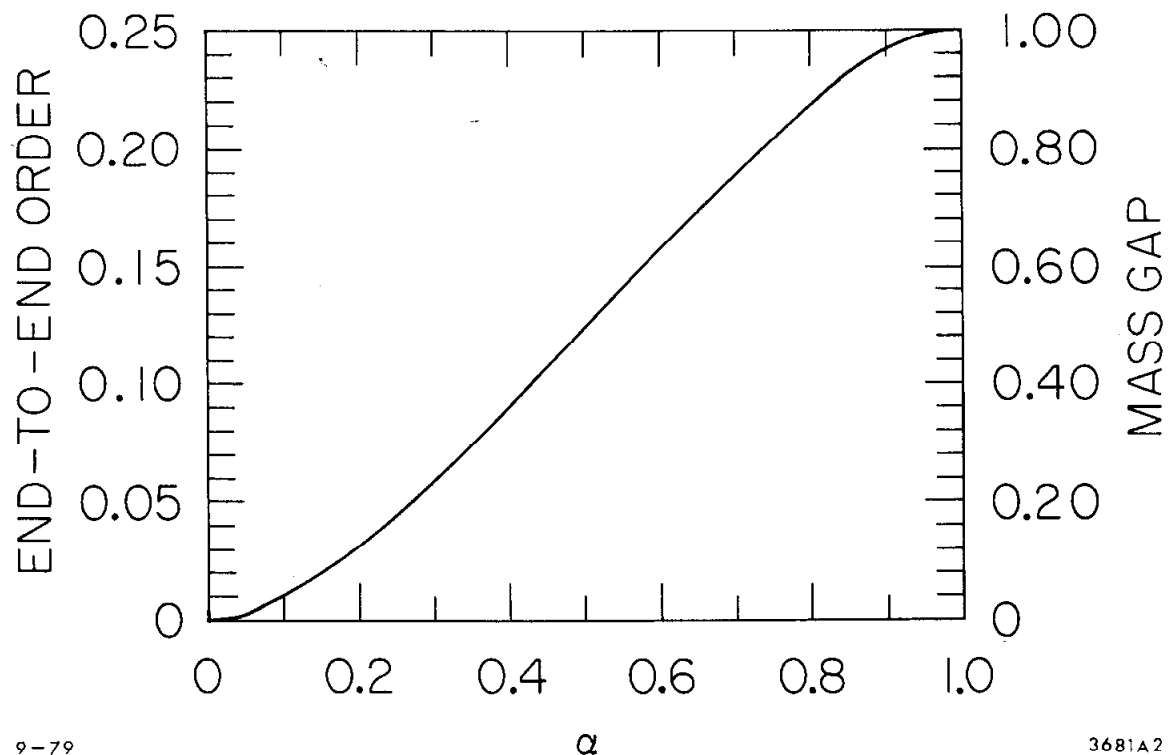


Fig. 11. Comparison of the exact ground state energy density for HOrbach (lower curve) with the result of the renormalization group calculation (upper curve).



9-79

$\alpha$

3681A2

Fig. 12. Results of the renormalization group calculation of the end-to-end order  $|\langle \vec{S}(1) \cdot \vec{S}(N) \rangle|$  and the mass gap for  $H_{\text{Orbach}}$ .

the results of the present calculation for the end-to-end order and the mass gap. Note that the energy density and mass gap both refer to the Hamiltonian used by Orbach, which differs slightly from that used here:

$$\begin{aligned} H_{\text{Orbach}} &= \sum_i \left\{ (1-\alpha) \left[ S_x(i) S_x(i+1) + S_y(i) S_y(i+1) \right] + S_z(i) S_z(i+1) \right\} \\ &= \frac{1}{\gamma} \sum_i \left[ S_x(i) S_x(i+1) + S_y(i) S_y(i+1) + \gamma S_z(i) S_z(i+1) \right], \quad (3.21) \end{aligned}$$

with

$$\gamma = \frac{1}{1-\alpha},$$

so that the region  $1 \leq \gamma \leq \infty$  corresponds to  $0 \leq \alpha \leq 1$ . Due to the factor  $1/\gamma$  in Eq. (3.21), the RG results for the order and the mass gap for this Hamiltonian differ only by a factor of 4, as shown in Fig. 12. The greatest error in the energy density is the 12% error at  $\alpha = 0$ , and the general shape of the curve is correct. According to Eq. (3.20b) the curve in Fig. 12 behaves as  $\alpha^{1.6}$  for  $\alpha$  near zero, whereas in fact both the gap<sup>29</sup> and the order<sup>30</sup> are known to vanish exponentially as  $\alpha \rightarrow 0^+$ . This substitution of power-law for exponential behavior is a common feature of simple block-spin calculations of this type and can be corrected by improving the calculation using variational techniques.<sup>5</sup> Except for this feature, the results of the simple RG calculation given here are completely consistent with the known properties of this model.

### 3. Two-Site Calculation for the Isotropic Heisenberg Model

A rule of thumb for block-spin calculations states that theories involving half-integral spins or fermionic degrees of freedom should be

treated using an odd number of sites per block to preserve these features. The consequences of ignoring this good advice will now be examined by applying a two-site blocking procedure to the isotropic Heisenberg model:

$$H = \sum_{i=1}^{N-1} \vec{S}(i) \cdot \vec{S}(i+1) . \quad (3.22)$$

Decomposing the Hamiltonian into pieces which do and do not connect different two-site blocks yields:

$$\begin{aligned} H &= H_{\text{in}} + H_{\text{out}} , \\ H_{\text{in}} &= \sum_k \vec{S}(k,1) \cdot \vec{S}(k,2) , \\ H_{\text{out}} &= \sum_k \vec{S}(k,2) \cdot \vec{S}(k+1,1) . \end{aligned} \quad (3.23)$$

Anticipating that tensor operators will be useful in the description of the integer spin block states, I write the operators appearing here in terms of raising and lowering operators:

$$\vec{S}(k,a) \cdot \vec{S}(k',a') = S_0(k,a)S_0(k',a') - S_1(k,a)S_{-1}(k',a') - S_{-1}(k,a)S_1(k',a') , \quad (3.24)$$

where  $S_0 \equiv S_z$  and  $S_{\pm 1} \equiv \mp (1/\sqrt{2}) (S_x \pm iS_y)$ .

The block Hamiltonian is introduced by

$$\begin{aligned} H_{\text{in}} &= \sum_k H_{\text{block}}(k) , \\ H_{\text{block}} &= \vec{S}(1) \cdot \vec{S}(2) . \end{aligned} \quad (3.25)$$

The eigenstates of  $H_{\text{block}}$  form the familiar singlet and triplet which will be labelled as follows:

$$\left. \begin{aligned} |+> &= |\uparrow\uparrow> \\ |0> &= \frac{1}{\sqrt{2}} (|\uparrow\downarrow> + |\downarrow\uparrow>) \\ |-> &= |\downarrow\downarrow> \end{aligned} \right\} \quad \text{energy} = + \frac{1}{4},$$

$$|x> = \frac{1}{\sqrt{2}} (|\uparrow\downarrow> - |\downarrow\uparrow>) , \quad \text{energy} = - \frac{3}{4} . \quad (3.26)$$

The Hamiltonian must now be rewritten in terms of block spin operators which act on the states (3.26). To keep rotational invariance explicit, it is useful to define spherical tensor operators of rank 1,  $Q_i$  and  $T_i$ ,  $i = -1, 0, +1$ , by:

$$Q_0 = S_z, \quad Q_{\pm 1} = \mp \frac{1}{\sqrt{2}} (S_x \pm iS_y) , \quad (3.27)$$

$$\langle 0|T_0|x> = 1, \quad \langle x|T_0|0> = 1 ,$$

$$\langle +|T_1|x> = 1, \quad \langle x|T_1|-> = -1 ,$$

$$\langle -|T_{-1}|x> = 1, \quad \langle x|T_{-1}|+> = -1 ,$$

$$\text{all other matrix elements of } T_i = 0 , \quad (3.28)$$

where  $S_x$ ,  $S_y$ ,  $S_z$  are the usual spin operators for a spin-1 particle whose states are  $|+>$ ,  $|0>$ ,  $|->$ ; these operators annihilate the spinless state  $|x>$ .  $Q_i$  thus acts only within the spin-1 subspace while  $T_i$  connects the spin-0 state to the spin-1 states. It is easy to check

that the following relations between matrix elements of the spin- $\frac{1}{2}$  operators appearing in  $H_{\text{block}}$  and of the operators introduced in (3.27) and (3.28) hold between any pair of the states  $|+\rangle$ ,  $|0\rangle$ ,  $|-\rangle$ ,  $|x\rangle$ :

$$\langle S_i(1) \rangle = \frac{1}{2} \langle Q_i + T_i \rangle , \quad \langle S_i(2) \rangle = \frac{1}{2} \langle Q_i - T_i \rangle . \quad (3.29)$$

These relations may be inverted:

$$\langle Q_i \rangle = \langle S_i(1) + S_i(2) \rangle , \quad \langle T_i \rangle = \langle S_i(1) - S_i(2) \rangle . \quad (3.30)$$

Thus, for example,  $\vec{S}(k,2) \cdot \vec{S}(k+1,1)$  may be replaced by the scalar operator

$$\frac{1}{4} \sum_i (-1)^i [Q_i(k) - T_i(k)] [Q_{-i}(k+1) + T_{-i}(k+1)] \equiv \frac{1}{4} [Q(k) - T(k)] [Q(k+1) + T(k+1)].$$

It is also possible to record the diagonalization of  $H_{\text{block}}$  in the form:

$$\langle \vec{S}(k,1) \cdot \vec{S}(k,2) \rangle = -\frac{3}{4} + \frac{1}{2} \langle Q^2(k) \rangle , \quad (3.31)$$

since  $Q^2 = 2$  in the spin-1 subspace and  $Q^2 = 0$  in the spin-0 subspace.

Using (3.29) and (3.31), the effective Hamiltonian after the first blocking may be written:

$$H^{(0)} = \sum_{k=1}^{N/2} [E_0 + c_0 \Delta_0 Q^2(k)] + \sum_{k=1}^{(N/2)-1} c_0 [Q(k) - g_0 T(k)] [Q(k+1) + g_0 T(k+1)], \quad (3.32)$$

where  $E_0 = -3/4$ ,  $c_0 = 1/4$ ,  $\Delta_0 = 2$ ,  $g_0 = 1$ . It is important to realize that no approximation has been made yet because  $|+\rangle$ ,  $|0\rangle$ ,  $|-\rangle$  and  $|x\rangle$  form a complete set of block states. A new basis in Hilbert space has

simply been chosen, so that the Hamiltonian (3.32) now describes a lattice of length  $N/2$  with a spin-1 triplet state and a spin-0 singlet state at each site. The change of basis and its inverse are described by Eqs. (3.29) - (3.31).

Since the sum of two integer spins is again an integer, it will be possible to implement a two-site RG transformation under which (3.32) retains its form. In fact, restricting  $H^{(0)}$  to a particular two-site block produces a block Hamiltonian:

$$H_{\text{block}}^{(0)} = 2E_0 + c_0 \Delta_0 [Q^2(1) + Q^2(2)] + c_0 [Q(1) - g_0 T(1)][Q(2) + g_0 T(2)]. \quad (3.33)$$

According to the general rules for combining spins,  $H_{\text{block}}$  will have sixteen eigenstates: two spin-0 singlets, three spin-1 triplets, and a spin-2 quintet. In order to preserve the form of (3.32) an effective Hamiltonian will be written for the subspace of states built from the lowest-lying singlet and triplet eigenstates of (3.33). These states are readily found to be:

$$|0,0\rangle = \left(3 + r_0^2\right)^{-\frac{1}{2}} (r_0 |xx\rangle + |00\rangle - |+-\rangle - |-+\rangle), \quad \text{energy} = E_1, \quad (3.34a)$$

$$|1,1\rangle = \left(2 + 2s_0^2\right)^{-\frac{1}{2}} \left[ s_0 (|++\rangle + |x+\rangle) + (|0+\rangle - |+0\rangle) \right],$$

$$|1,0\rangle = \left(2 + 2s_0^2\right)^{-\frac{1}{2}} \left[ s_0 (|0x\rangle + |x0\rangle) + (|-\rangle - |+\rangle) \right],$$

$$|1,-1\rangle = \left(2 + 2s_0^2\right)^{-\frac{1}{2}} \left[ s_0 (|-x\rangle + |x-\rangle) + (|-0\rangle - |0-\rangle) \right],$$

$$\text{energy} = E'_1, \quad (3.34b)$$

where:

$$r_0 = \sqrt{3 + \left( \frac{2\Delta_0 - 1}{g_0^2} \right)^2} + \frac{2\Delta_0 - 1}{g_0^2}, \quad (3.34c)$$

$$s_0 = \sqrt{1 + \left( \frac{2\Delta_0 - 1 + g_0^2}{4g_0} \right)^2} + \frac{2\Delta_0 - 1 + g_0^2}{4g_0}, \quad (3.34d)$$

$$E_1 = 2E_0 + c_0 (4\Delta_0 - 2 - r_0 g_0^2), \quad (3.34e)$$

$$E'_1 = 2E_0 + c_0 (4\Delta_0 - 1 - 2s_0 g_0), \quad (3.34f)$$

The next step is to define new tensor operators  $Q'_i$  and  $T'_i$  which act on the states (3.34a,b) exactly as  $Q_i$  and  $T_i$  acted on the states (3.26):  $\langle 0,0 | T'_0 | 1,0 \rangle = 1$ , etc. The resulting relationships between matrix elements are:

$$\langle Q_i(k, a) \rangle = u_a \langle Q'_i(k) \rangle + v_a \langle T'_i(k) \rangle, \quad ,$$

$$\langle T_i(k, a) \rangle = w_a \langle Q'_i(k) \rangle + z_a \langle T'_i(k) \rangle, \quad ,$$

$$u_1 = u_2 = \frac{1}{2}, \quad ,$$

$$v_1 = -v_2 = 2 \left( 2 + 2s_0^2 \right)^{-\frac{1}{2}} \left( 3 + r_0^2 \right)^{-\frac{1}{2}}, \quad ,$$

$$w_1 = -w_2 = \frac{s_0}{1 + s_0^2}, \quad ,$$

$$z_1 = z_2 = s_0 (1 + r_0) \left( 2 + 2s_0^2 \right)^{-\frac{1}{2}} \left( 3 + r_0^2 \right)^{-\frac{1}{2}}. \quad (3.35)$$

The Hamiltonian (3.32) has the decomposition as  $H_{in} + H_{out}$ :

$$H^{(0)} = \sum_{k=1}^{N/4} H_{block}^{(0)}(k) + \sum_{k=1}^{(N/4)-1} c_0 [Q(k,2) - g_0^T(k,2)] [Q(k+1,1) + g_0^T(k+1,1)],$$

and use of (3.34e,f) and (3.35) leads to a new, approximate, effective Hamiltonian of the same form as (3.32). In fact, the general RG equations are readily seen to be:

$$H^{(m)} = \sum_k \left\{ E_m + c_m (\Delta_m Q^2(k) + [Q(k) - g_m^T(k)][Q(k+1) + g_m^T(k+1)]) \right\} , \quad (3.36a)$$

$$\left. \begin{aligned} c_{m+1} &= c_m \left( \frac{1 + 2g_m s_m + s_m^2}{2 + 2s_m^2} \right)^2, \\ g_{m+1} &= \left( \frac{c_m}{c_{m+1}} \right)^{\frac{1}{2}} \frac{2 + g_m s_m (1 + r_m)}{(2 + 2s_m^2)^{\frac{1}{2}} (3 + r_m^2)^{\frac{1}{2}}}, \\ \Delta_{m+1} &= \frac{c_m}{2c_{m+1}} \left( 1 - 2g_m s_m + g_m^2 r_m \right), \\ E_{m+1} &= 2E_m + c_m \left( 4\Delta_m - 2 - r_m g_m^2 \right), \end{aligned} \right\} \quad (3.36b)$$

where

$$\begin{aligned} r_m &= \sqrt{3 + \left( \frac{2\Delta_m - 1}{g_m^2} \right)^2} + \frac{2\Delta_m - 1}{g_m^2}, \\ s_m &= \sqrt{1 + \left( \frac{2\Delta_m - 1 + g_m^2}{4g_m} \right)^2} + \frac{2\Delta_m - 1 + g_m^2}{4g_m}, \\ E_0 &= -\frac{3}{4}, \quad c_0 = \frac{1}{4}, \quad \Delta_0 = 2, \quad g_0 = 1. \end{aligned}$$

As usual, the energy per original lattice site is to be computed as

$$\lim_{m \rightarrow \infty} E_m / 2^{m+1}.$$

Numerical iteration of Eqs. (3.36) leads to a ground state energy density of -0.4210, only 5% higher than the exact result -0.4431. Because the isotropic Heisenberg model is massless, one would expect to find  $c_m \rightarrow 0$ . In fact, one finds that  $g_m \rightarrow 1$ ,  $\Delta_m \rightarrow 0$ , but  $c_m \rightarrow$  a nonzero constant! This limiting theory with  $\Delta_\infty = 0$  can be solved exactly by using Eqs. (3.30) and (3.31) to rewrite it on an underlying spin- $\frac{1}{2}$  lattice (recall that this transformation is exact). The condition  $\Delta_\infty = 0$  means that the two sites within any one block on the spin- $\frac{1}{2}$  lattice are uncoupled. The spin- $\frac{1}{2}$  couplings are therefore as shown in Fig. 13. This theory has a four-fold degenerate ground state in which each coupled pair of sites has total spin 0 while the uncoupled sites at the ends of the lattice have total spin 0 or 1. There is a finite mass gap to the highly degenerate first excited state in which some pair of coupled spins have total spin 1, and additional mass gaps separate the higher excited states. Clearly this bears no resemblance to the physics of the isotropic Heisenberg model with its massless spin wave excitations. What went wrong?

Recalling the calculation of Sect. 2, suppose that here also the Heisenberg model  $\Delta = 2$ ,  $g = 1$  is an unstable fixed point of the more general model of Eqs. (3.36). The RG calculation should find this fixed point, but being an approximate calculation it need not locate it precisely at  $\Delta = 2$ ,  $g = 1$ . In such a case the RG equations with Heisenberg model initial conditions will iterate away from the unstable fixed point, toward a stable fixed point with totally different physics.

Figure 14 shows the qualitative behavior of the RG trajectories resulting from Eqs. (3.36) near the Heisenberg point  $\Delta = 2$ ,  $g = 1$  and supports the picture just sketched. The unstable fixed point is quite close, at  $\Delta = 1.7$ ,  $g = 0.84$ , but the Heisenberg model iterates to the stable

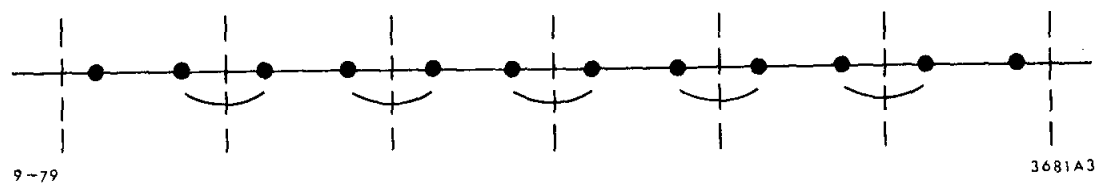


Fig. 13. Couplings for the spin-1/2 theory equivalent to the  $m \rightarrow \infty$  integer-spin theory (3.36).

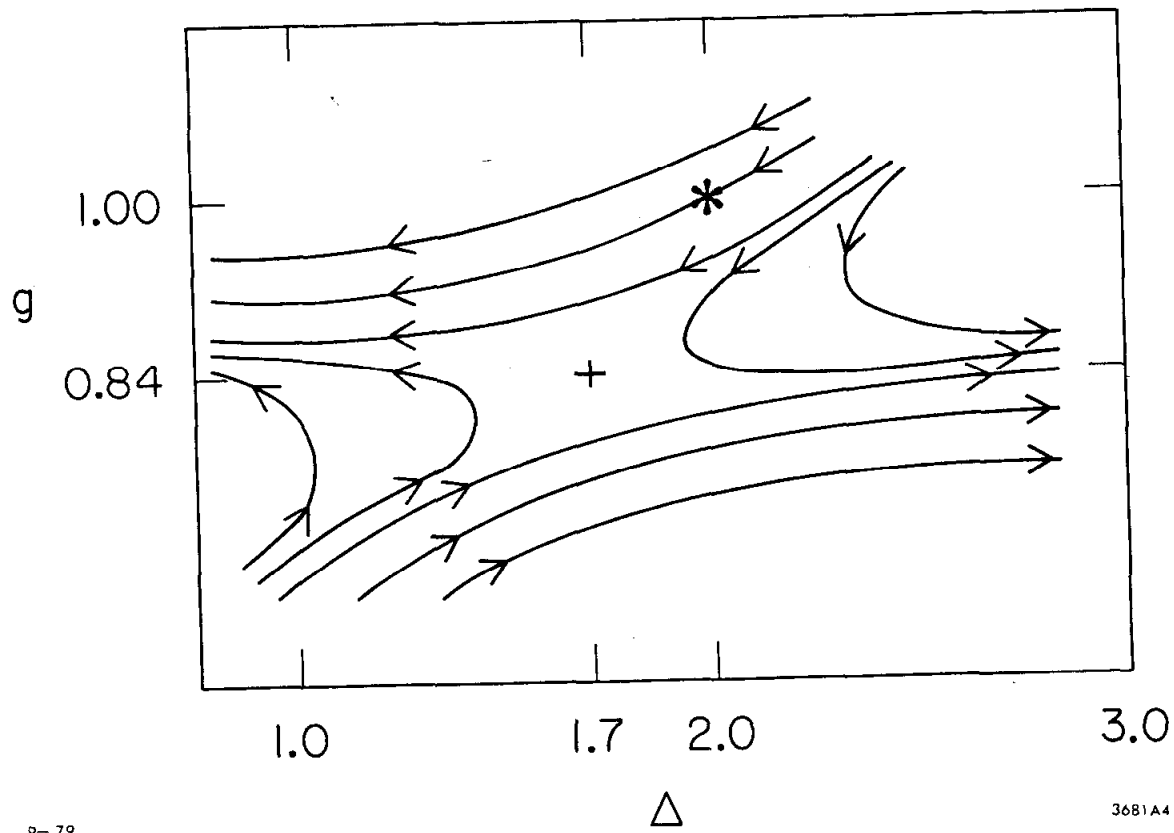


Fig. 14. Qualitative behavior of RG trajectories in the two-site calculation. The point \* is the Heisenberg model point and + is the unstable fixed point.

9-79

3681A4

fixed point  $\Delta=0$ . There is also a stable fixed point at  $\Delta=\infty$ . At the unstable fixed point the Hamiltonian just rescales by a factor less than 1 at each iteration, leading to the correct massless behavior.

The result that the nearest-neighbor Heisenberg chain and the fully dimerized chain of Fig. 13 correspond respectively to unstable and stable fixed points of a model with more free parameters is familiar in solid-state physics. One-dimensional chains of atoms with nearest-neighbor spring forces as well as Heisenberg spin interactions are unstable against spontaneous distortion into a chain of atom pairs, paired atoms being closer together than atoms in adjacent pairs. An RG treatment of this Peierls distortion, which is related to the Peierls instability in one-dimensional conductors, has been given by Caspers<sup>6</sup> using three-site blocking and obtaining the same fixed-point structure.

Recalling that the  $\gamma=1$  unstable fixed point of the three-site calculation was located correctly as a consequence of rotational invariance, it is natural to ask whether the model (3.36a) possesses some symmetry at the Heisenberg point which is not preserved by the RG transformation. Intuitively this symmetry is just the translational symmetry of the spin-1/2 form of the Heisenberg model, Eq. (3.22). I now show that such a symmetry can be defined as invariance under a duality transformation.

To define the duality transformation it is convenient to rewrite the Hamiltonian (3.36a) in the generic form:

$$H = \sum_k \left\{ E + GQ^2(k) + A Q(k)Q(k+1) + B T(k)T(k+1) + D [Q(k)T(k+1) - T(k)Q(k+1)] \right\} , \quad (3.37)$$

where  $G = c\Delta$ ,  $A = c$ ,  $B = -cg^2$ ,  $D = cg$ .

The change in notation is necessary because the duality transformation will not preserve the form of the nearest-neighbor couplings in the Hamiltonian (3.36a) except for special values of the parameters.

The first step is to use Eqs. (3.30) and (3.31) to write a spin-1/2 Hamiltonian equivalent to (3.37). This is the same trick used to solve exactly the fixed point Hamiltonian. It yields a spin- $\frac{1}{2}$  Hamiltonian which, if blocked using two-site blocks, would reproduce (3.37). The spin- $\frac{1}{2}$  Hamiltonian is:

$$H = \sum_k \left\{ E + \frac{3}{2} G \vec{S}(k,1) \cdot \vec{S}(k,2) + (A+B) \vec{S}(k,1) \cdot \vec{S}(k+1,1) + (A+B) \vec{S}(k,2) \cdot \vec{S}(k+1,2) + (A-B-2D) \vec{S}(k,1) \cdot \vec{S}(k+1,2) + (A-B+2D) \vec{S}(k,2) \cdot \vec{S}(k+1,1) \right\} . \quad (3.38)$$

The spin- $\frac{1}{2}$  lattice is now shifted one unit to the right by letting  $(k,1) \rightarrow (k,2)$  and  $(k,2) \rightarrow (k+1,1)$  (periodic boundary conditions are useful here). This shift interchanges interblock couplings with intrablock couplings. Finally, blocking the Hamiltonian back to the integer spin form using Eqs. (3.29) and (3.31) produces the dual Hamiltonian:

$$\tilde{H} = \sum_k \left\{ \tilde{E} + \tilde{G} Q^2(k) + \tilde{A} Q(k) Q(k+1) + \tilde{B} T(k) T(k+1) + \tilde{D} [Q(k) T(k+1) - T(k) Q(k+1)] + \tilde{F} [Q(k) - T(k)] [Q(k+2) + T(k+2)] \right\},$$

where

$$\tilde{E} = E + \frac{3}{2} G - \frac{3}{4} (A - B + 2D),$$

$$\tilde{G} = \frac{1}{2} (A - B + 2D),$$

$$\tilde{A} = \frac{1}{2} (A + B + G),$$

$$\tilde{B} = \frac{1}{2} (A + B - G),$$

$$\tilde{D} = \frac{1}{2} G,$$

$$\tilde{F} = \frac{1}{4} (A - B - 2D).$$

(3.39)

Notice that the dual gap parameter  $\tilde{G}$  depends on the original couplings  $A$ ,  $B$ , and  $D$  while the original gap parameter contributes to the dual couplings. Next-nearest-neighbor couplings have also appeared.  $H$  and  $\tilde{H}$  clearly describe the same system in different ways and have the same spectrum and other properties. A system is self-dual in the sense that  $H = \tilde{H}$  if its spin- $\frac{1}{2}$  form is translationally invariant. The self-duality condition reduces to  $A - B = 2D = G$  which implies  $\Delta = 2$ ,  $g = 1$ . Only multiples of the Heisenberg Hamiltonian are self-dual. Therefore, a calculation which respected translational invariance would lead to the correct physics for the Heisenberg model.

The RG transformation will not preserve self-duality (translational invariance). Indeed, RG calculations of this type treat intrablock and

interblock couplings quite differently. The former are diagonalized and contribute to the gap parameter at the next iteration, while the latter contribute to the new couplings. In the present calculation the initial Hamiltonian was self-dual while the  $\Delta = 0$  fixed point which was finally reached was not. This fixed point corresponds to  $A - B = 2D \neq 0$ ,  $G = 0$ . It is dual to the point  $A = B = 2D = 0$ ,  $G \neq 0$  which is the  $\Delta = \infty$  fixed point of Fig. 14. The  $\Delta = \infty$  fixed point corresponds to Fig. 13 with the coupling pattern shifted one unit to the right.

Several remarks should be made regarding the problem with this calculation and its resolution as discussed above.

(1) Although the RG equations, naively applied, lead to the wrong fixed point, a glance at the trajectories of Fig. 14 is sufficient to reveal the problem and indicate the correct physics. Unfortunately, models with long-range interactions such as (3.1) involve an infinite number of different couplings, so that RG trajectories cannot be mapped out. Without the trajectories there is no way to locate unstable fixed points. Thus, the two-site calculation of this section cannot be reliably used to study the phases of the model (3.1) even though it may well yield a good ground state energy density.

(2) The problem encountered in the two-site calculation is clearly very general: it may occur in any theory when the first RG blocking embeds the theory at or near an unstable fixed point of a more general model. However, the following considerations suggest a rule for determining which of several possible calculations may be most seriously affected by the failure of the RG technique to preserve self-duality. In the two-site calculation, the ground state in a block was a singlet.

In order to get the correct massless physics it would have been necessary for both the gap parameter  $G$  and the couplings  $A, B, D$  to iterate to zero. This did not happen because the RG calculation treats gaps and couplings asymmetrically. In the three-site calculation the ground state in a block was a doublet, and the subspace of lattice states formed from these doublet block states was isomorphic to the space of states of the original Heisenberg model. This would remain true even in a three-site calculation using all eight block states. As long as all couplings iterate to zero in such a calculation, this subspace contains massless excitations yielding the correct spectrum even if nonzero gaps separate the lowest doublet from the other states in one block. This suggests the following rule of thumb: given a choice, one should prefer that calculation for which the ground state in a block has the highest multiplicity. This maximizes the number of lattice states that can be constructed from the block ground states alone. Physics which depends on this sector of lattice states only will be independent of gaps between block states, and therefore independent of asymmetrical treatment of gaps and couplings.

(3) The duality transformation introduced here has applications beyond this particular model. Such a transformation can be defined in any calculation in which all the block states are kept at the first blocking, so that the blocking is "reversible". In a two-site calculation the square of the duality transformation is unity; in a calculation using  $m$ -site blocks the duality transformation generates a  $Z_m$  symmetry group. The relation of this transformation to the existing complex of "duality" ideas in the literature is under investigation.

(4) In addition to its utility in classifying fixed points, the duality transformation may be used to increase the accuracy of the RG calculation itself. Consider the following scheme. Beginning with the Hamiltonian  $H^{(0)}$  of Eq. (3.32), one blocks as usual to obtain  $H^{(1)}$ .  $H^{(2)}$  is obtained by blocking the dual Hamiltonian  $\tilde{H}^{(1)}$  (note that this blocking removes the next-nearest-neighbor couplings introduced by the duality transformation) and one continues by alternately applying the duality transformation and the blocking procedure. Since the underlying spin- $\frac{1}{2}$  lattice is shifted to the right at each iteration of this scheme, one might hope that more translationally invariant states than usual are being constructed and that edge effects due to the walls of the blocks are being "smeared out". This scheme does in fact improve the energy density found in the two-site calculation very slightly.

#### 4. Improving the Three-Site Calculation

One might try to improve the three-site calculation for the isotropic Heisenberg model ( $\gamma = 1$  in the notation of Sect. 2) in a variety of ways. One method is to keep more than two of the block states (3.5). One might keep both spin- $\frac{1}{2}$  doublets, or even all eight states in which case a duality transformation could be employed. Alternatively one might try to select a better pair of states to keep, which need not be eigenstates of  $H_{\text{block}}$ . In this problem, symmetry considerations make this impossible: rotational symmetry forbids mixing spin-3/2 with spin- $\frac{1}{2}$  states, and parity rules out a linear combination of the two spin- $\frac{1}{2}$  multiplets. A third course is to use larger blocks. In this section, I describe a way to improve the three-site calculation by using it to approximate a nine-site calculation.

Consider performing a nine-site calculation by keeping only the lowest-lying spin- $\frac{1}{2}$  doublet of eigenstates on a block at each iteration. Such a calculation can only be done with the aid of a computer. However, two iterations of the three-site calculation have the effect of constructing a pair of spin- $\frac{1}{2}$  states on a nine-site block. The  $S_z = \frac{1}{2}$  member of this pair is (cf., Eq. (3.5)):

$$|\psi\rangle = \frac{1}{\sqrt{6}} \left[ 2 \left| \frac{1}{2}, \frac{1}{2} \right\rangle_1 \left| \frac{1}{2}, -\frac{1}{2} \right\rangle_1 \left| \frac{1}{2}, \frac{1}{2} \right\rangle_1 - \left| \frac{1}{2}, \frac{1}{2} \right\rangle_1 \left| \frac{1}{2}, \frac{1}{2} \right\rangle_1 \left| \frac{1}{2}, -\frac{1}{2} \right\rangle_1 - \left| \frac{1}{2}, -\frac{1}{2} \right\rangle_1 \left| \frac{1}{2}, \frac{1}{2} \right\rangle_1 \left| \frac{1}{2}, \frac{1}{2} \right\rangle_1 \right],$$

where  $\left| \frac{1}{2}, \frac{1}{2} \right\rangle_1 = \frac{1}{\sqrt{6}} \left( 2 |\uparrow\uparrow\uparrow\rangle - |\uparrow\uparrow\downarrow\rangle - |\uparrow\downarrow\uparrow\rangle \right)$  ,

and  $\left| \frac{1}{2}, -\frac{1}{2} \right\rangle_1 = \frac{1}{\sqrt{6}} \left( -2 |\uparrow\uparrow\downarrow\rangle + |\downarrow\uparrow\uparrow\rangle + |\uparrow\downarrow\downarrow\rangle \right)$  .

(3.40)

If the Hamiltonian on a nine-site block is written in the form:

$$H_{\text{block}} = H_0 + V ,$$

$$H_0 = \vec{S}(1) \cdot \vec{S}(2) + \vec{S}(2) \cdot \vec{S}(3) + \vec{S}(3) \cdot \vec{S}(4) + \vec{S}(4) \cdot \vec{S}(5) + \vec{S}(5) \cdot \vec{S}(6) + \vec{S}(6) \cdot \vec{S}(7) + \vec{S}(7) \cdot \vec{S}(8) + \vec{S}(8) \cdot \vec{S}(9) ,$$

$$V = \vec{S}(3) \cdot \vec{S}(4) + \vec{S}(6) \cdot \vec{S}(7) ,$$
(3.41)

then  $|\psi\rangle$  is an eigenstate of  $H_0$  with eigenvalue -3. To the extent that  $V$  can be regarded as "small",  $|\psi\rangle$  approximates an exact nine-site eigenstate. In actuality  $V$  will mix  $|\psi\rangle$  with the additional states  $V|\psi\rangle$ ,  $V^2|\psi\rangle$ , etc., of which the most important will be  $V|\psi\rangle$  if  $V$  is "small". It is then reasonable to do a nine-site blocking calculation using as the  $S_z = \frac{1}{2}$  state the lower-lying state obtained by diagonalizing the matrix of  $H_{\text{block}}$  in the subspace spanned by  $|\psi\rangle$  and  $V|\psi\rangle$  only. This is a  $2 \times 2$  matrix and the calculation is not difficult. It yields a

ground-state energy density in error by 5.4% as compared to 11.7% for the three-site and 5.0% for the two-site calculation. Like the three-site calculation, it also yields the correct massless spectrum. Although perturbative in spirit, this method is not a consistent expansion to some particular order in  $V$  as is the method of Ref. 7. However, it can easily be improved further by diagonalizing the matrix of  $H_{\text{block}}$  in a larger subspace spanned by more of the states  $|\psi\rangle$ ,  $V|\psi\rangle$ ,  $V^2|\psi\rangle$ , ... , and choosing the lowest-lying state. Eventually these states will span the entire spin- $\frac{1}{2}$ ,  $S_z = \frac{1}{2}$ , even parity subspace on nine sites and one is back to the exact nine-site calculation. This technique should also be suitable for studying the model (3.1) with long-range interactions.

##### 5. Concluding Remarks

In this chapter block-spin calculations for the isotropic Heisenberg model employing both two-site and three-site blocks have been discussed in great detail. The three-site calculation and its nine-site generalization gave good results and will be suitable for studying the model (3.1) with long-range interactions. The two-site calculation is not reliable for this purpose. The duality transformation introduced in Sect. 3 can be defined for models other than the one studied here, and it is hoped that it will be useful in other calculations of this type.

After this work was completed, I learned from Marvin Weinstein that improving the two-site calculation by variational techniques suffices to obtain the correct massless spectrum. In such an improved calculation,

the block states are allowed to depend on one or more variational parameters. These parameters are adjusted to minimize the ground state energy computed after many RG iterations, rather than to diagonalize the block Hamiltonian. This "feedback" mechanism allows the physics at scales much larger than the block size to influence the selection of block states.— This very powerful generalization of the real-space RG technique is not used in the calculations reported in this thesis. See, however, Refs. 5 and 8.

## CHAPTER IV

### THE LONG-RANGE HEISENBERG ANTIFERROMAGNET<sup>31</sup>

#### 1. Introduction

In this chapter I take up the study of the one-dimensional Heisenberg antiferromagnetic chain,

$$H = \frac{1}{2} \sum_{\substack{i,j=1 \\ i \neq j}}^N (-1)^{i-j+1} \frac{1}{|i-j|^p} \vec{s}(i) \cdot \vec{s}(j) , \quad (4.1)$$

using the zero-temperature, real-space RG methods illustrated in Chapter III. The infinite-volume limit  $N \rightarrow \infty$  will generally be implied. Chapter III established that the simple three-site blocking scheme correctly predicts the qualitative behavior of this model in the  $p \rightarrow \infty$  limit and is quantitatively accurate at about the 15% level. The nine-site calculation improves this to the 5% level.

Models such as (4.1) arise naturally as effective Hamiltonians describing particular sectors of states in the strong-coupling limit of lattice field theories with fermions, provided that the fermions are treated by the SLAC method described in Chapter II.<sup>8,15</sup> Consider for example the Schwinger model (massless QED in 1+1 dimensions):

$$H = a \sum_x \frac{1}{2} E^2(x) + a^2 \sum_{x,y} \psi^\dagger(x) \frac{1}{i} \alpha D(x-y) \psi(y) U(x,y) ,$$
$$U(x,y) = \exp iea \sum_{z=x}^y A(z) . \quad (4.2)$$

Rescaling  $E \rightarrow eE$  and  $A \rightarrow A/e$  and changing to dimensionless variables gives:

$$H = \frac{1}{a} \left[ \frac{1}{2} g^2 \sum_x E^2(x) + \sum_{x,y} \psi^\dagger(x) \frac{1}{i} \alpha D(x-y) \psi(y) U(x,y) \right] ,$$

$$U(x,y) = \exp i \sum_{z=x}^y A(z) , \quad [A(x), E(x')] = i \delta_{x,x'} ,$$

$$\left\{ \psi_\alpha^\dagger(x), \psi_\beta(x') \right\} = \delta_{\alpha\beta} \delta_{x,x'} ,$$

$$D(x) = (-1)^{x/x} . \quad (4.3)$$

Here the fields, the coupling constant  $g=ea$ , and the lattice coordinates  $x,y,z$  are all dimensionless.  $U(x,y)$  creates one unit of electric flux on each link between  $x$  and  $y$ , oriented from  $x$  to  $y$ .

At strong coupling the first term in  $H$  is taken as the unperturbed Hamiltonian and the second as the perturbation  $V$ . The unperturbed ground states are those with no charge and no flux links. In second-order perturbation theory their energies are

$$\mathcal{E}_n = 0 + \sum_{k \neq n} \frac{\langle n | V | k \rangle \langle k | V | n \rangle}{E_k^0} . \quad (4.4)$$

The perturbation connects the ground states to states with flux running from  $x$  to  $y$ , with energy  $\mathcal{E}_k^0 = (1/2a)g^2|x-y| \neq 0$ . An effective Hamiltonian for the fluxless sector can now be defined by

$$\mathcal{E}_n = \langle n | H_{\text{eff}} | n \rangle , \quad H_{\text{eff}} = \sum_k - \frac{1}{\mathcal{E}_k^0} v | k \rangle \langle k | v ,$$

$$H_{\text{eff}} = \frac{1}{a^2} \sum_k \sum_{x,y,x',y'} D(x-y) D(x'-y') \frac{2a}{g^2 |x-y|}$$

$$\times \psi^\dagger(x) \alpha \psi(x) U(x,y) |k\rangle \langle k| \psi^\dagger(x') \alpha \psi(y') U(x',y') . \quad (4.5)$$

The only terms in  $H_{\text{eff}}$  which take fluxless states into fluxless states are those with  $x = y'$  and  $x' = y$ . Introducing also the representation

$$\psi = \begin{pmatrix} b \\ d^\dagger \end{pmatrix} , \quad \alpha = \begin{pmatrix} 1 & 0 \\ 0 & -1 \end{pmatrix} ,$$

gives

$$H_{\text{eff}} = - \frac{2}{ag^2} \sum_{\substack{x,y \\ x \neq y}} \frac{1}{|x-y|^3} \left\{ b^\dagger(x) b(x) [1 - d^\dagger(y) d(y)] + d^\dagger(x) d(x) [1 - b^\dagger(y) b(y)] + 2b^\dagger(x) d^\dagger(x) d(y) b(y) \right\} . \quad (4.6)$$

In the fluxless sector only two states can appear on any site: either the vacuum  $|0\rangle$  or the fermion-antifermion pair  $|\pm\rangle = b^\dagger d^\dagger |0\rangle$ . Thus in this sector  $b^\dagger(x) b(x) = d^\dagger(x) d(x) \equiv N(x)$ , and a convenient spin representation is introduced by

$$S_+(x) = (-1)^x b^\dagger(x) d^\dagger(x) , \quad S_-(x) = (-1)^x d(x) b(x) ,$$

$$S_z(x) = N(x) - \frac{1}{2} ,$$

in terms of which, up to a constant,

$$H_{\text{eff}} = \frac{4}{ag^2} \sum_{x \neq y} \frac{1}{|x-y|^3} [(-1)^{x-y+1} S_+(x) S_-(y) + S_z(x) S_z(y)] . \quad (4.7)$$

The nearest-neighbor piece of  $H_{\text{eff}}$  is now the isotropic Heisenberg antiferromagnet considered in Chapter III; the full  $H_{\text{eff}}$  is similar to the model (4.1) for  $p = 3$  but has a staggered anisotropy in the  $z$ -direction. A similar analysis for the  $Q = 0$  sector of the Thirring model<sup>15</sup> leads again to Eq. (4.7) with  $|x-y|^3$  replaced by  $|x-y|^2$  (no factor  $|x-y|$  appears in the energy denominator). And 1+1 dimensional QCD leads to an  $SU(4)$  generalization of the  $O(3)$  antiferromagnet (4.7).<sup>8</sup>

To obtain agreement with known properties of the continuum Thirring model, it was argued (but not proved) in Ref. 15 that the corresponding  $H_{\text{eff}}$  has a massless excitation spectrum like the nearest-neighbor Heisenberg antiferromagnet. This suggests that the model (4.1) is in a single phase from  $p = \infty$  at least down to  $p = 2$ . Other results along these lines are those of Dyson<sup>25</sup> and Ruelle<sup>26</sup> showing that the Ising model obtained from (4.1) by  $\vec{S} \rightarrow S_z$  is disordered at all finite temperatures for all  $p > 2$  but is ordered below a critical temperature if  $p < 2$ . The result of the RG calculations in this chapter is that the model (4.1) is in a single phase from  $p = \infty$  down to approximately  $p = 1.85$ . The exact value is probably  $p = 2$ .

The discussion in this chapter is organized as follows. Section 2 presents some exact results for the cases  $p = 0$  and  $p \rightarrow \infty$ . Section 3 reviews the simple three-site blocking calculation used in Chapter III and applies it to the model (4.1). Renormalization group equations are derived which are sufficiently simple to be studied analytically. In particular, it can be seen explicitly how the non-nearest-neighbor interactions in (4.1) disappear as the RG equations are iterated when  $p$  exceeds a certain critical value. Section 4 shows that the results

of the three-site calculation do not change qualitatively when one goes to a more accurate calculation using nine-site blocks. The latter calculation, unfortunately, must be carried out numerically. Section 5 contains the conclusions.

## 2. Exact Results

Although very little is known about the model (4.1) some rigorous results can be obtained by considering the limiting cases  $p \rightarrow \infty$  and  $p = 0$ .

For  $p \rightarrow \infty$  the model becomes the Heisenberg antiferromagnet with nearest-neighbor interactions which was discussed by block-spin methods in Chapter III. This model is exactly soluble<sup>32</sup> and for the present work its relevant properties are as follows. The ground state energy density is -0.4431 and the low-lying excitations are massless spin waves. The end-to-end order  $\langle \vec{S}(1) \cdot \vec{S}(N) \rangle$  vanishes in the infinite-volume limit and the cluster property

$$\lim_{N \rightarrow \infty} [\langle \vec{S}(1) \cdot \vec{S}(N) \rangle - \langle \vec{S}(1) \rangle \cdot \langle \vec{S}(N) \rangle] = 0$$

is satisfied.

For  $p = 0$  the Hamiltonian (4.1) becomes:

$$H = \frac{1}{2} \sum_{\substack{i,j=1 \\ i \neq j}}^N (-1)^{i-j+1} \vec{S}(i) \cdot \vec{S}(j) \quad . \quad (4.8)$$

All spins interact with equal strength and the fact that they form a linear chain becomes irrelevant. This Hamiltonian can also be solved exactly, by introducing the two sublattices containing respectively only even-numbered sites and only odd-numbered sites.  $N$  is assumed to be even

so that each sublattice contains  $\frac{1}{2}N$  sites. The Hamiltonian (4.8) may be rewritten as:

$$\begin{aligned}
 H &= \sum_{\substack{i \text{ even} \\ j \text{ odd}}} \vec{s}(i) \cdot \vec{s}(j) - \frac{1}{2} \sum_{\substack{i, j \text{ even} \\ i \neq j}} \vec{s}(i) \cdot \vec{s}(j) - \frac{1}{2} \sum_{\substack{i, j \text{ odd} \\ i \neq j}} \vec{s}(i) \cdot \vec{s}(j) \\
 &= \sum_{i \text{ even}} \vec{s}(i) \cdot \sum_{j \text{ odd}} \vec{s}(j) - \frac{1}{2} \left[ \sum_{i \text{ even}} \vec{s}(i) \right]^2 - \frac{1}{2} \left[ \sum_{i \text{ odd}} \vec{s}(i) \right]^2 + \frac{3}{8} N \\
 &= \vec{s}_{\text{even}} \cdot \vec{s}_{\text{odd}} - \frac{1}{2} s_{\text{even}}^2 - \frac{1}{2} s_{\text{odd}}^2 + \frac{3}{8} N \\
 &= \frac{1}{2} s_{\text{total}}^2 - s_{\text{even}}^2 - s_{\text{odd}}^2 + \frac{3}{8} N \quad , \tag{4.9}
 \end{aligned}$$

where I have introduced the total spins on the entire lattice and on the even and odd sublattices. The ground state evidently has  $s_{\text{total}} = 0$ ,  $s_{\text{even}} = s_{\text{odd}} = \frac{1}{4}N$ , and an energy given by

$$E_0 = - \frac{\frac{N^2}{8} + N}{8} . \tag{4.10}$$

The energy density diverges linearly with  $N$  and the infinite-volume limit of the theory does not exist. The first excited state has  $s_{\text{total}} = 1$ ,  $s_{\text{even}} = s_{\text{odd}} = \frac{1}{4}N$ , and the excitation energy is 1. This contrasts with the massless excitations in the  $p \rightarrow \infty$  theory. The end-to-end order  $\langle \Phi_0 | \vec{s}(1) \cdot \vec{s}(N) | \Phi_0 \rangle$  in the ground state  $|\Phi_0\rangle$  can be obtained as follows. The fact that all spins on a single sublattice are equivalent implies that  $\langle \vec{s}(i) \cdot \vec{s}(j) \rangle$  depends only on the parities of  $i$  and  $j$ . Therefore,

$$\begin{aligned}
 \langle \vec{s}(1) \cdot \vec{s}(N) \rangle &= \frac{4}{N^2} \sum_{\substack{i \text{ odd} \\ j \text{ even}}} \langle \vec{s}(i) \cdot \vec{s}(j) \rangle \\
 &= \frac{4}{N^2} \langle \vec{s}_{\text{odd}} \cdot \vec{s}_{\text{even}} \rangle \\
 &= \frac{2}{N^2} \langle s_{\text{total}}^2 - s_{\text{even}}^2 - s_{\text{odd}}^2 \rangle \\
 &= -\frac{1}{4} - \frac{1}{N} , \tag{4.11}
 \end{aligned}$$

which explicitly shows the breakdown of clustering due to the long-range interactions.

Additional information can be obtained by using the  $p = 0$  ground state  $|\Phi_0\rangle$  as a variational trial state to study the full theory (4.1). The variational energy obtained in this way is

$$\langle \Phi_0 | H | \Phi_0 \rangle = \frac{1}{2} \sum_{i \neq j} (-1)^{i-j+1} \frac{1}{|i-j|^p} \langle \Phi_0 | \vec{s}(i) \cdot \vec{s}(j) | \Phi_0 \rangle . \tag{4.12}$$

It follows from Eq. (4.11) and the sublattice structure that

$$\langle \Phi_0 | \vec{s}(i) \cdot \vec{s}(j) | \Phi_0 \rangle = (-1)^{i-j} \left( \frac{1}{4} + \frac{1}{N} \right) .$$

Therefore,

$$\begin{aligned}
 \langle \Phi_0 | H | \Phi_0 \rangle &= -\left(\frac{1}{8} + \frac{1}{2N}\right) \sum_{i \neq j} \frac{1}{|i-j|^p} \\
 &= -\left(\frac{1}{4} + \frac{1}{N}\right) \left[ (N-1) \frac{1}{1^p} + (N-2) \frac{1}{2^p} + \dots + \frac{1}{(N-1)^p} \right] \\
 &= -\left(\frac{1}{4} + \frac{1}{N}\right) \left( N \sum_{k=1}^{N-1} \frac{1}{k^p} - \sum_{k=1}^{N-1} \frac{1}{k^{p-1}} \right) . \tag{4.13}
 \end{aligned}$$

The exact ground state energy density is therefore bounded above by

$$\frac{E_0}{N} \leq -\left(\frac{1}{4} + \frac{1}{N}\right) \left( \sum_{k=1}^{N-1} \frac{1}{k^p} - \frac{1}{N} \sum_{k=1}^{N-1} \frac{1}{k^{p-1}} \right) . \quad (4.14)$$

This shows that the infinite-volume limit does not exist for  $p \leq 1$ . Since the spin operators in  $H$  have bounded matrix elements there can be no divergence in  $E_0/N$  for  $p > 1$ , so the theory does exist in this region.

In view of the radically different properties of the theory at  $p \rightarrow \infty$  and  $p = 0$ , two possibilities exist. Either the theory remains in the  $p = \infty$  phase all the way down to  $p = 1$  where the infinite-volume limit ceases to exist, or a phase transition occurs for some  $p > 1$ . In the remainder of this paper block-spin techniques are applied to resolve this question.

### 3. Simple Calculation Using Three-Site Blocks

#### A. Derivation of RG Equations

This section applies the three-site blocking algorithm used in Chapter III to the model (4.1), which is conveniently rewritten in the form:

$$H = \frac{1}{2} \sum_{\substack{i,j=1 \\ i \neq j}}^N (-1)^{i-j+1} F(i-j) \vec{s}(i) \cdot \vec{s}(j) ,$$
$$F(i-j) \equiv \frac{1}{|i-j|^p} . \quad (4.15)$$

One begins by dividing the lattice into three-site blocks and relabelling each lattice site with an ordered pair  $(k,a)$ , where  $k = 1, 2, \dots, N/3$  labels the blocks and  $a = 1, 2, 3$  labels the sites within a block. The

Hamiltonian is separated into the piece  $H_{in}$  which only couples sites in the same block, and the remainder  $H_{out}$ :

$$H = H_{in} + H_{out},$$

$$H_{in} = \frac{1}{2} \sum_{k-a,a'} \sum_{a,a'} (-1)^{a-a'+1} F(a-a') \vec{S}(k,a) \cdot \vec{S}(k,a'), \quad (4.16)$$

$$H_{out} = \frac{1}{2} \sum_{k \neq k'} \sum_{a,a'} (-1)^{k-k'+a-a'+1} F[3(k-k') + a-a'] \vec{S}(k,a) \cdot \vec{S}(k',a').$$

Singling out a particular block for attention, I write:

$$H_{in} = \sum_k H_{block}(k),$$

$$\begin{aligned} H_{block} &= F(1) [\vec{S}(1) \cdot \vec{S}(2) + \vec{S}(2) \cdot \vec{S}(3)] - F(2) \vec{S}(1) \cdot \vec{S}(3) \\ &= \frac{1}{2} F(1) \left\{ [\vec{S}(1) + \vec{S}(2) + \vec{S}(3)]^2 - [\vec{S}(1) + \vec{S}(3)]^2 - \frac{3}{4} \right\} \\ &\quad - \frac{1}{2} F(2) \left\{ [\vec{S}(1) + \vec{S}(3)]^2 - \frac{3}{2} \right\}. \end{aligned} \quad (4.17)$$

This shows that the eigenstates of  $H_{block}$  are just the simultaneous eigenstates of the total spin on a block and  $[\vec{S}(1) + \vec{S}(3)]^2$ . These states are [notation is  $|S, S_z\rangle$ ; the subscript, when present, gives the value of the spin  $\vec{S}(1) + \vec{S}(3)$ ]:

$$\begin{aligned}
 |\frac{3}{2}, \frac{3}{2}\rangle &= |\uparrow\uparrow\uparrow\rangle \\
 |\frac{3}{2}, \frac{1}{2}\rangle &= \frac{1}{\sqrt{3}} (|\uparrow\uparrow\uparrow\rangle + |\uparrow\uparrow\downarrow\rangle + |\uparrow\downarrow\downarrow\rangle) \\
 |\frac{1}{2}, \frac{1}{2}\rangle_0 &= \frac{1}{\sqrt{2}} (|\uparrow\uparrow\downarrow\rangle - |\uparrow\downarrow\downarrow\rangle), \text{ energy} = \frac{3}{4}F(2) , \\
 |\frac{1}{2}, \frac{1}{2}\rangle_1 &= \frac{1}{\sqrt{6}} (2|\uparrow\uparrow\downarrow\rangle - |\uparrow\uparrow\downarrow\rangle - |\uparrow\downarrow\downarrow\rangle), \text{ energy} = -F(1) - \frac{1}{4}F(2) ,
 \end{aligned}
 \right\} \text{energy} = \frac{1}{2}F(1) - \frac{1}{4}F(2) ,$$

(4.18)

plus the four corresponding states with all spins flipped and negative total  $S_z$ . It can be seen that  $|\frac{1}{2}, \pm\frac{1}{2}\rangle_1$  have the lowest energy regardless of the value of  $p$ . One then hopes to get a reasonable picture of the low-lying states of the lattice by restricting attention to those lattice states which are built from the block states  $|\frac{1}{2}, \pm\frac{1}{2}\rangle_1$  only. The next step is to write an effective Hamiltonian which has the same matrix elements as the original Hamiltonian within this sector of states. For this purpose I introduce new spin operators  $\vec{S}'$  which act on the states  $|\frac{1}{2}, \pm\frac{1}{2}\rangle_1$  in the usual manner:  ${}_1\langle \frac{1}{2}, \frac{1}{2} | S'_z | \frac{1}{2}, \frac{1}{2} \rangle_1 = \frac{1}{2}$ , etc.  $\vec{S}'$  is in fact just the total block spin, and the Wigner-Eckart theorem gives:

$$\begin{aligned}
 \langle \vec{S}(k, a) \rangle &= u_a \langle \vec{S}'(k) \rangle , \\
 u_1 = u_3 &= \frac{2}{3} , \quad u_2 = -\frac{1}{3} ,
 \end{aligned}$$

(4.19)

where the notation  $\langle \rangle$  indicates any one of the four matrix elements involving the states  $|\frac{1}{2}, \pm\frac{1}{2}\rangle_1$ . Using (4.19) to express  $H_{\text{out}}$  in terms of the block spin operators  $\vec{S}'$  and observing that  $H_{\text{in}}$  is diagonal in the sector of states of interest produces the effective Hamiltonian:

$$\begin{aligned}
 H^{(1)} &= \sum_k \left[ -F(1) - \frac{1}{4} F(2) \right] + \frac{1}{2} \sum_{k \neq k'} (-1)^{k-k'+1} \sum_{a,a'} (-1)^{a-a'} \\
 &\quad \times u_a u_{a'} F[3(k-k') + a - a'] \vec{s}'(k) \cdot \vec{s}'(k') \\
 &\equiv \sum_k E_1 + \frac{1}{2} \sum_{k \neq k'} (-1)^{k-k'+1} F_1(k-k') \vec{s}'(k) \cdot \vec{s}'(k') . \quad (4.20)
 \end{aligned}$$

Since this Hamiltonian has the same form as the original one, apart from the overall energy shift  $E_1$ , the blocks of the original lattice may be viewed as sites of a new lattice and the whole blocking procedure iterated. This generates a sequence  $H^{(m)}$  of effective Hamiltonians obeying the RG equations:

$$H^{(m)} = \sum_{k=1}^{N/3^m} E_m + \frac{1}{2} \sum_{\substack{k,k'=1 \\ k \neq k'}}^{N/3^m} (-1)^{k-k'+1} F_m(k-k') \vec{s}(k) \cdot \vec{s}(k') , \quad (4.21a)$$

$$E_{m+1} = 3E_m - F_m(1) - \frac{1}{4} F_m(2) , \quad E_0 = 0 , \quad (4.21b)$$

$$F_{m+1}(j) = \sum_{a,a'=1}^3 (-1)^{a-a'} u_a u_{a'} F_m(3j+a-a') , \quad F_0(j) = F(j) , \quad (4.21c)$$

i.e.,

$$F_{m+1}(j) = F_m(3j) + \frac{4}{9} [F_m(3j-2) + F_m(3j-1) + F_m(3j+1) + F_m(3j+2)] , \quad (4.21d)$$

where the primes on the spin operators have been dropped for convenience. Note that the formula (4.21d) preserves the symmetry property  $F_m(j) = F_m(-j)$  which was assumed in writing Eqs. (4.17) and (4.18). After roughly  $m = \log_3 N$  iterations of the blocking procedure the entire lattice will be reduced to a single block of energy  $E_m$ . The energy per original lattice

site is therefore  $\mathcal{E}_m \equiv E_m/3^m$ . In the infinite-volume limit the energy density is given by  $\mathcal{E}_\infty$ , with  $\mathcal{E}_m$  satisfying

$$\mathcal{E}_{m+1} = \mathcal{E}_m - \frac{1}{3^{m+1}} \left[ F_m(1) + \frac{1}{4} F_m(2) \right] , \quad \mathcal{E}_0 = 0 . \quad (4.21e)$$

This will always be a variational upper bound on the exact ground state energy density. The problem now is to iterate the RG equations many times to find the Hamiltonian which describes the physics at very large length scales.

### B. Analysis of RG Equations

A procedure for numerically iterating RG equations like (4.21) has been given by Drell, Svetitsky, and Weinstein.<sup>3</sup> At each iteration a finite set of function values, say  $F_m(1), \dots, F_m(100)$ , are explicitly computed and stored in an array. For  $|j| > 100$ ,  $F_m(j)$  is parametrized as  $F_m(j) = \frac{1}{|j|^p} \left( A_m + \frac{B_m}{j^2} + \frac{C_m}{j^4} + \frac{D_m}{j^6} \right)$ , with only even order terms being required due to  $F_m(j) = F_m(-j)$ . The initial conditions are  $A_0 = 1$ ,  $B_0 = C_0 = D_0 = 0$ , and substituting this form for  $F_m$  into (4.21d) and applying the binomial theorem produces formulas from which  $A_m - D_m$  can be computed recursively. The error introduced by using this asymptotic form for  $F_m$  is comparable to the inherent roundoff error in double precision computer arithmetic. I have performed the numerical calculation using this procedure, but due to the simplicity of Eq. (4.21d) all the important results can be obtained by an analytic study of the RG equations. This is done by considering Eq. (4.21d) in the limit of very large  $j$  where it simplifies considerably. Physically this corresponds to looking at the interaction between very distant spins. Since the RG equations by definition relate the physics of different length scales

they can be used to extend conclusions valid at large  $j$  to smaller and smaller values of  $j$ , as will now be shown.

When  $j$  is large,  $F(j)$  is sufficiently slowly varying that  $F(3j \pm 1)$  and  $F(3j \pm 2)$  can be approximated by  $F(3j)$ . Then the first ( $m = 0$ ) iteration of Eq. (4.21d) becomes

$$F_1(j) = \frac{25}{9} F_o(3j) = \frac{1}{3^p} \frac{25}{9} F_o(j) \equiv C F_o(j), \text{ for } j \text{ sufficiently large.} \quad (4.22)$$

To extend this to smaller values of  $j$  assume now that  $j$  is not "sufficiently large" but that  $3j-2$  is, so that  $F_1(3j-2) = C F_o(3j-2)$ . Then the next iteration of Eq. (4.21d) looks like this:

$$\begin{aligned} F_2(j) &= F_1(3j) + \frac{4}{9} [F_1(3j-2) + F_1(3j-1) + F_1(3j+1) + F_1(3j+2)] \\ &= C \left\{ F_o(3j) + \frac{4}{9} [F_o(3j-2) + F_o(3j-1) + F_o(3j+1) + F_o(3j+2)] \right\} \\ &= C F_1(j), \end{aligned} \quad (4.23)$$

and this is valid for values of  $j$  roughly  $1/3$  as large as those for which Eq. (4.22) was valid. Continuing to iterate Eq. (4.21d) produces equations analogous to (4.23) holding for smaller and smaller values of  $j$  until ultimately one obtains simply

$$F_{m+1}(j) = C F_m(j) \text{ for all } j > 1 \text{ and all sufficiently large } m. \quad (4.24)$$

The restriction to  $j \neq 1$  comes about because according to Eq. (4.21d),  $F_{m+1}(1)$  depends on  $F_m(1)$ ; in fact,

$$F_{m+1}(1) = F_m(3) + \frac{4}{9} [F_m(1) + F_m(2) + F_m(4) + F_m(5)]. \quad (4.25)$$

The reasoning leading to Eq. (4.24) assumed that the smallest argument

appearing on the right side of Eq. (4.21d), namely  $3j-2$ , was greater than  $j$ , and this is only true if  $j > 1$ . This fact is crucial physically, since it means that the nearest-neighbor coupling  $F_m(1)$  may behave differently under renormalization group transformations than the longer-range couplings. The results (4.24) and (4.25) are sufficient to reveal the physical content of the RG equations.

Proceeding with the analysis, the definition  $C = 25/3^{p+2}$  shows that  $C > 1$  for  $p < \log_3 25 - 2 \approx 0.93$ , and  $C < 1$  for  $p > 0.93$ . By Eq. (4.24) this implies that

$$\lim_{m \rightarrow \infty} F_m(j) = \begin{cases} 0 & \text{if } p > 0.93 \\ \infty & \text{if } p < 0.93 \end{cases} . \quad (4.26)$$

Actually this follows from Eq. (4.24) only for  $j > 1$ , but it holds for  $j = 1$  as well: Eq. (4.25) shows that it is not possible to have  $F_m(j) \rightarrow 0$  or  $\infty$  for all  $j > 1$  without having  $F_m(1) \rightarrow 0$  or  $\infty$  (respectively) also. The value  $p = 0.93$  is strikingly close to the anticipated  $p = 1$ ; unfortunately,  $p = 0.93$  is not to be identified as the point at which the energy density diverges and the theory ceases to exist. It is clear from Eq. (4.21e) that the divergence of  $F_m(j)$  is not sufficient to produce a divergence in  $\mathcal{E}_m$  unless  $F_m(j)$  grows by a factor of at least 3 at each iteration. This happens for  $C \geq 3$ , so that  $p \leq -0.07$  is needed before this block-spin approximation can detect the divergence in  $\mathcal{E}_m$ . The significance of  $p = 0.93$  is that for  $p > 0.93$  this approximate calculation predicts that the theory has a massless spectrum: any mass gap, if present, must vanish along with the couplings  $F_m(j)$  as  $m \rightarrow \infty$ . For  $p < 0.93$  no statement can be made without actually solving the theory:

Eq. (4.26) does not imply an infinite mass gap because a massless theory remains massless even when multiplied by a large scale factor.

The really interesting question, left open by Eq. (4.26), is how  $F_m(1)$  behaves relative to the other terms in the Hamiltonian. In particular, under what conditions will  $F_m(1) \rightarrow \infty$  relative to the other  $F_m(j)$  so that the effective Hamiltonian ultimately contains only nearest-neighbor interactions? According to Eq. (4.25), if  $F_m(1)$  is much greater than the other  $F_m(j)$  then  $F_{m+1}(1) = \frac{4}{9}F_m(1)$ . Comparing this with Eq. (4.24) requires  $C < 4/9$  if the assumption  $F_m(1) \gg F_m(j > 1)$  is to be maintained as  $m \rightarrow \infty$ .  $C < 4/9$  corresponds to  $p > \log_3 \frac{25}{4} \approx 1.67$ , and it is easy to see that  $p > 1.67$  is sufficient as well as necessary for  $H^{(m)}$  to approach nearest-neighbor form. On the other hand, for  $p < 1.67$  it is impossible to have  $F_m(1) \rightarrow \infty$  relative to the other  $F_m(j)$ . But  $F_m(1) \rightarrow 0$  relative to the other  $F_m(j)$  is also impossible since by Eq. (4.25)  $F_{m+1}(1) > F_m(3) = \frac{1}{C}F_{m+1}(3)$  for large  $m$ ; thus  $F_m(1)/F_m(3)$  is bounded below by  $1/C$  as  $m \rightarrow \infty$ . Assuming that  $H^{(m)}$  does in fact iterate to a fixed form, the only possibility for  $p < 1.67$  is that all the ratios  $F_m(1)/F_m(j)$  approach finite nonzero values as  $m \rightarrow \infty$ . The interaction thus remains long-range; furthermore, since  $F_m(j) \sim 1/j^p$  for large  $j$ , the form of the interaction will be different for each  $p$ . In this sense each  $p < 1.67$  is in the domain of a separate fixed point.

The energy density computed numerically from Eq. (4.21e) is displayed as the upper curve in Fig. 15. The precise location of the vertical asymptote ( $p = -0.07$ ) is not apparent due to the limited range on the vertical axis. As discussed in Chapter III, the curve lies 12% above the exact answer in the nearest-neighbor limit  $p \rightarrow \infty$ .

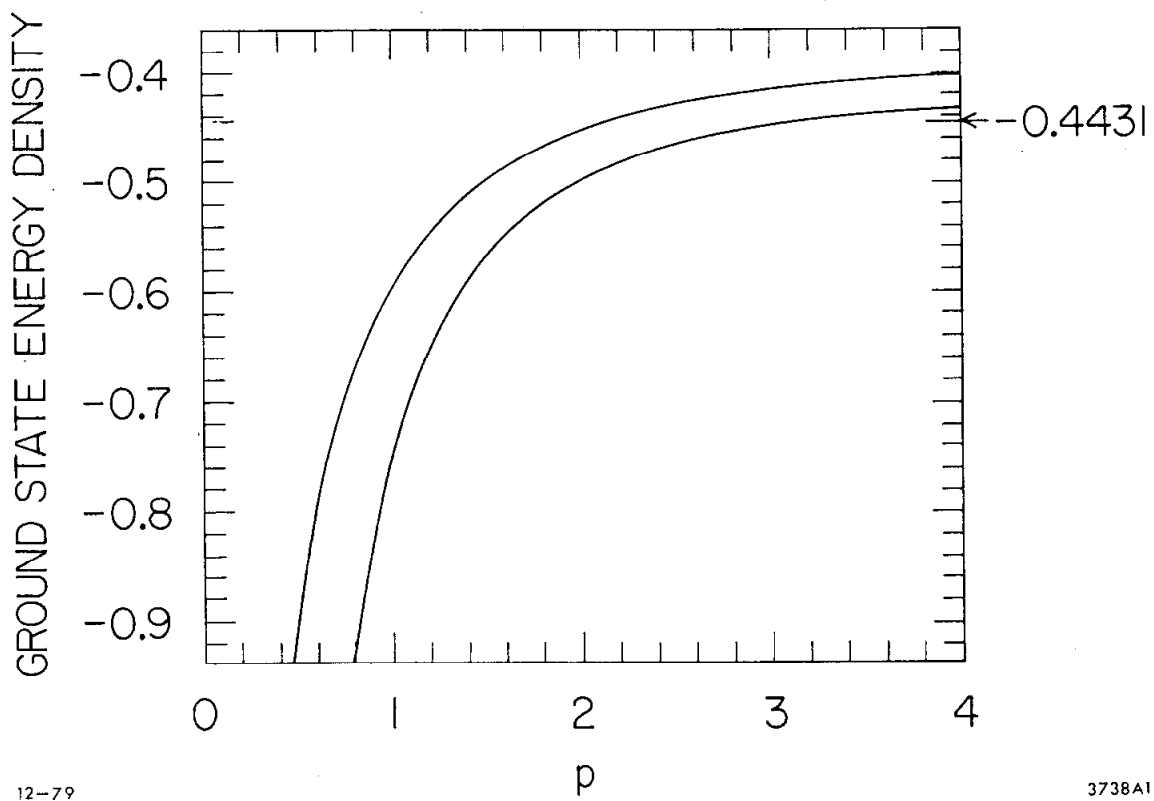


Fig. 15. Renormalization group results for the ground state energy density of the Heisenberg model with (distance)<sup>-p</sup> interactions. The upper (lower) curve is the three (nine)-site calculation of Sect. 3(4). The exact result in the limit  $p \rightarrow \infty$ , -0.4431, is marked.

C. Discussion

Several remarks are in order regarding the significance of each of the three points  $p = -0.07$ ,  $0.93$  and  $1.67$  at which the character of the fixed-point Hamiltonian  $H^{(\infty)}$  changes. (Of course, it is the change in the behavior of  $H^{(\infty)}$  that is significant, rather than the precise numerical values found for the critical points. One would not expect the critical points to be very accurately located by the present crude calculation.) It should be realized at the outset that there are basically two ways to obtain information about a theory from a block-spin calculation such as this one. The first way is to solve the fixed-point Hamiltonian. In the present case this will not work for  $p < 1.67$  where the fixed-point Hamiltonian contains long-range interactions and is at least as difficult to solve as the original theory. The second way is to study the lattice states iteratively constructed by the blocking procedure. This is not always practical, and in the present case it will not distinguish the phases of the theory because the same lattice states are constructed for all values of  $p$ . Therefore, the conclusions drawn from the present calculation are necessarily rather sketchy.

The present calculation does not detect the energy density divergence until  $p \leq -0.07$ , which compares poorly enough with the anticipated  $p \leq 1$  to warrant some discussion. Recall that the ground state energy density was identified as  $\lim_{m \rightarrow \infty} E_m / 3^m$  on the basis of an argument which iterated the blocking procedure until the entire lattice was reduced to a single block. Suppose instead that one performs some fixed number  $M$  of iterations, then takes the infinite-volume limit and studies the resulting Hamiltonian  $H^{(M)}$ . The energy density may be

estimated by  $3^{-M} \langle \phi | H^{(M)} | \phi \rangle$  with some variational trial state  $|\phi\rangle$ . In particular, since  $F_M(j) \sim 1/j^p$  asymptotically, the expectation value of  $H^{(M)}$  in the ordered state  $|\Phi_0\rangle$  of Sect. 2 will contain a divergence at  $p = 1$  coming from the operator part of  $H^{(M)}$ . In this way one recovers the correct result. This illustrates that it is always better, when possible, to extract information from the effective Hamiltonian than to continue iterating until the lattice is reduced to a single block. The point is simply that in any variational approximate calculation better trial states exist than the ones being used. In the present case, for  $p$  near 1 the state  $|\Phi_0\rangle$  is better than the states built using the blocking procedure.

As noted above, the significance of the point  $p = 0.93$  is that for  $p > 0.93$  the theory is expected to be massless based on the RG equations alone, while for  $p < 0.93$  the issue cannot be resolved without further study of the fixed-point Hamiltonian. The theory may be massless for  $p < 0.93$  or a mass gap may exist. It might seem that the mass gap would have to be infinite if nonzero because it should diverge with the coupling function  $F_m(j)$ , but this is not correct. The proper conclusion is that the blocking procedure has identified a class of block states whose energies diverge with the block size when  $p < 0.93$ . These states certainly need not be the lowest-lying excitations in the system, although to the extent that they are not, the motivation for the blocking scheme as a probe of the low-lying spectrum is weakened. Nevertheless, the suppression of this class of excitations at finite temperature is useful thermodynamic information.

For example, if the Ising model analogous to Eq. (4.15) is treated by the block-spin method of this section one finds that  $\lim_{m \rightarrow \infty} F_m(j) = \infty$  for  $p < 2$ . This discussion is given in Appendix B. The states constructed by the blocking procedure in this case are the exact ground states plus states formed by flipping blocks of spins. The divergence of  $F_m(j)$  means that at finite temperature flips of large blocks of spins are suppressed. This is responsible for the persistence of order in this model up to a finite critical temperature when  $p < 2$ . Based on this example one may conjecture that the Heisenberg antiferromagnet also is ordered at low temperatures in some range of  $p$ , given as  $p < 0.93$  in this very crude calculation.

The point  $p = 1.67$  represents the approximate location of a true phase transition, separating the "nearest-neighbor phase"  $p > 1.67$  from the "long-range phase"  $p < 1.67$ . The phases may be distinguished, for example, by the behavior of the correlation function  $\langle \vec{S}(i) \cdot \vec{S}(j) \rangle$  of very widely separated spins. The correlation function will be governed by the fixed-point Hamiltonian which is quite different in the two phases. In practice one may consider the translationally invariant correlation function  $C(k) = \lim_{N \rightarrow \infty} \frac{1}{N} \sum_i \langle \vec{S}(i) \cdot \vec{S}(i+k) \rangle$  so as to average out edge effects associated with the block walls in a block-spin calculation. Following the treatment of the Hamiltonian,  $\vec{S}(i) \cdot \vec{S}(i+k)$  is replaced by an effective operator at each iteration, using Eq. (4.19). When the Hamiltonian achieves its fixed form the required expectation values are computed in its ground state. If the fixed-point Hamiltonian is not solvable, one has no recourse but to continue iterating until the dot products of spins are reduced to squares of single spins with expectation

value  $3/4$ . This yields much poorer results: in the present case it leads to correlation functions with no dependence on  $p$ , since the block states have none! Indeed, one may be skeptical about the results of the present calculation on the grounds that the same variational trial states are used for all values of  $p$ . This problem is corrected in the improved calculation to be discussed next.

#### 4. Improved Calculation Using Nine-Site Blocks

Although the three-site calculation definitely indicates the presence of a phase transition at  $p \approx 1.67$ , one would like some assurance that the conclusions do not change qualitatively when more accurate calculations are done. The greatest single drawback of the three-site calculation is that the block eigenstates are completely determined by the rotational invariance, rather than the detailed structure, of the interactions. The nine-site calculation to be discussed now does not suffer from this problem.

The algorithm employed here is just as in Sect. 3. One restricts the full Hamiltonian (4.15) to a nine-site block and, by diagonalizing, determines the lowest-lying spin-1/2 doublet of eigenstates. Taking matrix elements between these states produces the relations analogous to (4.19):

$$\langle \vec{S}(k,a) \rangle = u_a \langle \vec{S}'(k) \rangle , \quad a = 1, 2, \dots, 9, \quad (4.27)$$

which may be used to construct the effective Hamiltonians. The  $u_a$ , however, will no longer be constants but will change with the value of  $p$  and from iteration to iteration. The RG equations will take the form:

$$H^{(m)} = \sum_{k=1}^{N/9^m} E_m + \frac{1}{2} \sum_{\substack{k, k' = 1 \\ k \neq k'}}^{N/9^m} (-1)^{k-k'+1} F_m(k-k') \vec{s}(k) \cdot \vec{s}(k') , \quad (4.28a)$$

$$F_{m+1}(j) = \sum_{a, a'=1}^9 (-1)^{a-a'} u_a^{(m)} u_{a'}^{(m)} F_m(9j+a-a') , \quad F_0(j) = F(j) , \quad (4.28b)$$

$$E_{m+1} = 9E_m + e_m , \quad E_0 = 0 , \quad (4.28c)$$

where  $e_m$  are the "energies" (eigenvalues of the operator part of  $H_{\text{block}}^{(m)}$ , dropping the constant  $E_m$ ) of the doublet of states constructed at successive iterations. These RG equations must be iterated numerically using the method of Drell, Svetitsky, and Weinstein described in Sect. 3.

Although there are 512 independent states on a nine-site block, one does not need to diagonalize  $512 \times 512$  matrices to carry out the above program. It suffices to determine the  $S_z = 1/2$  member of the lowest-lying spin-1/2 doublet, which will have even parity. Simple combinatorics shows that there are exactly 22 spin-1/2,  $S_z = 1/2$ , even parity states on a nine-site block. One of these states can be constructed by two iterations of the three-site blocking procedure [compare Eq. (4.18)]:

$$|\psi\rangle = \frac{1}{\sqrt{6}} \left[ 2 |\frac{1}{2}, \frac{1}{2}\rangle_1 |\frac{1}{2}, -\frac{1}{2}\rangle_1 |\frac{1}{2}, \frac{1}{2}\rangle_1 - |\frac{1}{2}, \frac{1}{2}\rangle_1 |\frac{1}{2}, \frac{1}{2}\rangle_1 |\frac{1}{2}, -\frac{1}{2}\rangle_1 - |\frac{1}{2}, -\frac{1}{2}\rangle_1 |\frac{1}{2}, \frac{1}{2}\rangle_1 |\frac{1}{2}, \frac{1}{2}\rangle_1 \right] ,$$

$$\text{where } |\frac{1}{2}, \frac{1}{2}\rangle_1 = \frac{1}{\sqrt{6}} (2 |\uparrow\uparrow\uparrow\rangle - |\uparrow\uparrow\downarrow\rangle - |\uparrow\downarrow\uparrow\rangle) ,$$

$$\text{and } |\frac{1}{2}, -\frac{1}{2}\rangle_1 = \frac{1}{\sqrt{6}} (-2 |\uparrow\uparrow\downarrow\rangle + |\uparrow\downarrow\uparrow\rangle + |\uparrow\downarrow\downarrow\rangle) . \quad (4.29)$$

The next state is obtained by applying the block Hamiltonian to  $|\psi\rangle$  and eliminating the component of the resulting state along  $|\psi\rangle$ , and the remaining 20 states are constructed by repeatedly applying the block Hamiltonian to the last state constructed and orthonormalizing the whole set. The matrix to be diagonalized is then  $22 \times 22$ . Some technical points concerning the numerical calculation are discussed in Appendix C.

In Chapter III an alternative scheme was suggested, in which only the  $2 \times 2$  matrix representing the block Hamiltonian in the subspace spanned by  $|\psi\rangle$  and  $H_{\text{block}}|\psi\rangle$  is diagonalized to obtain approximate nine-site eigenstates. This is based on the idea that  $|\psi\rangle$  is already a reasonable approximation to a nine-site eigenstate and in perturbation theory would mix most strongly with the state  $H_{\text{block}}|\psi\rangle$ . Indeed, one finds by diagonalizing the  $22 \times 22$  matrices that the exact lowest-lying eigenstate typically gets about 90% of its amplitude from the two states  $|\psi\rangle$  and  $H_{\text{block}}|\psi\rangle$ . Since the error in an energy goes as the square of the error in a state vector, energies computed by the  $2 \times 2$  diagonalization typically are within 1% of the exact nine-site energies. The approximation is thus very good. For definiteness, however, the results to be reported in this section come from the exact nine-site diagonalization using  $22 \times 22$  matrices.

Numerical iteration of the RG equations (4.28) shows that there are still three critical values of  $p$  with the same qualitative properties discussed in Sect. 3. The region in which the energy density diverges is found to be  $p \lesssim 0.18$  (as compared to  $-0.07$  from the previous, less accurate, calculation), the couplings  $F_m(j)$  diverge for  $p \lesssim 1.11$  (as compared to 0.93), and the transition separating the long-range and

nearest-neighbor phases occurs at  $p \approx 1.85 \pm 0.05$  (as compared to 1.67).

This last value is hard to estimate from numerical data because as the transition point is approached from above the long-range couplings  $F_m(j > 1)$  decay more and more slowly. Very near the transition it is impossible to tell whether the long-range couplings ultimately vanish or not. However, it is significant that this critical point moved up from 1.67. Had it moved down one might have suspected that an exact calculation would reveal no transition in the "physical region"  $p > 1$ .

The ground state energy density resulting from this calculation is given by the lower curve in Fig. 15. For  $p \rightarrow \infty$  the energy density is -0.4212, 5% above the correct value.

Since the block states now depend on  $p$ , correlation functions computed using nine-site blocks will have  $p$ -dependence and will distinguish the long-range and nearest-neighbor phases. In a simple block-spin calculation of the present type (non-variational) one obtains a power-law falloff at large distances, where the exponent is a constant throughout the nearest-neighbor phase but depends on  $p$  once the long-range phase is entered. It is worth emphasizing that no evidence will be found for the violation of the cluster property known to occur at  $p = 0$ . The effective operator representing the end-to-end order after  $m$  iterations satisfies the RG equation:

$$\left[ \vec{S}(1) \cdot \vec{S}(N) \right]_{\text{Eff}}^{(m+1)} = u_1^{(m)} u_9^{(m)} \left[ \vec{S}(1) \cdot \vec{S}(N) \right]_{\text{Eff}}^{(m)}, \quad (4.30)$$

and since  $u_1^{(m)}, u_9^{(m)} < 1$  [this follows from Eq. (4.27) and the fact that the magnitude of the expectation value of  $S_z$  in a non-eigenstate is less

than  $1/2$ ] one has  $\lim_{N \rightarrow \infty} \langle \vec{S}(1) \cdot \vec{S}(N) \rangle = 0$ . This is because a cluster property is really built into block-spin calculations: at any iteration correlations between spins in different blocks are ignored. This is also why the calculations locate the energy density divergence poorly. The most one could hope for is that if the cluster property is violated, then  $\langle \vec{S}(1) \cdot \vec{S}(N) \rangle$  will go to zero more slowly as the accuracy of the calculation is improved.

##### 5. Concluding Remarks

The most accurate calculation I have performed indicates that the Heisenberg antiferromagnet (4.1) has a phase transition at  $p \approx 1.85$ . The phases can be distinguished by the form of the fixed-point Hamiltonian and the behavior of correlation functions such as  $\langle \vec{S}(i) \cdot \vec{S}(j) \rangle$ . The large- $p$  phase has the physics of the nearest-neighbor antiferromagnet while for  $p \lesssim 1.85$  there is a line of fixed points. The calculation predicts that the model is massless for  $p \gtrsim 1.11$ . More detailed statements cannot be made due to the intractability of the fixed-point Hamiltonian for  $p \lesssim 1.85$ .

It is interesting to speculate on how these numbers will change in more accurate calculations. As the accuracy increases, the point at which the energy density begins to diverge must approach  $p=1$ . The point at which the couplings begin to diverge must be at a larger value of  $p$ , since the couplings must grow by a factor  $L$  at each iteration to get a divergent energy density, with  $L$  the number of sites per block. The calculations done here suggest that the divergent couplings and the divergent energy density are separated by about 1 unit of  $p$ . It is

tempting to suppose that the onset of the divergent couplings occurs at  $p \approx 2$  and coincides with the nearest-neighbor to long-range phase transition. The divergent couplings in the long-range phase then make it possible that there is long-range order at finite temperature in this phase since the excitations whose energies are diverging will not be present at finite temperature.

It is difficult to recommend reliable ways to improve the present calculations. Simply going to bigger blocks soon becomes cumbersome due to the size of the matrices to be diagonalized. Another possibility is to write effective Hamiltonians valid for more block states than just the lowest pair. This method generally gives large increases in numerical accuracy because the additional states contain information on energy levels and the density of states not present in the lowest-lying pair of states alone. For example, the two-site calculation using four states per block for the nearest-neighbor Heisenberg model (Chapter III) gives almost the same accuracy in the energy density as the nine-site calculation discussed here. However, this method will not preserve the form of the original Hamiltonian but will embed it in a more general (and more complicated) theory after the first iteration. As discussed in Chapter III, it is then necessary to study the phases of the more general theory and to understand how the original theory has been embedded. Finally, variational calculations in which the block states are chosen to minimize the ground state energy after many iterations rather than to diagonalize the block Hamiltonians can give excellent results,<sup>5,8</sup> but how to choose good variational trial states is an open question.

## APPENDIX A

I prove that, given a set of Feynman rules periodic in all momenta, periodic  $\delta$ -functions can be used to do trivial momentum integrations just as ordinary  $\delta$ -functions are used in continuum theories.

It suffices to show that if

$$I \equiv \int_{-\Lambda}^{\Lambda} dk_1 \dots dk_n F(k_1, \dots, k_n) \delta_{\text{per}}[k_1 - G(k_2, \dots, k_n)] , \quad (\text{A.1})$$

where  $F$  is periodic in  $k_1$  with period  $2\Lambda$ , then

$$I = \int_{-\Lambda}^{\Lambda} dk_2 \dots dk_n F[G(k_2, \dots, k_n), k_2, \dots, k_n] . \quad (\text{A.2})$$

To do this, write (A.1) as

$$I = \sum_{m=-\infty}^{\infty} \int_{-\Lambda}^{\Lambda} dk_1 \dots dk_n F(k_1, \dots, k_n) \delta[k_1 - G(k_2, \dots, k_n) + 2m\Lambda] . \quad (\text{A.3})$$

In the  $m^{\text{th}}$  term change variables from  $k_1$  to  $k'_1 = k_1 + 2m\Lambda$ , giving

$$\begin{aligned} I &= \sum_{m=-\infty}^{\infty} \int_{(2m-1)\Lambda}^{(2m+1)\Lambda} dk'_1 \int_{-\Lambda}^{\Lambda} dk_2 \dots dk_n F(k'_1 - 2m\Lambda, k_2, \dots, k_n) \delta[k'_1 - G(k_2, \dots, k_n)] \\ &= \int_{-\infty}^{\infty} dk'_1 \int_{-\Lambda}^{\Lambda} dk_2 \dots dk_n F(k'_1, k_2, \dots, k_n) \delta[k'_1 - G(k_2, \dots, k_n)] \\ &= \int_{-\Lambda}^{\Lambda} dk_2 \dots dk_n F[G(k_2, \dots, k_n); k_2, \dots, k_n] , \end{aligned} \quad (\text{A.4})$$

by periodicity.

If the function  $F$  is initially defined only for  $-\Lambda < k_1 < \Lambda$  then  
the above holds if  $F$  is extended periodically.

APPENDIX B

Although the Ising model with long-range interactions is quite trivially soluble at zero temperature, it is illuminating to study it using the three-site RG algorithm of Chapter IV. The RG equations are very similar to those for the Heisenberg model, and the interpretation of the various critical values of  $p$  can be justified by known properties of the model.

The Hamiltonian is written as

$$H = \frac{1}{2} \sum_{i \neq j}^N (-1)^{i-j+1} F(i-j) S_z(i) S_z(j) ,$$
$$F(i-j) = \frac{1}{|i-j|^p} , \quad (B.1)$$

and restricting it to a three-site block leads to a block Hamiltonian:

$$H_{\text{block}} = F(1) [S_z(1)S_z(2) + S_z(2)S_z(3)] - F(2) S_z(1) S_z(3) . \quad (B.2)$$

The lowest-lying pair of eigenstates of  $H_{\text{block}}$  is clearly

$$|+\frac{1}{2}\rangle = |\uparrow\uparrow\uparrow\rangle , \quad |-\frac{1}{2}\rangle = |\downarrow\uparrow\downarrow\rangle , \quad \text{energies} = -\frac{1}{2}F(1) - \frac{1}{4}F(2) . \quad (B.3)$$

Within the sector of states built from  $|\pm \frac{1}{2}\rangle$  the relation between the single-site operators and the block spin operators is just [compare Eq. (4.19)]:

$$\langle S_z(k,a) \rangle = u_a \langle S'_z(k) \rangle ,$$
$$u_1 = u_3 = 1 , \quad u_2 = -1 . \quad (B.4)$$

It is evident that this sector of states contains both of the degenerate true ground states of the model:  $|\Phi_I\rangle \equiv |\uparrow\uparrow\uparrow\downarrow\dots\rangle$  and the state  $|\uparrow\uparrow\downarrow\uparrow\dots\rangle$ .

The RG equations analogous to Eqs. (4.21) are:

$$H^{(m)} = \sum_k E_m + \frac{1}{2} \sum_{k \neq k'} (-1)^{k-k'+1} F_m(k-k') S_z(k) S_z(k') , \quad (B.5a)$$

$$F_{m+1}(j) = \sum_{a,a'} (-1)^{a-a'} u_a u_{a'} F_m(3j+a-a') , \quad F_0(j) = F(j) , \quad (B.5b)$$

i.e.,

$$F_{m+1}(j) = 3F_m(3j) + 2F_m(3j-1) + 2F_m(3j+1) + F_m(3j-2) + F_m(3j+2) , \quad (B.5c)$$

$$\mathcal{E}_{m+1} = \mathcal{E}_m - \frac{1}{3^{m+1}} \left[ \frac{1}{2} F_m(1) + \frac{1}{4} F_m(2) \right] . \quad (B.5d)$$

These equations may be analyzed by exactly the same methods applied to Eqs. (4.21). By considering first large values of  $j$  one finds that Eq. (B.5c) implies:

$$F_{m+1}(j) = C' F_m(j) , \quad j > 1 \text{ and } m \text{ sufficiently large,}$$

$$\text{where } C' = \frac{1}{3^p} (3 + 2 + 2 + 1 + 1) = \frac{9}{3^p} , \quad (B.6)$$

while the nearest-neighbor coupling obeys:

$$F_{m+1}(1) = 3F_m(3) + 2F_m(2) + 2F_m(4) + F_m(1) + F_m(5) . \quad (B.7)$$

The condition for the energy density to diverge is again  $C' \geq 3$ , which implies  $p \leq 1$ . This is exactly the correct result (recall that  $p \leq -0.07$  was obtained for the Heisenberg model), as it must be since the true ground states are in the sector to which the Hamiltonian  $H^{(m)}$  applies. The range of  $p$  for which the model is in the nearest-neighbor phase is found by requiring  $C'$  to be less than the coefficient of  $F_m(1)$  in Eq. (B.7):  $C' < 1$  means  $p > 2$ . The model is in the long-range phase for

$1 < p < 2$ . Finally, Eqs. (B.6) and (B.7) show that for  $C' > 1$  or  $p < 2$ ,  
 $\lim_{m \rightarrow \infty} F_m(j) = \infty$ . For  $C' < 1$  however, it is easy to see that  $F_m(j > 1) \rightarrow 0$   
but  $F_m(1) \rightarrow \text{constant} > 0$ . This last fact, that  $F_m(1) \neq 0$  for  $p > 2$ ,  
squares with the known nonzero mass gap of the nearest-neighbor Ising  
model. The point  $p = 2$  is thus analogous to both of the points  $p = 0.93$ ,  
1.67 in the Heisenberg case.

The significance of the fact that for  $p > 2$  the mass gap is finite  
while for  $p < 2$  it is apparently infinite will now be explained. By  
virtue of the structure of the block states (B.3), after  $m$  iterations of  
the RG equations, flipping a single spin in the ground state  $|\Phi_I\rangle$   
corresponds to flipping a block of  $3^m$  spins on the original lattice.  
The effective Hamiltonian  $H^{(m)}$  therefore describes the true ground  
states plus those excited states formed by flipping blocks of  $3^m$  spins.  
(For the remainder of this paragraph, a "spin" always means a spin of  
the original lattice.) For the nearest-neighbor Ising model ( $p = \infty$ ) it  
costs the same amount of energy to flip a block of spins of any size.  
For  $p$  large but finite the first excited state has exactly one spin  
flipped, and it costs progressively more energy to flip larger blocks.  
However, this energy remains finite as the block size goes to infinity  
provided  $p > 2$ . At finite temperatures arbitrarily large blocks can be  
excited and flipped. This will destroy the end-to-end order of the  
ground state, as proved by Ruelle.<sup>26</sup> For  $p < 2$  the energy required to  
flip a block of spins diverges with the size of the block. The resulting  
suppression of large-scale fluctuations suggests that the order in the  
ground state may persist at low temperatures at least, although a  
rigorous proof is required and was supplied by Dyson.<sup>25</sup> Obviously the

first excited state has only a single spin flipped, is not in the sector governed by  $H^{(m)}$ , and the mass gap to this state is perfectly finite down to  $p = 1$  despite the divergence in  $F_m(j)$ .

The Ising model differs from the Heisenberg model in that the zero-temperature ground state of the Ising model is the same for all values of  $p$ . The long-range and nearest-neighbor phases of the Ising model are distinguished only by their finite-temperature properties, which stem from the distribution in energy of the excited states.

## APPENDIX C

This Appendix describes in more detail the organization of the computer program which carries out the nine-site RG calculation of Chapt. IV, Sect. 4. At each iteration of the RG equations (4.28) the program must:

- 1) Find the lowest-lying spin- $\frac{1}{2}$ ,  $S_z = \frac{1}{2}$  eigenstate of  $H^{(m)}$  restricted to a nine-site block,  $\phi^{(m)}$ , and its energy  $E_{m+1}$ .
- 2) Compute the parameters  $u_a^{(m)}$  of Eq. (4.27) from  $\langle \phi^{(m)} | S_z(a) | \phi^{(m)} \rangle = \frac{1}{2} u_a^{(m)}, \quad a = 1, 2, \dots, 9.$
- 3) Compute the new long-range coupling function  $F_{m+1}(j)$  from Eq. (4.28b).

To begin with, one needs a convenient and efficient representation for the 512 basis states on a nine-site block. They are naturally labelled by the integers from 0 to 511 themselves: write each integer as a nine-bit binary number and interpret a 0 or 1 in the nth position as a spin down or up, respectively, on the nth site in the block.

Those binary numbers containing exactly five 1's represent states in the  $S_z = \frac{1}{2}$  sector of interest. There are exactly 126 such states, and their binary code numbers are given labels from 1 to 126. Each  $S_z = \frac{1}{2}$  basis state thus has an essentially arbitrary label, plus nonarbitrary binary and decimal code numbers which directly give the spin configuration of the state. A series of lookup tables allows any of these three numbers to be determined given any other. A state in the  $S_z = \frac{1}{2}$  sector can now be given as a 126-component vector, each component giving the amplitude of a unique basis state.

It is very simple to apply an operator  $\vec{S}(a) \cdot \vec{S}(b)$  to a basis state in binary form. Thus,  $\sigma_+(a) \sigma_-(b) + \sigma_-(a) \sigma_+(b)$  interchanges the  $a$ th and  $b$ th binary bits if these are different and annihilates the state otherwise, while  $\sigma_z(a) \sigma_z(b)$  multiplies the state by  $\pm 1$ . A simple subroutine can rapidly apply the block Hamiltonian to any  $S_z = \frac{1}{2}$  state.

To find the eigenstate  $\phi^{(m)}$ , the block Hamiltonian  $H_{\text{block}}^{(m)}$  is written as a  $22 \times 22$  matrix in the spin- $\frac{1}{2}$ ,  $S_z = \frac{1}{2}$ , even parity sector. Numerical accuracy requires that one remove from  $H_{\text{block}}^{(m)}$  its c-number piece  $E_m$ , which is growing as  $9^m$ , leaving an operator  $M$ . The basis states  $\psi_i$ ,  $i = 1, 2, \dots, 22$ , in this sector are generated by the Lanczos method.<sup>33</sup> Taking for  $\psi_1$  the state of Eq. (4.29),  $\psi_2$  is taken as  $M\psi_1 - \langle \psi_1 | M | \psi_1 \rangle \psi_1$ , normalized to unity, so that  $\langle \psi_2 | \psi_1 \rangle = 0$ . In principle,  $\psi_{n+1}$  can be defined by  $M\psi_n - \langle \psi_n | M | \psi_n \rangle \psi_n - \langle \psi_{n-1} | M | \psi_n \rangle \psi_{n-1}$ , normalized to unity.

One shows inductively that  $\psi_{n+1}$  is automatically orthogonal to  $\psi_\ell$  if  $\ell < n-1$ : assuming  $\psi_n$  was orthogonal to all previously constructed states, one has

$$\begin{aligned}\langle \psi_\ell | \psi_{n+1} \rangle &= \langle \psi_\ell | M | \psi_n \rangle = -\langle \psi_n | M \psi_\ell \rangle \\ &= \langle \psi_n | \text{combination of } \psi_1, \psi_2, \dots, \psi_{n-1} \rangle = 0 .\end{aligned}$$

In practice, however, enough numerical error builds up in constructing 22 126-component states that  $\psi_{n+1}$  must be explicitly orthogonalized to all previous states. The matrix of  $M$  is automatically tridiagonal in this basis:  $\langle \psi_\ell | M | \psi_n \rangle = 0$  unless  $\ell = n$  or  $n \pm 1$ , so relatively few matrix elements have to be computed.

Another danger introduced by numerical error is that the states  $\psi_i$  may have components outside the spin- $\frac{1}{2}$  even parity sector of interest. Fortunately, as discussed in the text,  $\phi^{(m)}$  is predominantly composed of the first few  $\psi_i$ , which are also the most accurate. I explicitly checked that  $\phi^{(m)}$  always had spin- $\frac{1}{2}$  to several decimal places.

Diagonalizing the  $22 \times 22$  matrix of  $M$  gives the eigenstate  $\phi^{(m)}$ , its "energy"  $e_m$ , and the parameters  $u_a^{(m)}$ . Defining the  $9 \times 9$  matrix  $R_{aa'}^{(m)} = (-1)^{a-a'} u_a^{(m)} u_{a'}^{(m)}$ , the RG equation (4.28b) becomes

$$F_{m+1}(j) = \sum_{a,a'} R_{aa'}^{(m)} F_m(9j + a - a') . \quad (C.1)$$

The remaining problem is how to compute the infinitely many parameters  $F_{m+1}(j)$ .

As mentioned in the text, only the parameters  $F_m(j)$ ,  $j = 1, 2, \dots, 100$  are actually stored for each  $m$ . For  $j > 100$  one writes

$$F_m(j) = \sum_{k=0}^6 A_{k+1}^{(m)} j^{-p-k} , \quad A_k^{(0)} = \delta_{k,1} , \quad (C.2)$$

and stores the seven additional parameters  $A_k^{(m)}$  (of which three vanish because  $F_m$  is even). Then  $A_k^{(m)}$  obeys the recursion relation following from Eq. (C.2),

$$A_k^{(m+1)} = \sum_{a,a'=1}^9 \sum_{\ell=1}^k \frac{1}{9^{\ell+p}} R_{aa'}^{(m)} A_{\ell}^{(m)} B_{\ell,k-\ell+1} (a - a')^{k-\ell} , \quad (C.3)$$

where  $(a - a')^{k-\ell}$  means 1 if  $a = a'$  and  $k = \ell$ , and  $B$  is a matrix of convenient binomial coefficients:

$$\left(1 + \frac{\delta}{9}\right)^{-p-k} = \sum_{q=0}^{\infty} B_{k+1,q+1} \delta^q .$$

The calculation of  $F_{m+1}$  from  $F_m$  proceeds using Eqs. (C.1-3).

REFERENCES

1. K. G. Wilson and J. Kogut, Phys. Reports 12C, 75 (1974) and references therein.
2. J. B. Kogut, Rev. Mod. Phys. 51, 659 (1979) and references therein.
3. D. Horn and S. Yankielowicz, Nucl. Phys. B161, 533 (1979); S. D. Drell, B. Svetitsky and M. Weinstein, Phys. Rev. D17, 523 (1978); S. D. Drell and M. Weinstein, ibid. D17, 3203 (1978); R. Jullien, J. N. Fields and S. Doniach, ibid. B16, 4889 (1977); R. Jullien and P. Pfeuty, ibid. B19, 4646 (1979); E. Fradkin and S. Raby, ibid. D20, 2566 (1979).
4. S. D. Drell, M. Weinstein and S. Yankielowicz, Phys. Rev. D14, 487 (1976).
5. M. Aelion, Ph. D. thesis, Stanford University (unpublished) (1979).
6. W. J. Caspers, Phys. Reports 63, 223 (1980) and references therein.
7. J. E. Hirsch and G. F. Mazenko, Phys. Rev. B19, 2656 (1979).
8. B. Svetitsky, S. D. Drell, H. R. Quinn and M. Weinstein, Phys. Rev. D22, 490 (1980).
9. M. Creutz, L. Jacobs and C. Rebbi, Phys. Rev. D20, 1915 (1979) and Phys. Rev. Lett. 42, 1390 (1979); L. McLerran and B. Svetitsky, Phys. Lett. 98B, 195 (1981).
10. S. D. Drell, H. R. Quinn, B. Svetitsky and M. Weinstein, Phys. Rev. D19, 619 (1979).
11. H. S. Sharatchandra, Phys. Rev. D18, 2042 (1978).

12. L. H. Karsten and J. Smit, Phys. Lett. 85B, 100 (1979).
13. A. Guth, Phys. Rev. D21, 2291 (1980).
14. K. G. Wilson, Phys. Rev. D10, 2445 (1974) and in New Phenomena in Subnuclear Physics, ed. A. Zichichi, Plenum Press, New York, 1977.
15. S. D. Drell, M. Weinstein and S. Yankielowicz, Phys. Rev. D14, 1627 (1976). Actually the "SLAC derivative" seems to have been introduced by G. Wentzel, Helv. Phys. Acta. 13, 269 (1940).
16. L. H. Karsten and J. Smit, Stanford preprint ITP-677, (September 1980).
17. W. Kerler, SLAC-PUB-2634 (October 1980).
18. H. B. Nielsen and M. Ninomiya, Rutherford Laboratory preprint RL-80-090 (November 1980).
19. L. H. Karsten and J. Smit, Nucl. Phys. B144, 536 (1978).
20. Y. Nakawaki, Prog. Theor. Phys. 59, 248 (1978) and 61, 1197 (1979).
21. J. B. Bronzan, Phys. Rev. D21, 2270 (1980).
22. W. Rudin, Principles of Mathematical Analysis, McGraw-Hill, 1964.
23. I thank Marvin Weinstein for stressing this point until I finally understood it.
24. The results of this chapter have been published in J. M. Rabin, Phys. Rev. B21, 2027 (1980).
25. F. J. Dyson, Comm. Math. Phys. 12, 91 (1969).
26. D. Ruelle, Comm. Math. Phys. 9, 267 (1968).
27. E. Lieb, T. Schultz and D. Mattis, Ann. Phys. 16, 407 (1961).
28. R. Orbach, Phys. Rev. 112, 309 (1958).

29. J. des Cloizeaux and M. Gaudin, J. Math. Phys. 7, 1384 (1966).  
In addition to the massive excitations, these authors erroneously found a massless state in the Heisenberg-Ising model with  $\gamma > 1$ . I thank Bill Sutherland for bringing this error to my attention.
30. R. J. Baxter, J. Stat. Phys. 9, 145 (1973).
31. Most of the results of this chapter appear in J. M. Rabin, Phys. Rev. B22, 2420 (1980).
32. H. Bethe, Z. Phys. 71, 205 (1931); L. Hulthén, Ark. Mat. Astron. Fys. 26A, No. 11 (1938); J. des Cloizeaux and J. J. Pearson, Phys. Rev. 128, 2131 (1962).
33. C. C. Paige, BIT 10, 183 (1970).